Lithospheric Thickness, Rift and Inversion Tectonics: The Formation and Deformation of the Neoproterozoic Katangan Basin of Central Africa.

M. C. Daly[1], M. Zimba[2], M. Purkiss[1] and F. Chibesakunda[3]

[1]Department of Earth Sciences, Oxford University, UK, [2]First Quantum Minerals Ltd., Solwezi, Zambia, [3]Geological Survey Department, Lusaka, Zambia.

Corresponding author: M. C Daly (mike.daly@earth.ox.ac.uk)

ORCID.org/0000-0002-3426-0164

Key Points:

- The Neoproterozoic Katangan basin developed between three craton margins, within what is today mapped as an elliptical zone of lithosphere, 140-170 km thick.
- Basin stratigraphy and structure proves crustal extension by rifting drove basin formation and increased dramatically from basin margins to a Central Rift Zone.
- Eo-Cambrian inversion of the basin, most intensely along the Central Rift Zone, reactivated rift structures and created potential pathways for metallic brines.

Abstract

The tectono-stratigraphic development of continental basins is key to our understanding of the location and scale of metal deposits required by the energy transition. We examine the Neoproterozoic Katangan copper basin of Central Africa to determine the link between lithosphere and crust and the generation of potential fluid pathways. Integration of lithospheric thickness, quantitative basin analysis and structure, defines a basin scale tectono-stratigraphic model for controls on potential fluid pathways. The basin developed along the thinned (140-170 km thick) margins of the Congo, Kalahari and Bangweulu cratons. Crustal scale fault zones define these margins and imply a mechanical weakness in the basin. Drill core and seismic data show extensional, half graben geometries. Basin subsidence analysis indicates two phases of rift-driven subsidence and increasing lithospheric extension from the basin boundary to a Central Rift Zone (CRZ). The CRZ also maps out as a sediment provenance boundary. Subsequent Late Ediacaran and Cambrian orogenesis and rift-fault inversion occurred most intensively within the CRZ. Basin expulsion and thrust tectonics resulted in a narrow belt of crustal thickening defined today by a ~50 km wide zone of garnet amphibolite facies metamorphism. The spatial coincidence of early crustal extension, relatively thin lithosphere, and later intense basin inversion along the CRZ, indicates that pre-existing crustal structure and weakness was a key tectonic control. The reactivated structures define several tectonic domains, control basin architecture within the zones and occur as potential fluid pathways for high volume fluid migration for metal bearing brines.

Plain Language Summary

The world requires copper to deliver the energy transition. Large sedimentary basins within the continents are a prolific source of copper, however our understanding of how deposits are formed remains unertain. Here we examine the world's most prolific copper bearing basin, the Central Africa Katangan basin to understand key aspects of copper deposit formation. Existing mines were largely discovered by the detection of surface indications of copper. To discover new copper we need to look deeper into unexplored rocks. By integrating four independent geological tools, we define pathways along which copper bearing fluids may move through the earth. This will enable us to find deep deposits unseen by conventional surface detection. Specifically, we look at the thickness, and therefore strength, of the continent, searching for regional weakness where a suitable basin may have formed. We then analyze the basin's geometry and rocks, to understand both how the basin formed, and how it filled with sediment and from where. Finally, we analyse how the basin has deformed since its formation. Merging these very different perspectives allows us to define a series of structural domains and potential fluid channels crucial to metal migration and deposit formation and enables their systematic discovery.

1. Introduction

The Neoproterozoic Katangan basin lies on inter-cratonic lithosphere between the Archean and Paleoproterozoic Congo, Kalahari and Bangweulu cratons of Central Africa. The basin context, structure and stratigraphy appears strongly related to the margins of these cratons. The basin is also the world's largest, sediment-hosted copper (Cu) and cobalt (Co) province (Selley et al 2006) and contributes about 14% and 60% respectively to the world's Cu and Co production. This unique mineral endowment has resulted in the mines and mineral deposits of the basin having been widely studied (Mendelsohn 1961, Fleischer et al 1976, Hitzman 2000 & Hitzmann et al. 2005, Selley et al. 2006). Although the basin history has been extensively analysed in the context of the local mining activities (Mendelsohn 1961, Fleischer et al 1976, Coward & Daly 1982, Daly et al. 1986, Porada & Berhorst 2000, Hitzman et al. 2012), there remain significant unknowns about the tectonostratigraphic development of the basin as a whole and the crustal controls on the basins tectonic and mineral development (Alessio et al. 2019).

The uncertainties of the tectonic and geodynamic development of the Katangan basin are in part due to the paucity of deep crustal data and modern basin analysis. Chronostratigraphic correlation between the well-known mining locations is difficult due to very few reliable age markers beyond two well recognized but non-diagnostic diamictite units. No quantitative analysis of the subsidence history of the basin has been published. Similarly, there is little geometric analysis of the nature of the basin wide rift tectonics and their relationship with the subsequent Ediacran and Cambrian basin inversion and thrust tectonics. These deficiencies and singular scientific approaches, result in differing perspectives on the basin formation process based on magmatic data (Kampunzu et al. 2000), stratigraphic correlations (Binda 1994, Werndorf 2003, Cailteaux & De Putter 2019), the

role of salt tectonics and brecciation (Jackson et al 2003, Mambwe et al 2023), and the distribution, heterogeneity and degree of deformation and metamorphism experienced by the basin (Coward & Daly 1984, Cosi et al 1992, John et al 2004).

We build on this earlier work to develop a tectono-stratigraphic model for the northern Katangan basin and the development of its major fluid pathways. We integrate four distinct but complementary geological perspectives of the basin into a single tectonostratigraphic model. The inputs include lithospheric thickness and basin location, the basin forming process and its variability, the stratigraphic provenance of basin fill, and the basins subsequent deformational history and tectonic development. These perspectives are summarized as several tectonic domains that reflect the current heterogeneity and architecture of the basin, and identify a range of potential fluid pathways that may ultimately assist in the deep exploration for copper and associated minerals.

2. Lithospheric context of the Katangan Basin of Central Africa

The Neoproterozoic Katangan basin extends some 2500 km from the Katanga province of the Democratic Republic of Congo, southwestwards across Zambia and southeastern Angola to northwestern Namibia (Figure 1). It lies between the Archean Congo craton to the northwest and the Archaean and Proterozoic Kalahari craton to the south. It is also bordered by the Neoarchean and Paleoproterozoic Bangweulu craton to the west. From western Zambia, southwestwards to the Kamanjab inlier of Namibia (Figure 1) the basin is covered by Mesozoic sediments of the Okavango basin and Plio-Pleistocene sands of the paleo-Kalahari Desert (Miller, 2013). Throughout this poorly exposed basin there is broad consistency in tectono-stratigraphic units

indicating a broadly contiguous basin with comparable tectonic and climatic environments (Miller 2013). However, the extensive evaporitic sections in the DRC and Zambia, and the associated breccias, are not significant in Namibia and, to date, nor are the extensive Cu deposits.

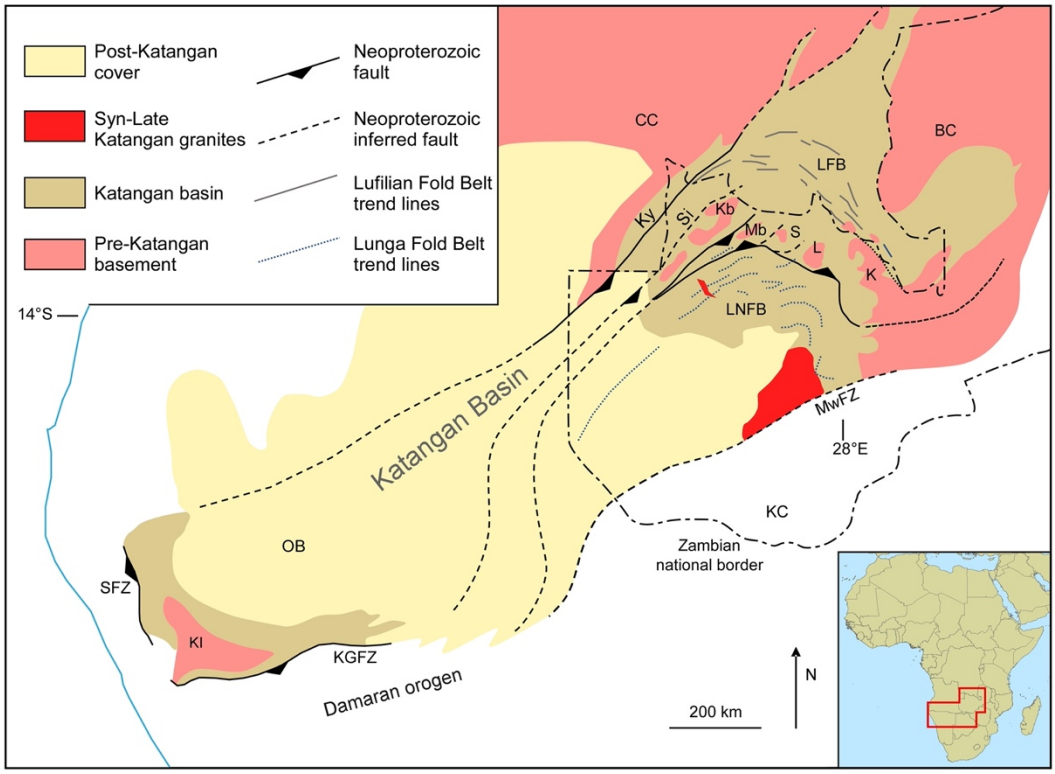

Figure 1. Map showing the Katangan basin, covered and exposed.
Geological outline of the greater Katangan basin from the DRC in the NE to Namibia in the SW. The map shows the central part of the basin is overlain by widespread cover of Mesozoic and Cenozoic sediments. The area discussed in this paper is the northeastern area known as the Central African Copper Belt (CACB). Abbreviations: CC Congo Craton; BC Bangweulu Craton; KC Kalahari craton; LFB Lufilian fold belt; LNFB Lunga fold belt; Ky Kanyama fault; Si Sailunga fault; Kb Kabompo Dome; Mb Mwombezhi Dome; S Solwezi Dome; L Luswishi Dome; K, Kafue Anticline; MwFZ Mwembeshi fault zone; KGFZ Kamanjab fault zone: KI Kamanjab inlier; Sesfontaine fault zone.

2.1. The cratonic margins of the Katangan basin

The cratonic boundaries of the Katangan basin appear to both influence the location, area and shape of the basin and also some major tectonic features within it (Figure 2). This section briefly describes the geophysical character of the bounding cratons and sets a fundamental context for the development of the entire basin.

During the past two decades Rayleigh wave tomography has been used to determine the thickness of continental lithospheric and, together with earthquake depths, has been used as a indicator of thick, cold and strong crust (Jackson et al 2001). Although only effective for lithospheric thicknesses greater than ~110 km, and with a lateral sensitivity of the order of 200 km and vertical resolution of 25 km, this technique has resulted in relatively stable models of continental lithospheric thickness globally (Jackson et al. 2021). Augmenting this view of lithospheric thickness, a less constrained, two-dimensional profile of lithospheric thickness across a part of the Katangan basin, has been made using magneto-telluric (MT) inversion (Sarafian et al. 2018). The technique maps lithospheric conductivity and resistivity variations driven by rock, fluid, or melts, and can give broad indications of the depth of sub-continental lithospheric mantle. Data from both techniques are used to define the cratonic margins of the Katangan basin. These geophysical data sources are supported by regional isotopic age data together with estimated Sm-Nd model ages (De Waele et al. 2006).

Raleigh wave Lithospheric thickness maps of southern Africa, derived from the model of Schaeffer & Lebedev (2013) (Figure 2a), are superposed with the regional fault structures of the Katangan basin in figure 2b. The contoured base map shows 10 km lithospheric thickness contours (LTC) from 100 km to 300 km. Southern Africa comprises two large areas of thick lithosphere that define the two cratonic areas of the Congo craton and the Kalahari craton. The two cratons reach thicknesses of over 250 km and are separated by a thinner, but still relatively thick lithosphere of about 140 km thick (Figure 2a & 2b). Both areas of thickened lithosphere comprise a composite make up of Archean and Proterozoic terranes within the thickened lithosphere that are not

distinguishable by the Raleigh wave technique. The map allows two differing scales of observation, the continental scale (~5000 km) and the basin scale (~1000) km, where the uncertainties still permit the identification of basin scale features (Figure 2a, b & c).

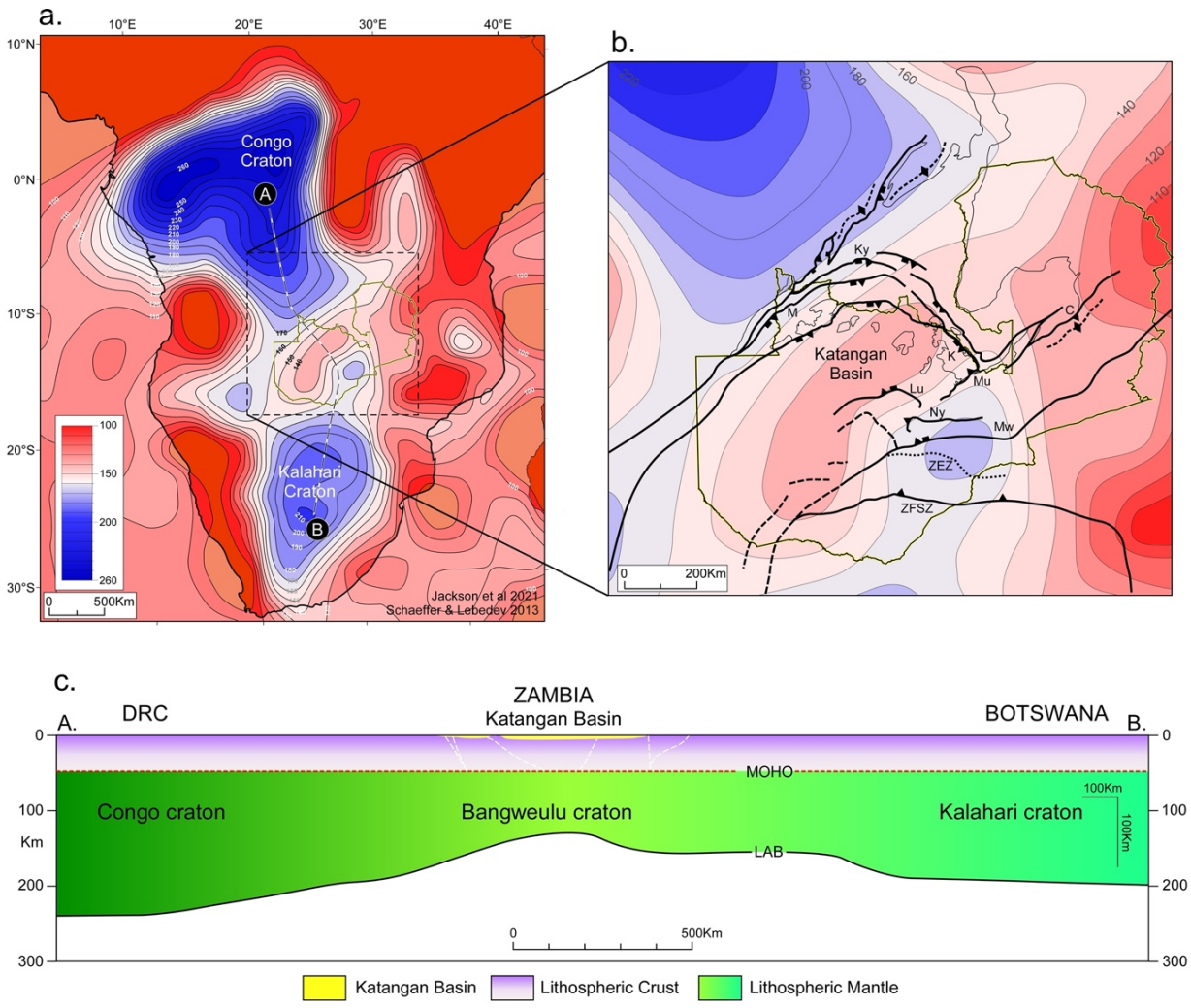

Figure 2 Lithospheric setting of the Katangan Basin

2a. Lithospheric thickness map of Southern Africa based on the Raleigh wave tomography model of Schaeffer & Lebedev (2013). Note the spatial relationship between the thick lithosphere of the Congo and Kalahari cratons and the elongate NE/SW elongate area of relatively thinner lithosphere beneath Zambia.
2b. A close-up of Zambian lithosphere and the major crustal scale faults that define the borders and major fault structures of the Neoproterozoic Katangan basin. The Katangan basin occupies a NE/SW trending elongate area of thinner (~140 km) lithosphere between the thicker (>200 km) lithosphere of the bounding cratons to north and south.
2c. A north-south cross section of the lithosphere showing the significant topography at the Lithosphere-Asthenosphere Boundary (LAB) between the Congo and Kalahari cratons. Katangan basin occupies the relatively thin zone between the two cratons to the north and south of it. The location of the section in marked in figure 1a.

2.1.1 The Congo craton margin

Figure 2 shows four features relevant to the southeastern margin of the Congo craton and its relationship with the overlying Katangan basin. Firstly, a parallelism of the northwestern Katangan basin margin with the southeastern thickness contours of the Congo craton, roughly paralleling a cratonic thickness of 160 km. This relationship extends for over 1000 km along strike (Figure 2a). The exposed geological outcrops between the Congo craton and the Katangan sedimentary basin have two distinct and overlapping modes: a flat to gently dipping stratigraphic onlapping relationship to the west of the Mwinilunga fault zone; a linear, east dipping monoclinal relationship along the NE/SW eastern margin of the Kibara mountain range (Francois 1969) (Figure 3). This ~800 km long, southeastern, faulted Congo cratonic margin is broadly linear and comprises several 100-200 km long, fault segments that define the margin. In addition to the margin parallel faults there is an extensive zone of andesitic and basaltic lava flows and volcanics and gabbroic intrusions that also roughly parallel the craton margin in Zambia (Linyunga et al. 2000) and to the north in the DRC (Kampunzu et al. 2000, Key et al. 2001 & Twite et al. 2017) (Figure 2b & 3).

Secondly the 140 km, closed lithospheric thickness contour beneath the centre of the Katangan basin broadly follows the trend and shape of the centre of the Katangan basin and its continuity to the SW. The steady gradient from the NW parallels the mappable fault zones (see section 3.1) between the Archean outcrop and the centre of the basin, implying the cratonic thickness change is potentially in-part fault controlled. Thirdly, the map also shows the central basin contour closing and thickening to the northeast towards the centre of the smaller Paleoproterozoic Bangweulu craton. These observations suggest a close relationship between lithospheric thickness change, the northwest boundary of the Katangan basin and the location of the basin.

2.1.2 The Bangweulu craton margin

The geophysical definition of the Bangweulu craton as a significant area of thickened, ancient lithosphere is less compelling on the surface wave tomography as that of the Congo and Kalahari cratons. However, its existence as cratonic lithosphere has long been postulated by field mapping of northeastern Zambia (Drysdall et al 1972, Daly & Unrug 1982, Andresen & Unrug 1984). More recently its physical existence has been supported by a magneto-telluric profile that concluded it comprised relatively thick and resistive lithosphere in comparison to the surrounding Proterozoic folded belts (Sarafian et al. 2018). In addition, the granites and volcanics that constitute the surface geology of the Bangweulu craton are well dated as Paleoproterozoic and reveal Archean Sm/Nd model ages indicating an Archean protolith (De Waele et al. 2006). To the SE and SW the Bangweulu craton and its overlying Mesoproterozoic sedimentary basins were deformed in the Irumide orogenic event between 1050 and 950 Ma (Daly 2006 & De Waele et al. 2006).

The contact between the Katangan sedimentary basin and the Bangweulu craton has two distinct modes: a flat to gently dipping onlapping relationship along the Luapula valley and the western side of the Chambeshi basin (Thieme 1968 & 1971); a linear, steeply dipping monoclinal relationship developed due to basement involved thrust faulting along the NE/SW Muchinga margin of the Chambeshi basin (Page 1973). A comparable NE facing monocline defines the and the NW/SE Kafue Dome margin of the Copperbelt (Daly et al. 1984). This linear, basement fault trend defines the eastern margin of the Kafue Dome (Coward & Daly 1984) and can be traced several hundred kilometers to the NW into the DRC (Figure 2b). Such continuous and linear fault zones are interpreted as a result of blind, crustal scale thrust structures.

The Bangweulu cratonic lithosphere thins to the SE and SW from the centre of the craton (Sarafian et al. 2018 and Schaeffer & Lebedev 2013) and constitutes the basement to the Katangan basin outcrop pattern (Figure 2b). Within the Katangan basin, in addition to the Kafue Dome, several other basement inliers record Paleoproterozoic ages broadly comparable to the Bangweulu craton (De Waele. et al 2006) and indicating that most of the Katangan basin of the Zambian copperbelt is underlain by an extensive Bangweulu craton margin (Figure 2b). The Bangweulu rock types and age connection can be traced to the southern boundary of the line of basement dome inliers (Figure 3 & 4). South of this line there is no further basement outcrop or drilled section within the basin.

2.1.3 The Kalahari craton margin

As with the Congo craton, the Kalahari craton comprises several geologically distinct Archean and Proterozoic units that amalgamate through the surface wave analysis to define a single, large, Kalahari craton (Figure 2a). The definition of the lithospheric shape and thickness of the Kalahari craton is relatively consistent across several studies as summarized by Jackson et al (2021). The northern margin of the craton lies to the south of the Katangan basin and is here considered as the southern, tectonic boundary of the Zambezi Belt as defined by the Zambezi Frontal Shear Zone (ZFSZ, Figure 2) and the Mesoproterozoic Choma-Kaloma Batholith of SW Zambia (Hanson 2003). The ZFSZ is defined geologically and on aeromagnetic data (Taverner-Smith 1961 & Loughlin 1979).

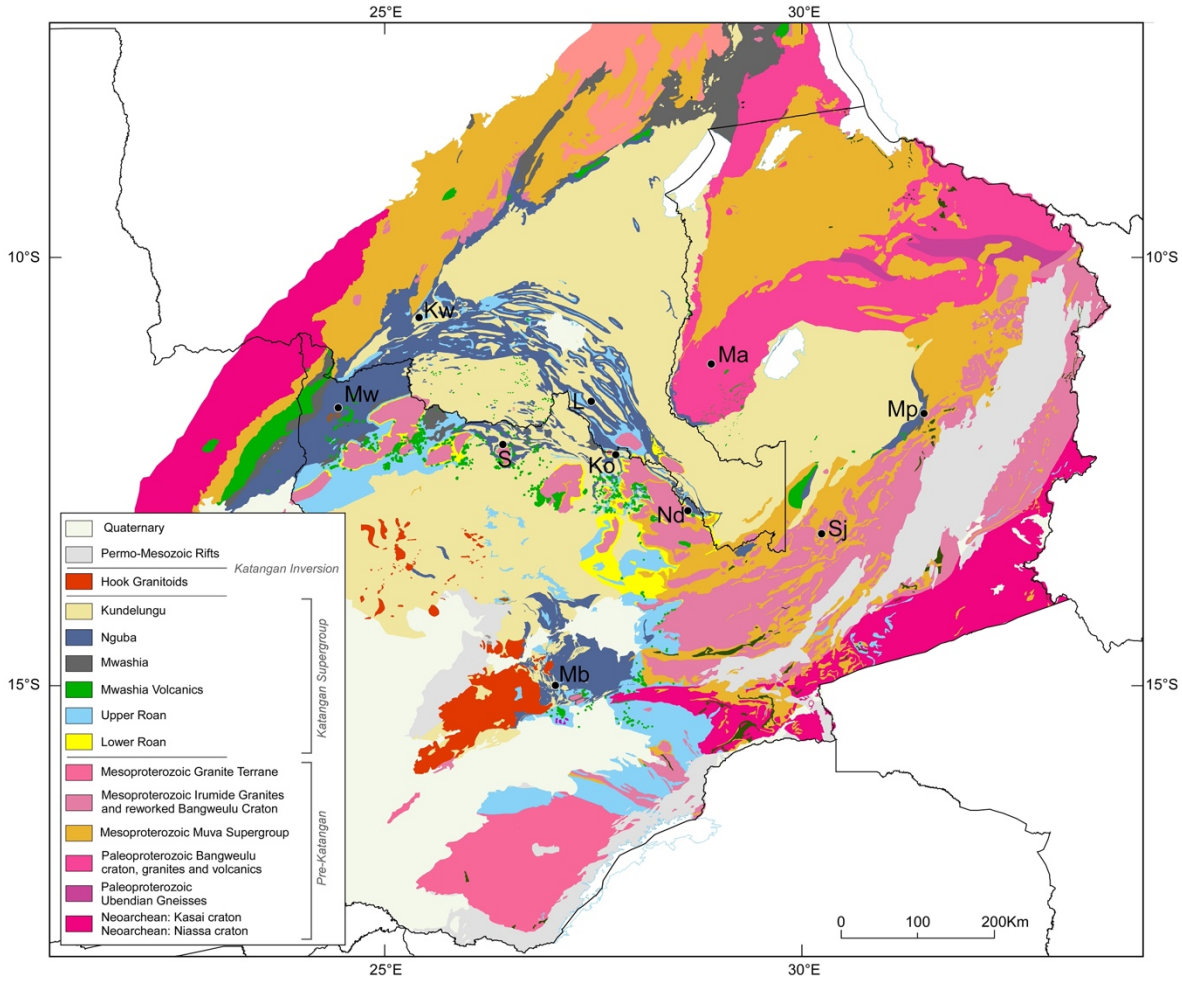

Figure 3. Geological Map of the Katangan basin and its surrounding area.
A geological map of the Katangan basin of Zambia and the southeastern DRC showing the detail of the basin geology and structure and more generally the major basement arches that define the basin today. (Modified after the Geological Map of the Republic of Zambia, Scale 1:1m (Thieme, J. G. & Johnson, R. L.1981). Abbreviations: Kw Kolwezi; Mw Mwinilunga; S Solwezi; K Konkola; Nd Ndola; Mb Mumbwa; Ma Mansa; Sj Serenje; and Mp Mpika.

2.2 Summary of the cratonic context of the Katangan basin

The observations above indicate that the three craton margins have influenced the location, shape, and arcuate trend of the Katangan basin, and consequently its structural and stratigraphic evolution. Given the different scales of observations, this is not yet a precise or simple influence. The relationship is most convincing along the northwestern boundary of the Katangan basin where the

onlapping edge of the basin closely follows the ~170 km LT contour and is marked by extensive Tonian aged gabbroic intrusions and extrusive basaltic and andesitic lavas and volcanics in both Zambia and the DRC (Figure 2 & 3). Equally compelling is the NE/SW trending zone of relatively thin, ~140 km thick lithosphere, underlying the centre of the Katangan basin in Zambia (Figure 2a, b & c). Some 300,000 km^2 in area, this curved, oval shape, trends NE/SW and defines a thin, central band of lithosphere that is bounded by all three cratons. The MT and geologically defined Bangweulu craton extends southwestwards beneath this central band of lithosphere and appears as a series of thrusted inliers widely described as domes (Coward & Daly 1984). The Kalahari craton broadly bounds the basin as the lithosphere thickens to the south (Figure 2b & 2c).

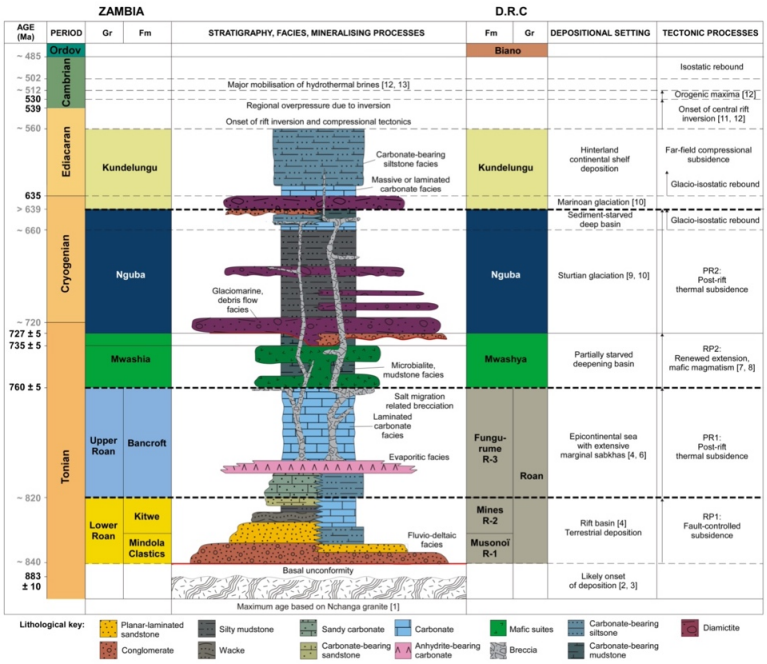

Figure 4 Katangan basin stratigraphic summary
Schematic stratigraphic column representing the Katangan basin lithostratigraphic nomenclature and general facies distribution. The southern part of the basin is on the left and the northern on the right. Stratigraphy and facies are represented in the central column with gross depositional environments and tectonic processes outlined on the right. On the left margin are stratigraphic ages from Cohen et al (2018). References numbers referred to: [1] Armstrong et al. (2005); [2] Selley et al. (2018); [3] Cahen et al. (1970)a; [4] Selley at al. (2006); [5] Muchez et al. (2015); [6] Binda (1994); [7] Key et al. (2001); [8] Kampunzu et al. (2000); [9] Rooney et al. (2015); [10] Halverson et al. (2020); [11] John et al. (2004); [12] Daly et al. (2020); [13] Torrealday et al. (2000).

3. Katangan Basin evolution

Based on the apparent lack of evident ocean crust within the Katangan basin, Binda (1994) argued that the Katangan basin was not rift related. However, the majority of publications assume the basin developed as a continental rift zone, argued largely on the basis of associated magmatism (Kampunzu et al. 2000) and analogues for the sedimentology and stratigraphic character of the early Roan sediments (Mendelshon 1961, Selley et al 2005 & Kennedy et al 2019).

Underpinning our approach is the extensive and detailed knowledge of the lithostratigraphy of the Katangan basin, based largely on the Zambia and the DRC Copperbelts and regional field mapping by the Geological Surveys of Zambia and the DRC (Mendelshon 1961, Francois 1969, Fleischer et al. 1976, Binda 1994, Cailteux et al.1994 & Cailteux et al 2019). Wendorff (2003 & 2011), working primarily in the DRC, added dynamic element to the lithostratigraphy and proposed discrete basin forming events that resulted in basin expansion to the north over time. Following the regional model of Porada and Berhorst (2000), Wendorff (2011) argued for two phases of Tonian rifting followed by a foreland basin developed during Ediacaran and Cambrian thrust tectonics. This history and our interpretation of the regional stratigraphy is summarized in the stratigraphic column of figure 4. To develop and test these interpretations we present quantitative estimates of crustal extension based on new regional data from deep diamond drill core and reflection seismic data. In addition, we use zircon provenance analysis to identify sediment provenance routing and depositional compartmentalization in the basin and the nature of sediment barriers and sediment entry routes through time.

296 ## 3.1 Basin formation

297 The primary tectonic drivers of basin formation are lithospheric extension and lithospheric loading,
298 the load either applied laterally (foreland basins) or from beneath (cratonic basins). The subsidence
299 profiles of these tectonic settings tend to be markedly different and is arguably an essential
300 characteristic for a basin to be attributed a tectonic mechanism (Xie & Heller 2009 & Allen &
301 Allen 2013). Stratigraphic and associated subsidence analysis has been widely used to constrain
302 basin driving mechanisms underpinning basin subsidence (Watts & Ryan 1976, Barton & Wood
303 1984, Xie & Heller 2009) and is deployed here in the Zambian part of the Katangan basin (Figure
304 5). The analysis is restricted to areas of minimal deformation of the basin's sedimentary section as
305 increasing strain and metamorphism makes interpretation of the original sedimentary section
306 increasingly unreliable. The analysis presents eight "type sections" based around a diamond drill
307 core interpretation with adjacent outcrop and supplementary data from the literature. The resultant
308 type sections are a best representation of the immediate area's stratigraphy. We have created such
309 type logs from the northeastern basin margin at Chilonga, to the Central Rift Zone (CRZ) around
310 Solwezi, an across strike section of approximately 200 km (Figure 5).

311

312 ### 3.1.1 Subsidence analysis and backstripping methodology

313 Quantitative subsidence analysis allows for the filling of a sedimentary basin to be quantified and
314 basin formation mechanisms to be constrained. Thicknesses of stratigraphic units at the time of
315 deposition are altered by the effects of subsequent sediment-loading and compaction. To see
316 through this complexity the process of back-stripping (Watts and Ryan 1976) allows present-day
317 stratigraphy to be corrected for the effects of sediment and water-loading. This allows basin
318 subsidence to be partitioned into top-down subsidence driven by sediment loading, and subsidence
319 driven by tectonic forces (Steckler and Watts, 1978; Watts and Ryan, 1976). By isolating tectonic

subsidence, comparisons can be made between different basin subsidence profiles and history. Different basin formation mechanisms create distinct tectonic subsidence profiles, with, for instance, rift basins being characterized by a concave profile of initially rapid tectonic subsidence which reduces exponentially as rifting attenuates and thermal cooling subsidence takes over (McKenzie, 1978; Steckler and Watts, 1978; Xie and Heller, 2009).

McKenzie (1978) proposed the uniform extension model to predict several aspects of rift evolution, including crustal thinning and subsidence. The uniform extension model invokes two stages of rift basin development: rapid initial fault-controlled subsidence, followed by thermal subsidence as the lithosphere cools. Both combined yield the characteristic concave-up tectonic subsidence profile observed in many rift basins (Steckler and Watts, 1978; Xie and Heller, 2009). Core logging and facies analysis was carried out on eight Katangan basin locations (Figure 8a). Type logs were established within a 1 km radius and detailed facies analysis was undertaken on each main core and adjacent cores and sections and estimates of water-depth ranges through time made. Decompaction of sedimentary columns and 1-D back-stripping was performed assuming Airy isostasy and analogue petrophysical parameters (Sclater & Christie1980, Turer and Maynard 2003 & Allen and Allen 2013). The calculations involved in decompaction, and back-stripping of sediment columns are well-established and are outlined in detail (Watts & Ryan 1976), Steckler & Watts 1978 and Allen & Allen 2013). The eustatic term in the back-stripping equation was omitted due to there being no reliable and continuous sea level curves for the Neoproterozoic.

The uniform stretching model (McKenzie 1978) was applied to estimate stretching (β) factors that best fit the tectonic subsidence profiles generated from back-stripping. It was assumed that the

fault-controlled subsidence phase lasted 10 Myr (Veevers 1981) and that the Lower Roan to Upper Roan transition represents the onset of thermal subsidence. Mwashia stretching factors were calculated using the stretched crust at the end of Roan rifting as the starting conditions for Mwashia extension. The type logs and parameters that were used in back-stripping and to compute stretching factors, are provided as Supplementary Data (1).

3.1.2 Katangan basin subsidence results

Back-stripping of the type logs shows a clear trend of tectonic subsidence increasing across the strike of the basin from east to west. This trend is particularly clearly developed in the four deepest cores (Figure 5b & 5c). In most of the cores and their associated type logs, evidence of two distinctive rift phases is also present, indicating an initial Lower Roan rifting event and a later Mwashia rifting event.

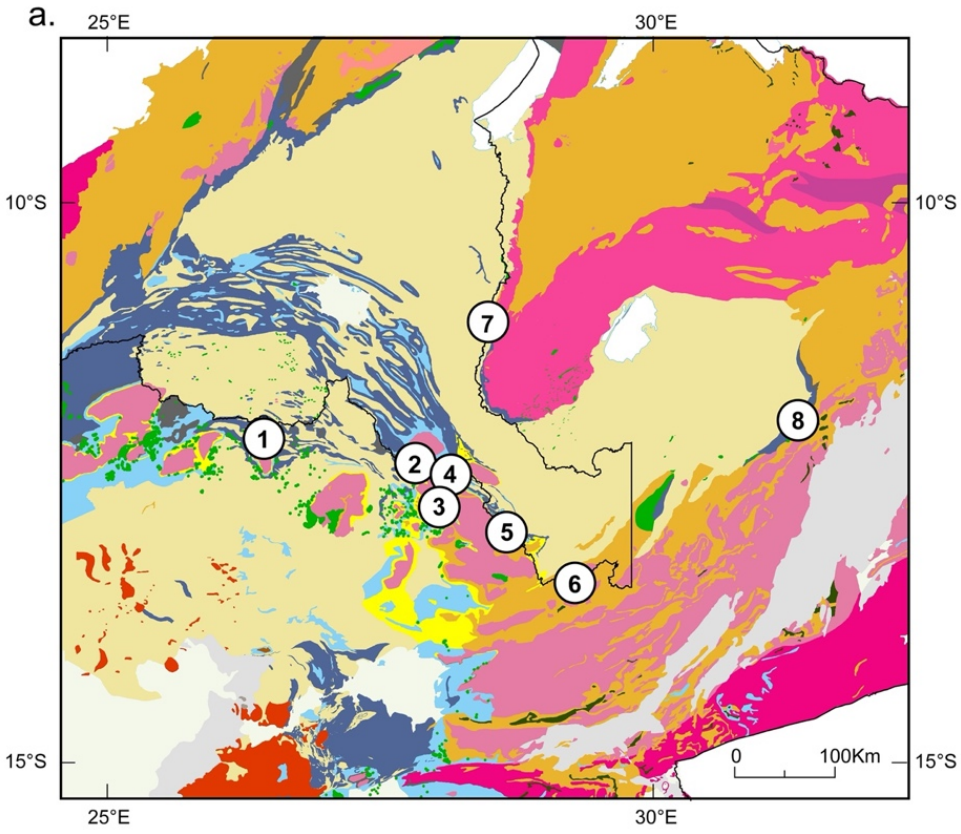

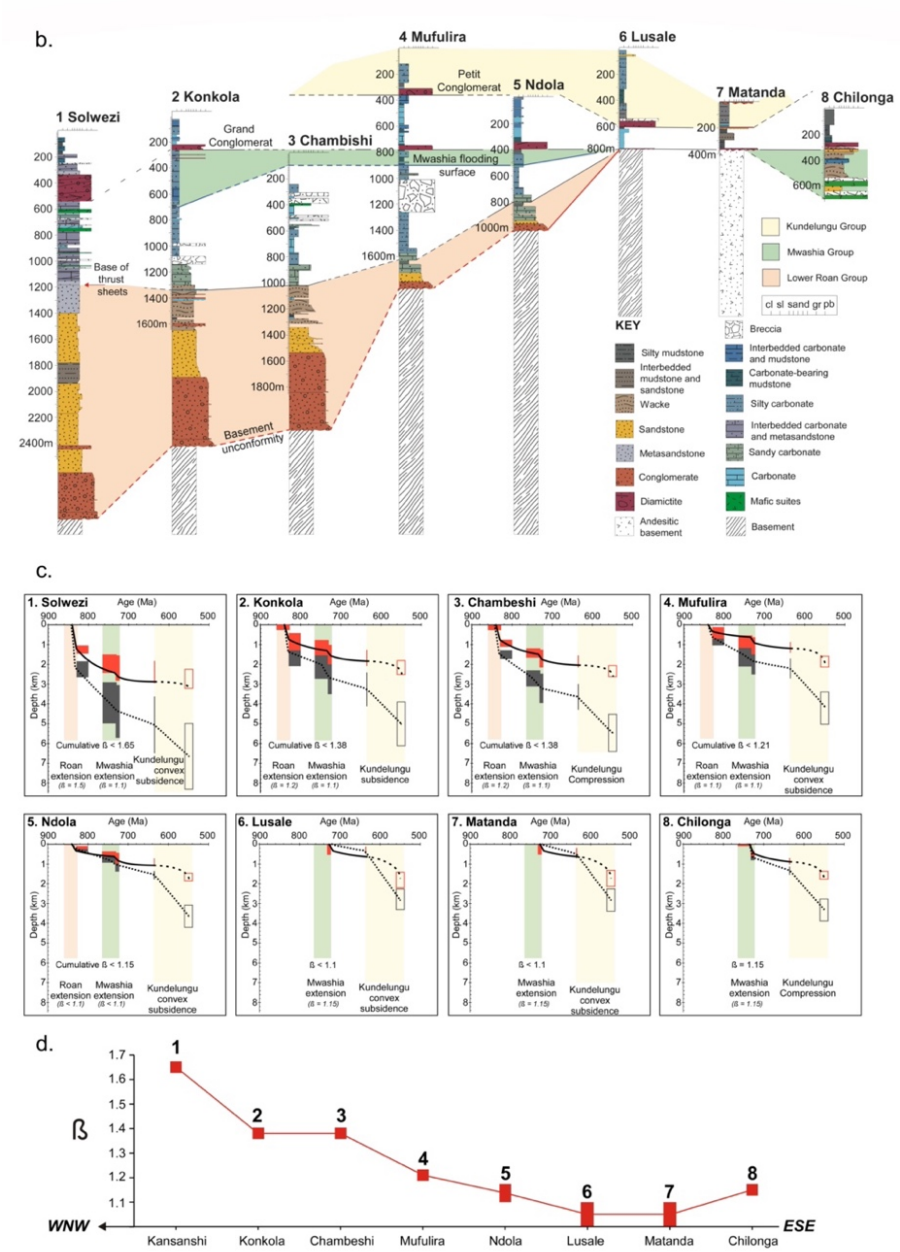

Figure 5 Analysis of the Katangan basin formation

5a A map showing the locations of the eight 'type logs' that have been used to determine the nature of basin subsidence and its distribution. The locations were chosen by the availability of deep, diamond drill cores, that were then integrated with adjacent data within a 1km radius to construct a local 'type log'.

5b The eight type logs constructed for the basin subsidence analysis.

5c The subsidence profiles of the eight type logs show the total subsidence profile (lower line) and the tectonic subsidence component (upper line). Error bars are included. The yellow and green columns highlight the Roan and Mwashia rifting event respectively.

5d. The chart shows the distribution of the calculated extension factor for the eight locations. It demonstrates the increase in cumulate extension from the eastern margin of the basin to the Central Rift Zone where cumulative lithospherical extension has exceeded 70%. The data also shows that the NE margin of the Bangweulu craton has experienced Mwashia extension.

The eight type cores show a clear increase in total subsidence from low in the east (Chilonga and Matanda) to high in the west (Konkola and Solwezi,) (Figure 5b & 5c). Cores with the thickest Lower Roan section in the west have the most pronounced concave-up subsidence signature during Roan extension. Initial subsidence during Roan extension was highest in the furthest west core from Solwezi, with the basin likely developing a syn-rift section greater than 2 km thick during the Lower Roan. Where Lower Roan clastic units are thinnest (< 100 m) near Ndola the Roan tectonic subsidence signature is most poorly developed, with minimal Lower Roan extension. The Konkola and Chambishi type logs show an intermediate Roan subsidence profile, falling between that of the Domes region and east of the Kafue Anticlines, with the basin subsiding to a depth of up to 1.5 km during the Lower Roan.

Best-fit β-factors match this trend in the associated tectonic subsidence profiles, with the degree of crustal stretching increasing to the WNW from Ndola to Solwezi. The Solwezi Region shows the highest degrees of Roan extension, 40% (a β-factor of 1.4), whereas in Lubambe this is reduced to 20% (a β-factor of 1.2). Around Ndola, the tectonic subsidence during Roan extension is small with a β-factor of a maximum of 1.1.

Mwashia extension is evident in all eight cores, but is generally less pronounced, more uncertain, largely due to the limitations of facies analysis in deep water successions and differently distributed. The tectonic subsidence recorded is generally of a lower magnitude than during Roan extension and has a smaller range. In Solwezi and Lubambe a β-factor of 1.1 fits the tectonic subsidence profile during Mwashia extension. It may have been significantly higher in Solwezi,

393 however the nappe emplacement prevents an appreciation of the full Mwashia section making the
394 outcome a minimum. In Ndola, the Mwashia extension is recorded in the core, but the magnitude
395 of extension is <10% suggesting crustal stretching during Mwashia and Nguba times was again
396 small in the SE Kafue anticline. In contrast the western basin borders in the DRC (Kennedy et al.
397 2019) and northeastern border in Zambia have thicker Mwashia sections and appear to show much
398 greater Mwashia age extension (e.g. at ~15% in Chilonga, Figures 5)
399
400 **3.1.3 Katangan basin formation**
401 Despite the limitations of the uniform extension model and 1-D Airy back-stripping, and water
402 depth estimations from facies analysis, the form of tectonic subsidence profiles and best-fit β-
403 factors provide satisfactory first-order results with significant implications. The concave-up
404 tectonic subsidence signatures of the back-stripped cores and their good agreement with
405 McKenzie's (1978) uniform extension model support and quantify a rift origin for the Katangan
406 Basin in Zambia. Lower Roan β-factors of 1.4 and 1.2 for Solwezi and Lubambe, respectively,
407 match those of other known rift systems, such as the North Sea, Baikal rift and Oslo Graben
408 (Barton and Wood 1984 & Huismans et al. 2001).
409
410 The increasing magnitude of tectonic subsidence and crustal stretching from the eastern margin of
411 the basin towards the CRZ is clear. Lusale, Matanda and Mpika are little affected by Roan
412 extension, with a Roan tectonic subsidence signature characteristic of distal extensional tectonic
413 regimes (Xie and Heller, 2009). Stepping into the basin, Ndola, Chambeshi, Konkola and Solwezi
414 show increasing and high degrees of extension. Solwezi being towards the deepest part of the

basin, with the full thickness of Solwezi syn-rift Roan stratigraphy approaching 2km and the whole rift prior to basin inversion likely to have exceeded 8-10 km.

Mwashia age extension appears to be generally less than in the Lower Roan and the resultant stretching estimates are more uncertain due to the deep-water facies dominating the lithostratigraphy. Although extensively present, the distribution of Mwashia stretching also appears to be different from the Lower Roan, with the greatest extension being focused on the northwestern flanks of the basin in the DRC (Kennedy et al) and the northeastern flanks of the basin in Zambia. This is evidenced by the fact that the magnitude of tectonic subsidence in IT26 during Mwashia extension is comparable to that during Roan extension. However, an alternative explanation is that the basin became partially starved during the Mwashia extension and there was no immediate stratigraphic response recorded to stretching. What is recorded however, is a strong volcanic and basic intrusion association with Mwashia age rifting. This is arguably best developed along the northwestern boundary of the basin in the Lwawu area of Zambia, within the Nzilo basin of the DRC and along the eastern margin of the Kibaran Arch (Kampunzu et al 1991 & 2000). An equivalent Mwashia volcanic and gabbroic suite is indicated in the east of the basin where mafic rocks are found in the Chilonga and Serenje areas (Figure 3 & 5a). In addition, extensive volcanic and basic igneous intrusions occur throughout the CRZ during this period.

Finally, the analysis also indicates that the stratigraphic sections of the Upper Roan and the Nguba, that developed between the rift phases represent post-rift periods of continued subsidence due to the thermal relaxation of the previously stretched and thinned continental lithosphere (Figure 5c & 5d). In addition, the significant extension trend implied by the Solwezi result raises the question of whether the Katangan extension resulted in lithospheric break up and part or extensive

formation of an ocean basin. Deformation and the degree of metamorphism to the southwest of Solwezi precludes further rift analysis via the subsidence analysis and back-stripping technique. The extensional gradient of the rifting reaching 60% extension along the Central Rift Zone (CRZ) at Solwezi and to the south of it, and the extensive basic igneous with the Mwashia rifting event, suggest there may have been a zone of failure of the lithosphere during Mwashia time to the southwest of the Solwezi area. If the lithosphere was broken it appears it was likely a small seaway and a local feature, not extending greatly to the east. Further to the SW the extension is unconstrained due to Quaternary cover. This same CRZ was later the location of the basins greatest deformational strain, displacements and metamorphism which will be discussed later in the paper.

The cumulative extension of both the Lower Roan and Mwashia rifting events outlined above resulted in a wide and deep area of rift basins and a subsequent thermal subsidence basin created a large Neoproterozoic epicontinental sea. . With cumulative extension of up to and beyond 70% in the Solwezi area and extensive coeval mafic magmatism of Large Igneous Province proportions, the formation of a deep and wide rift basin, south of Solwezi and east of Kabompo/Mwombezhi seems likely. The scale of this basin is difficult to judge but sediment provenance patterns and subsequent compressional tectonics will discuss this issue further.

3.1.4 Katangan rift basin geometry

Supporting the quantitative extension analysis presented above are two significant datasets acquired in the Zambian Copperbelt over the last decade. Firstly, the drilling of the 2.5 km deep KRX082 cored hole at Kansanshi mine and secondly, the acquisition of a 34 km seismic reflection line near Konkola. These both demonstrate the basement rifting, its structural geometry, and scale

463 to a degree not previously available. We will briefly discuss each of these datasets, their
464 interpretation and their implication for rift formation and subsequent deformation.

465

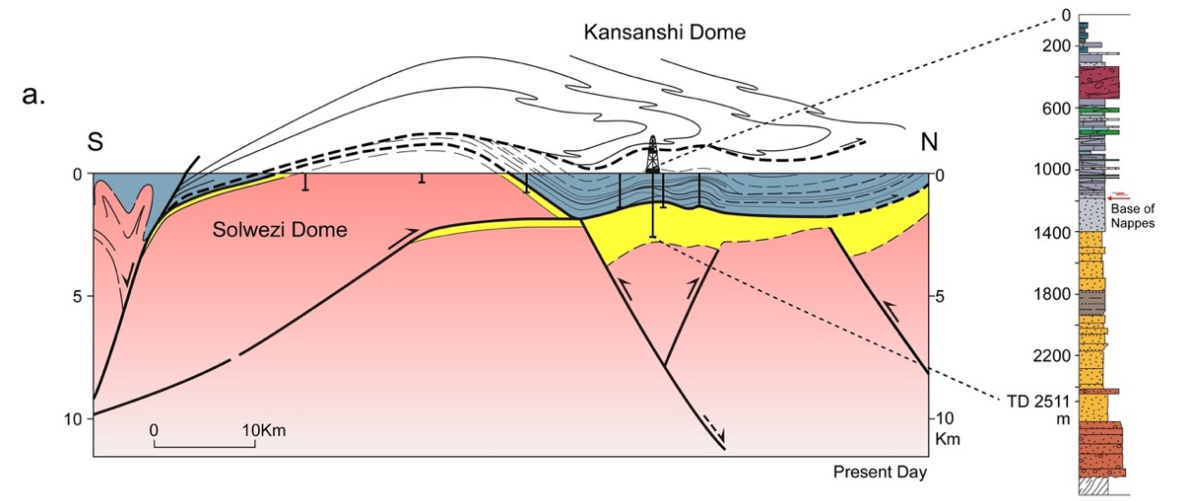

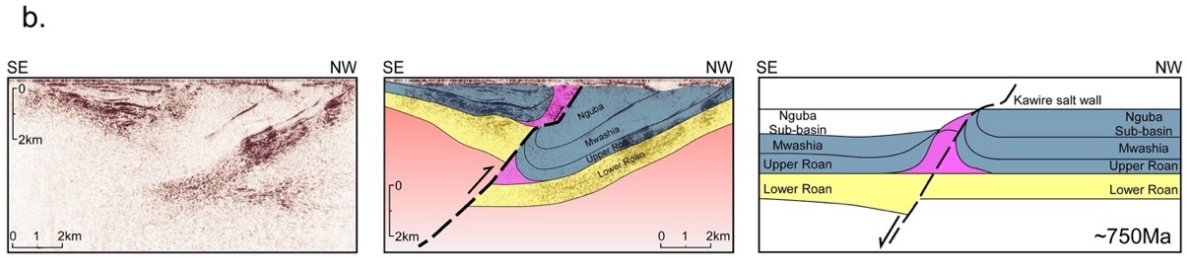

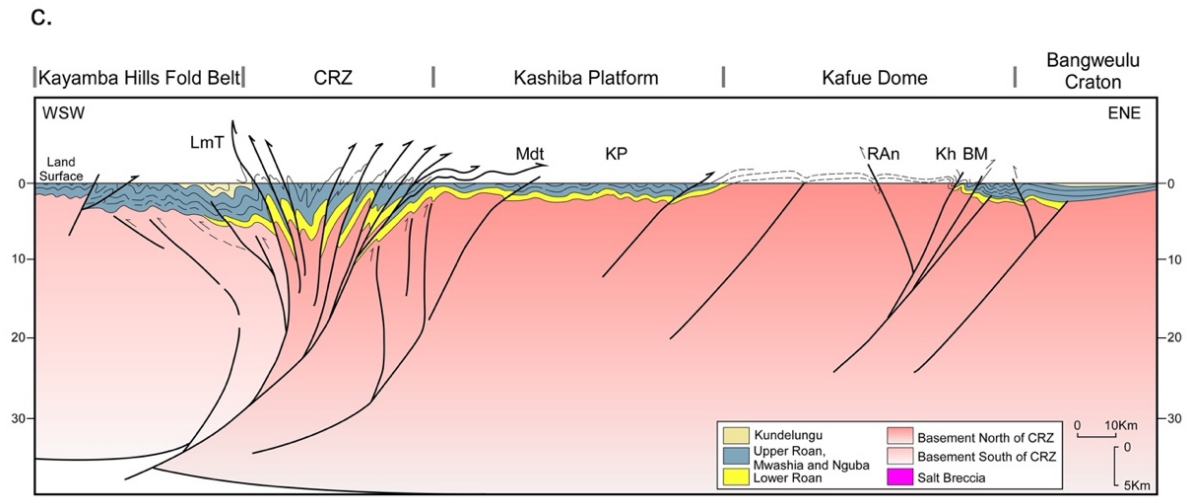

466
467

Figure 6 Extensional rift geometries in the Zambian Copperbelt.

(a) A core and field constrained section across the Solwezi basement dome (locate on figure 12 (section A). Showing the Solwezi half graben containing a proven minimum of 1400 m of clastic Lower Roan rock and an estimated 2000m based on regional stratigraphy. This undeformed section is overthrust by the metamorphic Solwezi nappe comprising a thin thrust sheet of recumbently folded Katanga metasediments. The formation of the dome is due to a later, basement cored fault, that elevates the basement to form the Solwezi dome.
(b) A section across the Kawiri fault of the Konkola area based on an interpretation of a pre-stack, depth migrated seismic line and local stratigraphy penetrations (Figure 12 section B). The basement cored fault that elevates the half graben is interpreted as an original extensional fault on the basis of the Lower Roan thickening towards the fault. The magenta wedge i the hanging wall and foot wall of the Kawiri fault is interpreted as a thick breccia zone resulting from salt migration from the Upper Roan, seen today in core and occasionally along the outcrop of the Kawiri fault zone. The quality of the seismic image is degraded over a triangular area below the breccia outcrop.
(c) A field based schematic cross section across the Kafue anticline and CRZ, from the Bangweulu craton margin to the Kayamba Hills (Figure 12 section C)). From the ENE it crosses the largely undeformed section of the Bangweulu craton to the ENE verging monoclinal structures of the margin of the Kafue anticline and the Bwana Mkubwa (BM) and Kaloko Kopie (Kh) areas. This northeast facing monocline is a continuation of the Kawire fault zone of the Konkola area (6b). In the centre of the Kafue anticline is the Roan Antelope (RAn) syncline resulting from a southerly verging reverse fault, and then the regional western dip of the Lower Roan clastics and Roan carbonate platform into the Kashiba platform (KP) area. Deformation of these rocks increases markedly to mylonitic and isoclinally folded marbles to the west where they dip sharply beneath the intensely deformed Luamala pelitic basin of Mwashia and Nguba age rocks seen in core-hole KE-11. This zone is bounded on the western side by the Luamala thrust (Lmt) where Upper Roan carbonates are thrust westwards over Nguba and Kundulungu age stratigraphy (Vajner 1998b). The western fold zone of the Kayambe Hills is moderately folded and has an upright deformation fabric of varying intensity.

A schematic cross section across the Solwezi Dome and through the location of the KRX082 collar (Figure 6a) shows a significant rift basin of half graben character. This interpretation is based on the thickening of the Roan syn-rift clastic section from 200m around the Solwezi dome (Arthur 1974) to a minimum of 1400m (Figure 5b & 6a). The clastic facies at the base of the KRX082 section is not the characteristic conglomeratic section at the base of a typical Lower Roan profile and suggests at least another 100-500m of clastic section is likely. Implying a potential thickness of the order of ~1.5-2 km of Lower Roan syn rift sediments. Also shown schematically in the profile is the allochthonous section of high-grade, garnet amphibolite rocks. These high-grade metamorphic rocks are interpreted as being derived from a basin to the south of the Solwezi dome and emplaced over the dome's basement as large nappe structures. These structures were later

elevated by a thick-skinned basement thrust that creates the present Solwezi Dome (Figure 6a). A partial and total restoration of the section shows these rocks coming from a larger basin to the south. A feature coherent with the quantitative subsidence analysis results of highly extended crust and a deep basin to the south.

Similar to the core and outcrop-based rift interpretation of Solwezi, the Konkola post stack depth migrated seismic data reveals a rift basin of half graben geometry (Figure 6b). The NNW-SSE profile across the Kawiri sub-basin (Figure 6b) shows a basement rooted thrust fault elevating a Lower Roan half graben along the northern flank of the Kafue Anticline. The structural setting of the half graben, in the hangingwall of the Kawiri reverse fault with the Roan section interpreted as thickening into the fault, indicates that the thrust reactivated an earlier Lower Roan extensional fault dipping to the SSW. The reactivated Kawiri fault continues to the SE and joins the Kafue fault zone that elevates the basement to form the Kafue Anticline as interpreted by Coward & Daly (1984). To the north the Katangan section is shown elevated by a blind basement thrust that also elevates and forms the exposed Konkola Dome to the NW. The rift basin interpretations from Solwezi and Konkola, are both data driven examples of rift basin geometry and stratigraphic change in the Katangan Basin. They complement the results of the quantitative crustal extension analysis by showing the structures resulting from the crustal extension. Both examples also exhibit the later impact of basement involved thrust tectonics and rift basin inversion.

These same structural themes occur to the southeast of Solwezi and Konkola and are shown in the schematic cross section of figure 6c. The section runs from east to west, from the margin of the Bangweulu craton to the edge of the Hook Granite Batholith and is also discussed in Section 4.1. The section shows the rift margin of the eastern flank of the Kafue Anticline inverted along the

east facing Kafue fault zone, the Kafue Anticline and the Kabisha platform of deformed Upper Roan carbonates (Gignoux, 2000) (Figure 6c). To the west this elevated section dips abruptly into the intensely deformed and tightly folded but poorly exposed rift basin of the CRZ comprising a thick, highly deformed section of phyllites whose protoliths are interpreted as Upper Roan and Mwashia in age (Vajner 1998). The western margin of this CRZ is marked by the Luamala Thrust (Vajner 1998) that emplaces the thick rift sequence westwards towards the Kayamba Hills fold belt that includes much younger stratigraphy (Figure 6c). This inverted rift interpretation is compatible with the well exposed sections from each margin. The Kabisha Carbonate platform displays the regionally present, intense, bedding parallel deformation fabric and localised isoclinal folding of bedding. This early fabric is folded by NW/SE trending open fold structures. Given this compelling evidence of Tonian rift basin formation, and later intense inversion of the CRZ, we now outline our chronostratigraphic interpretation of the basin and how that supports the rift model and shows the basin development through time.

3.2 Basin Chronostratigraphic summary

The two Tonian rifting events, and their subsequent periods of thermal subsidence generated and accommodated the Katangan Supergroup. The subsequent, and genetically poorly defined Kundulungu Group does not appear to have a rift origin. Its subsidence profile (Figure 5c) is interpreted here as a result of marginal load driven subsidence. The stratigraphic impact of these subsidence events is shown in the tectono-stratigraphic chart of figure 7 highlighting the major stratigraphic and structural features that have resulted from the formation of the basin. The section is drawn broadly west to east and is based on data from fieldwork and a series of publicly available well logs. The profile lies to the north of the Central Rift Basin (CRZ) where the constraints on

553 stratigraphic age and distribution are best available. Within the CRZ the degree of deformation
554 and metamorphism also make stratigraphic correlation extremely difficult and uncertain.
555

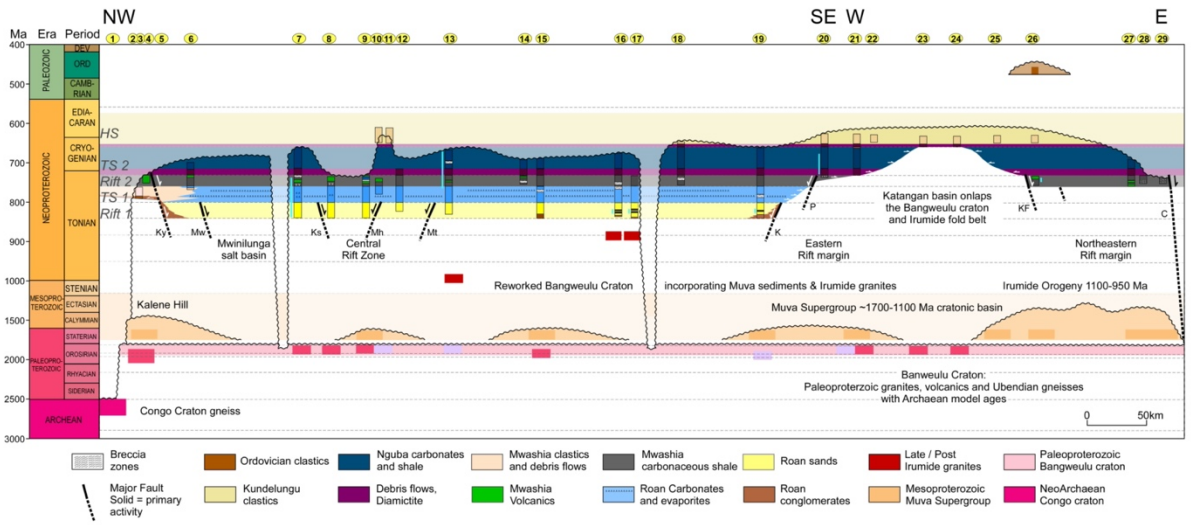

556
557
558 **Figure 7. Katangan basin chronostratigraphy.** A chronostratigraphic profile from west to east that shows
559 the basic form of the Katangan basin: the Congo craton; the narrow Mwashia rift in the west; the northern
560 rift basin with its eastern margin onlapping the Bangweulu craton; the Mwashia aged rift on the eastern side
561 of the Bangweulu craton.
562 Section 'fence post' localities: 1. Jimbe Bridge; 2.Kalene Hill; 3. Luawu Mission; 4. Sakeji River; 5. Nzilo
563 basin; 6. Mwinilunga; 7. Kabompo Dome; 8. Kisasa; 9. Mwombezhi Dome; 10. Matebo; 11. Kapiji Village;
564 12. Matebo; 13.Kansanshi Mine; 14. Kimabwe; 15. Luswishi; 16. Konkola; 17. Nchanga; 18. Mufulira; 19.
565 Mkubwa-Itawa; 20. Lusale; 21. Chief Mtanda; 22. Mombatuta Falls; 23. Milambo; 24. Mafula; 25. Lukulu
566 Falls; 26. Kasanka; 27. Chibwa; 28. Chilonga; 29. Danger Hill.
567

568 Traversing from west to east, the chart shows the pyroxene gneiss of the margin of the Congo
569 craton dated as ~2540-2560 Ma intruded by Paleoproterozoic porphyritic granites dated at ~ 2050
570 Ma (Key et al. 2001). Across the whole profile similar Paleoproterozoic Bangweulu granites and
571 volcanics are the most commonly exposed Katangan basement. In addition, Paleoproterozoic
572 quartz arenites and schists of the Muva Supergroup lay unconformably on the Archaean and the
573 associated Paleoproterozoic granite basement. The Muva quartz arenites and siltstones show no
574 metamorphism or penetrative deformation along the western flank of the Katangan basin and
575 preserve many shallow water sedimentary features such as crossbedding and ripple marks (Key &

Banda 2000). At Kalene Hill these rocks are seen dipping gently (5-15') to the east. They are in turn unconformably overlain by a thin quartz conglomerate of the Katangan Supergroup, thought to represent an Upper Roan age clastic facies, onlapping the basin margin to the west. The Lwawu fault and Kanyama faults appear to be active Mwashia aged due to their coeval relationship with the extensive Lwawu Continental Flood Basalts (CFB) and associated intrusions in the western margin of the basin. Their age is estimated as ~765 Ma by Key et al (2001). The Kanyama fault zone marks the western boundary fault of the major Lower Roan rift event and its connected structure, the Mwinilunga fault zone, marks the western margin of the thick section of the Mwinilunga Salt Basin (MSB). Indications of salt exist up to ~50 km west of Mwinilunga but to a much lesser extent than east of this major structure, as demonstrated in the mapping of Liyunga et al. (2002).

To the east the section touches the Kabompo, Mwombezhi and Solwezi inliers of largely Paleoproterozoic Bangweulu-aged granites with occasional Irumide age granites (Kang Kang et al. 2022) and continues to the Kafue anticline. The eastern margin of the Kafue anticline is defined by the Kafue fault zone which, similar to the Kanyama fault zone, marks the edge of the Lower Roan basin (Figure 7). To the west of this the Katangan stratigraphy appears to progressively onlap the Bangweulu craton. At the most central part of the Bangweulu craton, the Petit Conglomerat and Kundulungu stratigraphy sits unconformably upon the Paleoproterozoic granites of the Bangweulu craton. The extensive, overlying Kundulungu arenites and shales indicate a third subsidence event of different and more regional extent than the earlier Katangan episodes, suggesting a different subsidence process. There is a broad age coincidence with the onset of compressional tectonic regimes to the east and west along the Mozambique and Namibian margins

(Gascombe, 2020) with Kundulungu deposition. These may have instigated mid-continent, thick skinned thrusting and associated basin flexural subsidence. However, there is little evidence to support or deny this proposition. For now, we can be sure that the Bangweulu craton and most of the Katangan basin experienced subsidence and shallow water clastic and carbonate deposition after the Petit Conglomerat (Figure 4). What drove that subsidence remains to be established.

To the east of the central Bangweulu craton the Katangan basin reappears with what is interpreted as Upper Roan sediments and igneous rocks of Mwashia age onlapping from the south and east. Across the NNE trending Kasanka fault the Mwashia section reappears with extensive basic volcanics similar to the Nzilo area of the DRC. This Katanga section terminates abruptly due to uplift along major basement rooted faults of the Chilonga fault zone (Figure 7). The reoccurrence of Mwashia stratigraphy with coeval basalts and volcanics implies a degree of rifting and associated subsidence (Figure 5c). This may indicate the beginning of another large Katangan-connected basin to the east that has subsequently been eroded.

Finally, consideration of the basement rocks along the chronostratigraphic profile (Figure 7), shows the Archaean and Paleoproterozoic basement in the west is overlain by Muva and Katangan Supergroup stratigraphy. Moving eastwards, the Katangan basin basement, north of the CRZ and including the basement domal inliers, is dominantly of Paleoproterozoic Crosinian age (De Waele & Johnson 2007). These observations allow all of the major Zambian and DRC Copperbelt to be underlain by a Paleoproterozoic magmatic complex contiguous with the Paleoproterozoic granite and volcanics of the Bangweulu craton. This postulation is compatible with figure 2 and figure 3 and is further supported in the next section.

3.3 Katangan sedimentary provenance and age

In this section we present the results of 3223 zircon U-Pb analyses from 46 field outcrop samples collected during five field traverses of the Katangan basin and Bangweulu craton. The specific purpose of such a large sample set was to identify, at a regional scale within the Katangan basin, evidence of sediment routing and major changes in it, to understand rift and sub-basin-based compartmentalization within the basin. The work builds on several publications that have used provenance analysis to constrain Katangan basement geochronology and specific aspects of Katangan stratigraphic development. De Waele & Johnson (2007) illuminated the evolution of the regionally relevant Proterozoic igneous and volcanic rocks and Muva sediments of the Bangweulu craton, and more recently (Alessio, B.L. et al. 2019). have used similar analysis to argue for a southeastern extension of the Bangweulu craton and Muva Supergroup. Within the Katangan basin Kampunzo et al (2005) and Masters et al (2005) have used the technique to constrain sediment ages and provenance within specific parts of the DRC.

a.

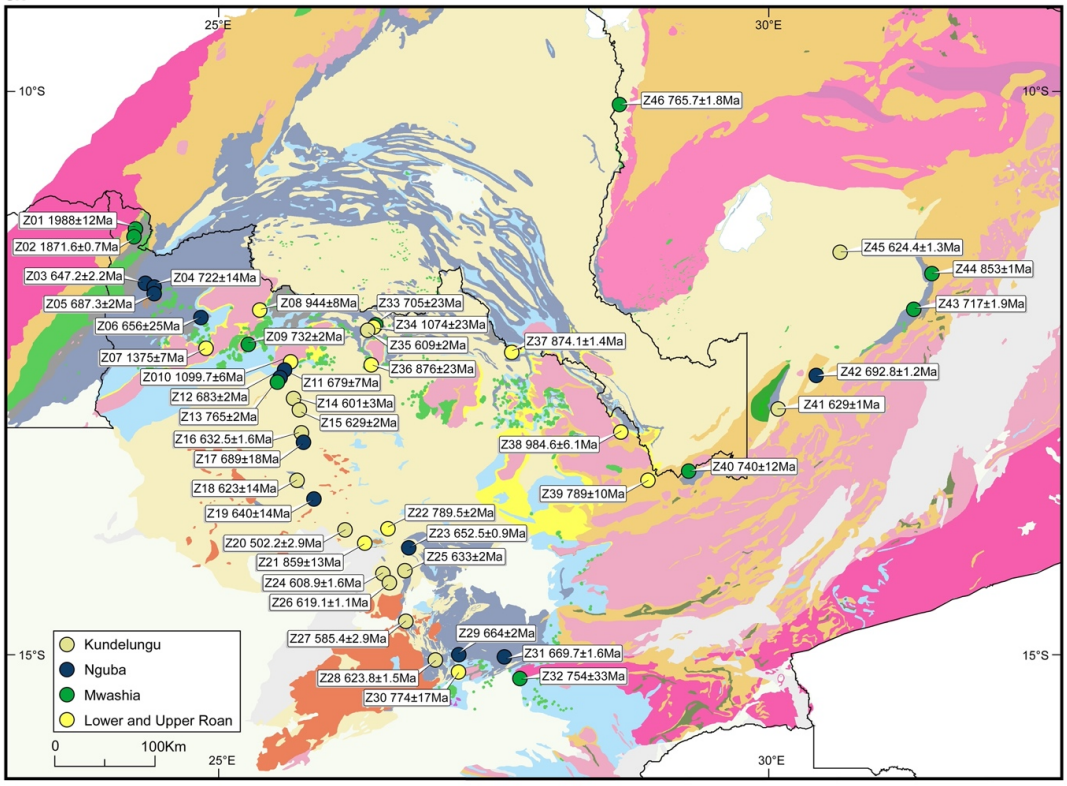

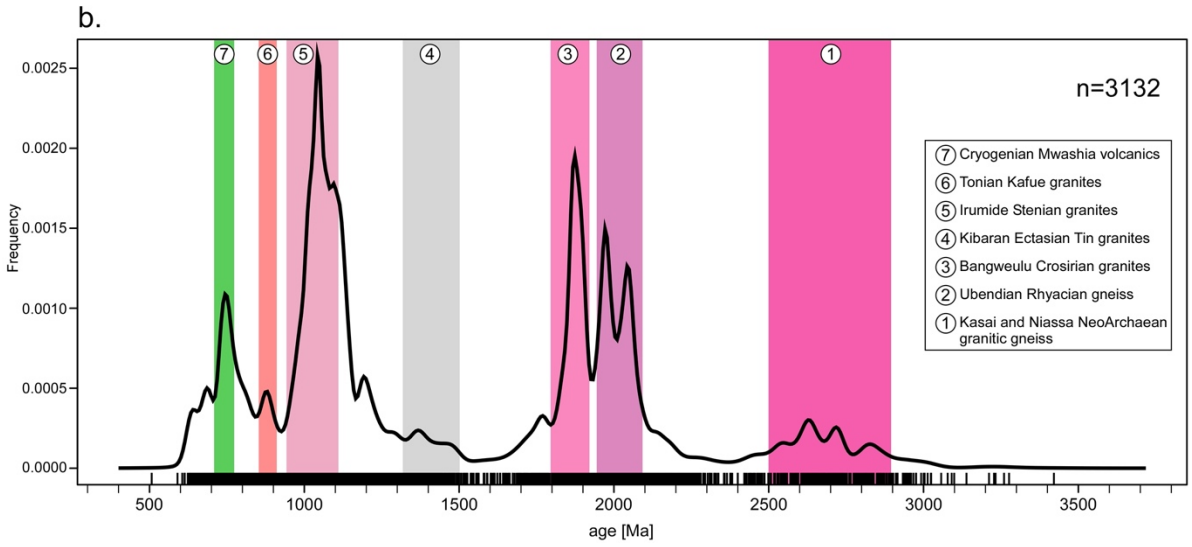

Figure 8.
Detrital U-Pb Zircon maximum ages and age frequency chart of Katangan stratigraphy.
8a. The geological map of the Katangan basin overlain with the U-Pb minimum provenance ages that define a maximum age for the stratigraphic section.
8b. An age - frequency plot from the whole zircon provenance U-Pb age dataset. The plot shows five distinctive age groupings of zircons deposited as a component of the sedimentary fill into the basin. A Neo-archean unit that includes a tail of Meso-archean zircons. These zircons are dominantly found in the west of the basin with one isolated occurrence in the east. A Paleo-proterozoic unit that comprises a broad peak of ages form 1800-2100 Ma with an indication of distinctive contributions of 1800-1900 Ma ages of 1950-2100 Ma ages. These two represent sources from the Ubendian, Rhyacian metamorphic terranes to the north and the 1800-1900 Ma Crosirian, Bangweulu cratonic granites. Thirdly, a small signal of 1300-1500 Ma, Ectasian zircons that appear to be coincident with the Kibaran tin granites of the DRC to the NW. The fourth high-frequency peak is of ~950-1100 Ma derived from the Stenian Irumide, syn and post tectonic granites. The highest frequency peak reflects the granites of the extensive Irumide terrane today exposed as the Muchinga mountain range today. A minor peak follows at 850-900 Ma the before the final, significant peak at 700-800 Ma that indicates a widespread and voluminous mafic igneous event associated with the Mwashia rifting event.

The well-established methodology of preparation, analytical process and isotopic result for each zircon is presented in “Supplemental Data 1: Katangan basin U-Pb Provenance and Age Studies”. The interpretation of the results of the individual outcrop samples is presented and discussed below and supported by figures 8, 9 and 10. The location and the maximum age of source provenance for each of the samples is presented in Table 1.

Sample_ID	Analysis	Sample_type	Coordinate_system	Longitude	Latitude	Lithology	Sample Weights (Kg)	Maximum depositional ages	No. of analysed zircons	No. of zircons used in KDE	Stratigraphy
Z01	Zircon U-Pb provenance age	Outcrop	LL_WGS84	24.2732	-11.2357	Hematitic arkosic metasandstone	3.1	1988±12Ma	30	30	Mwashya
Z02	Zircon U-Pb provenance age	Outcrop	LL_WGS84	24.2582	-11.3015	Arkosic metasandstone	5.715	1871.6±0.7Ma	100	63	Mwashya
Z03	Zircon U-Pb provenance age	Outcrop	LL_WGS84	24.3595	-11.7197	Arkosic metasandstone crosscut by speculraite veinlets	7.725	647.2±2.2Ma	62	37	Nguba
Z04	Zircon U-Pb provenance age	Outcrop	LL_WGS84	24.4426	-11.7527	Metasandstone with metasiltstone interbeds	2.4	722±14Ma	30	22	Nguba
Z05	Zircon U-Pb provenance age	Outcrop	LL_WGS84	24.4403	-11.813	Hematitic arkosic metasandstone	4.245	687.3±2Ma	100	73	Nguba
Z06	Zircon U-Pb provenance age	Outcrop	LL_WGS84	24.8612	-12.0176	Magnitite bearing diamictite	3.5	656±25Ma	80	74	Nguba
Z07	Zircon U-Pb provenance age	Outcrop	LL_WGS84	24.9093	-12.2923	Hematitic meta-quartz arenite	3.5	1375±7	30	29	Lower Roan
Z08	Zircon U-Pb provenance age	Outcrop	LL_WGS84	25.4024	-11.9532	Quartz sericite talc schist	4	944±8Ma	101	82	Lower Roan
Z09	Zircon U-Pb provenance age	Outcrop	LL_WGS84	25.2964	-12.2597	Meta-sandstone channel in carbonaceous phyllite	9.29	732±2Ma	41	23	Mwashya
Z10	Zircon U-Pb provenance age	Outcrop	LL_WGS84	25.68	-12.4059	Hematitic quartz sericite schist with imbricated quartz granules and pebbles	3.7	1099.7±6Ma	105	101	Lower Roan
Z11	Zircon U-Pb provenance age	Outcrop	LL_WGS84	25.6262	-12.4842	Quartz biotite schist	3.6	679±7Ma	40	39	Nguba
Z12	Zircon U-Pb provenance age	Outcrop	LL_WGS84	25.5885	-12.55	Calcareous quartz biotite schist	3.9	683±2Ma	101	60	Nguba
Z13	Zircon U-Pb provenance age	Outcrop	LL_WGS84	25.5576	-12.5832	Porphyroblastic phyllite, biotite porphyroblasts	3.8	765±2Ma	73	12	Mwashya
Z14	Zircon U-Pb provenance age	Outcrop	LL_WGS84	25.7054	-12.7303	Hematitic calcareous meta-arenite	3.8	601±3Ma	84	8	Kundelungu
Z15	Zircon U-Pb provenance age	Outcrop	LL_WGS84	25.7542	-12.8276	Meta-quartz arenite	3.8	629±2Ma	104	89	Kundelungu
Z16	Zircon U-Pb provenance age	Outcrop	LL_WGS84	25.7791	-13.0318	Arkosic metasandstone	4.24	632.5±1.6Ma	100	43	Kundelungu
Z17	Zircon U-Pb provenance age	Outcrop	LL_WGS84	25.7976	-13.12	Arkosic metasandstone	4.335	689±18Ma	66	60	Nguba
Z18	Zircon U-Pb provenance age	Outcrop	LL_WGS84	25.7396	-13.4572	Arkosic metasandstone	2.575	623±14Ma	67	56	Kundelungu
Z19	Zircon U-Pb provenance age	Outcrop	LL_WGS84	25.8876	-13.6179	Arkosic metasandstone	3.225	640±14Ma	60	45	Nguba
Z20	Zircon U-Pb provenance age	Outcrop	LL_WGS84	26.1703	-13.8877	Meta-sandstone	4.495	502.2±2.9Ma	51	23	Kundelungu
Z21	Zircon U-Pb provenance age	Outcrop	LL_WGS84	26.3581	-14.0083	Hematitic meta-quartz arenite	2.72	859±13Ma	100	77	Lower Roan
Z22	Zircon U-Pb provenance age	Outcrop	LL_WGS84	26.5684	-13.8834	Hematitic meta arenite	4.5	789.5±2Ma	110	108	Lower Roan
Z23	Zircon U-Pb provenance age	Outcrop	LL_WGS84	26.7501	-14.0463	Hematitic meta-quartz arenite	6.5	652.5±0.9Ma	111	108	Nguba
Z24	Zircon U-Pb provenance age	Outcrop	LL_WGS84	26.5221	-14.2749	Sub-arkosic metasandstone with hematite veinlets	3.51	608.9±1.6Ma	102	91	Kundelungu
Z25	Zircon U-Pb provenance age	Outcrop	LL_WGS84	26.7145	-14.2512	Hematitic meta-arenite crosscut by hemtite veinlets	2.9	633±2Ma	110	108	Kundelungu
Z26	Zircon U-Pb provenance age	Outcrop	LL_WGS84	26.5822	-14.3553	Meta-quartz arenite	8	619.1±1.1Ma	111	111	Kundelungu
Z27	Zircon U-Pb provenance age	Outcrop	LL_WGS84	26.7234	-14.6981	Sub-arkosic metasandstone crosscut by hematite veinlets	2.245	585.4±2.9Ma	100	91	Kundelungu
Z28	Zircon U-Pb provenance age	Outcrop	LL_WGS84	26.9913	-15.0392	Sericitic metasandstone	3.79	623.8±1.5Ma	100	83	Kundelungu
Z29	Zircon U-Pb provenance age	Outcrop	LL_WGS84	27.2128	-14.9964	Meta-quartz arenite interbedded with phyllite	4.25	664±2Ma	101	91	Nguba
Z30	Zircon U-Pb provenance age	Outcrop	LL_WGS84	27.2055	-15.1477	Quartz muscovite schistose conglomerate	4.365	774±17Ma	100	92	Lower Roan
Z31	Zircon U-Pb provenance age	Outcrop	LL_WGS84	27.628	-15.0167	Hematitic metasandstone interbedded with siltstone	3.31	699.7±1.6Ma	101	68	Nguba
Z32	Zircon U-Pb provenance age	Outcrop	LL_WGS84	27.7619	-15.202	Quartzite	2.865	754 ± 33Ma	60	34	Mwashya
Z33	Zircon U-Pb provenance age	Drillhole	LL_WGS84	26.451887	-12.083702	Calcareous metasandstone	1.77	705±23Ma	60	59	Mwashya
Z34	Zircon U-Pb provenance age	Drillhole	LL_WGS84	26.43214	-12.106977	Metasandstone	3.25	1074±23Ma	60	58	Lower Roan
Z35	Zircon U-Pb provenance age	Outcrop	LL_WGS84	26.384078	-12.133312	Quart biotite schist	9	609±2Ma	110	105	Kundelungu
Z36	Zircon U-Pb provenance age	Outcrop	LL_WGS84	26.412798	-12.433678	Meta-quartz arenite	2.945	876±23Ma	61	55	Lower Roan
Z37	Zircon U-Pb provenance age	Outcrop	LL_WGS84	27.692903	-12.325506	Arkosic metasandstone	5.75	874.1±1.4Ma	100	72	Lower Roan
Z38	Zircon U-Pb provenance age	Outcrop	LL_WGS84	28.6869	-13.0292	Metasandstone	3.915	984.6±6.1Ma	101	89	Lower Roan
Z39	Zircon U-Pb provenance age	Outcrop	LL_WGS84	28.9298	-13.4531	Arkosic metasandstone	5.075	789±10Ma	100	99	Lower Roan
Z40	Zircon U-Pb provenance age	Outcrop	LL_WGS84	29.3021	-13.3767	Cobble meta-conglomerate	5.64	740±12Ma	100	92	Mwashya
Z41	Zircon U-Pb provenance age	Outcrop	LL_WGS84	30.1103	-12.8265	Sericitic metasiltstone	3.825	629±1Ma	100	80	Kundelungu
Z42	Zircon U-Pb provenance age	Outcrop	LL_WGS84	30.4611	-12.5245	Meta-quartz arenite	3	692.8±1.2Ma	111	100	Nguba
Z43	Zircon U-Pb provenance age	Drillhole	LL_WGS84	31.348314	-11.947366	Metasandstone	3.5	717±1.9Ma	105	98	Mwashya
Z44	Zircon U-Pb provenance age	Outcrop	LL_WGS84	31.5152	-11.631	Conglomerate	2	853±1Ma	102	74	Mwashya
Z45	Zircon U-Pb provenance age	Outcrop	LL_WGS84	30.6793	-11.4406	Arkosic metasandstone	4.165	624.4±1.3Ma	101	45	Kundelungu
Z46	Zircon U-Pb provenance age	Outcrop	LL_WGS84	28.674	-10.1416	Metasandstone	4.665	765.7±1.8Ma	100	75	Mwashya

Table 1 The provenance dataset identifying the 46 sample location**,** rock types and stratigraphy with the maximum depositional age noted. The number of analysed zircons, and the number used to define the KDE charts are also specified. This data summary is expanded on in the supplementary data set available as S2.

3.3.1 Detrital zircons: U-Pb Sediment Provenance and Maximum Age Data

Zircon age results and their interpretation are discussed with a focus on sediment maximum age and provenance to examine the sedimentary routing into the basin. Sediment provenance and routing can identify the major tectonic boundaries causing basin segmentation. In addition, Table 1 highlights the minimum age of the sample's zircon population and is therefore a constraint on the maximum depositional age of the rock sampled and a test of the stratigraphic grouping. The data sampling roughly followed two profiles across the basin, one NW/SE from Jimbe Bridge to Mumbwa and a second along the basement inliers and domes of the Zambian Copperbelt and

northeastwards to Mpika (Figure 8a). The full suite of analytical data is presented in graphic form as Kernel Density Estimate (KDE) charts, one showing the entire dataset in a single chart (Figure 8b) and each sample (Figure 9a). An analytical assessment of the correlation between samples is represented on a multi-dimensional scaling (MDS) chart (Figure 9a & 9b). The MDS chart is then examined for clustering (Figure 10b) and the geographic implications and routing interpretation of the cluster distribution (Figure 10a). The detailed data behind these charts is presented in tabular form in Supplementary file (U-Pb zircon database).

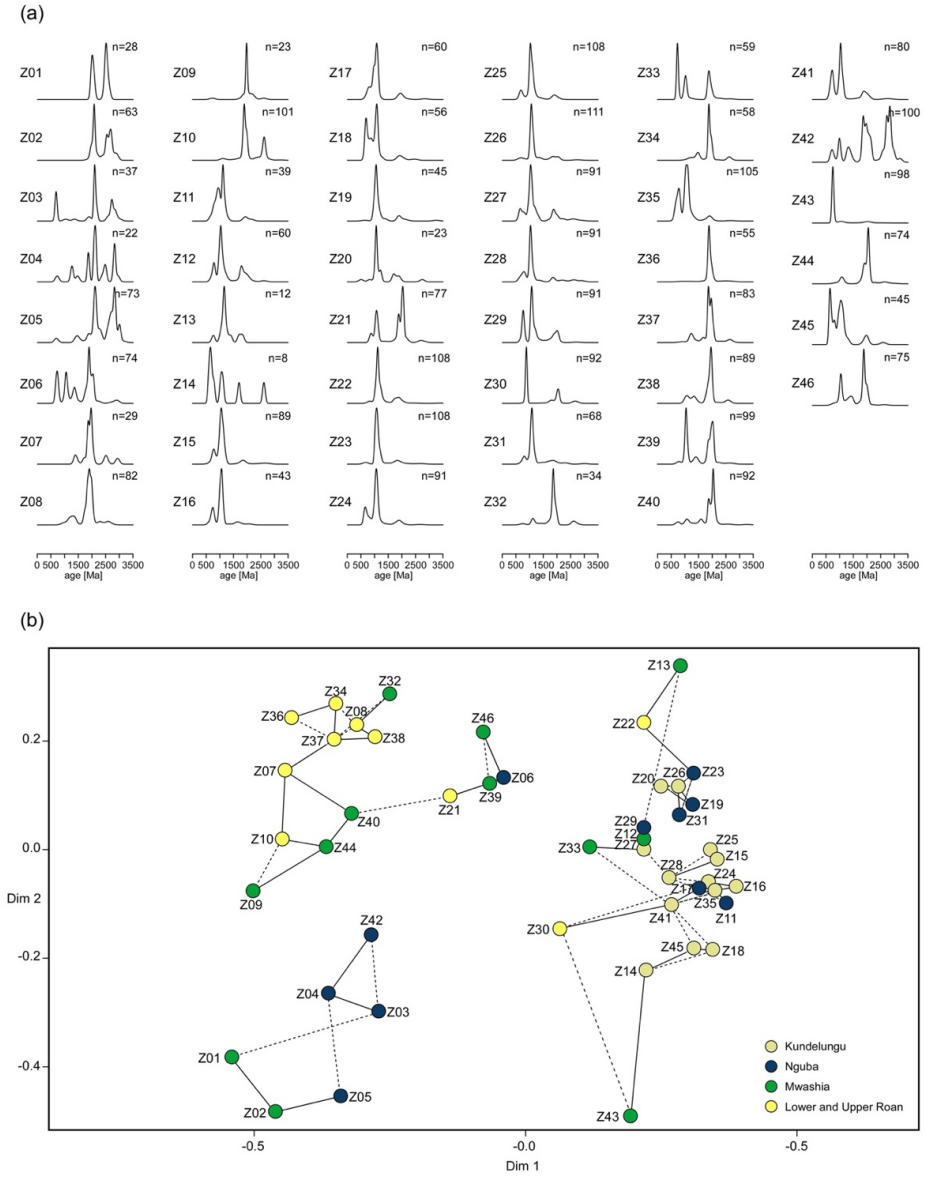

682

683 **Figure 9 Graphical representation of the provenance data.**

684 Figure (9a) shows the kernel density estimates (KDE) of the provenance data, highlighting the frequency
685 distributions of each of the 46 samples. There are visibly different groupings within the charts that
686 potentially indicate different provenance areas and different sediment routing systems.
687 Figure 9b examines the visible differences by the multi-dimensional scaling (MDS) of the zircon age
688 relationships, and divides the samples into three major clusters. Within each grouping, sub-groups are also
689 recognized that may indicate subtly different provenance changes. At the largest scale, three clusters are
690 recognized: MDS1, characterised by frequent Neo-Archean ages that end abruptly between the Kabompo
691 and Mwombezhi domes; MDS2, characterised by dominantly Paleoproterozoic ages of the Bangweulu
692 craton: MDS3 characterised by both frequent Paleoproterozoic and Mesoproterozoic age zircons.
693
694 The MDS chart (Figure 9) shows the stratigraphic unit the individual samples originate from. The
695 KDE data displays as three MDS clusters (Figure 9b) implying potentially three gross provenance
696 relationships. Cluster MSD 1 (Z01-05 & Z042 Figure 10) is characterised by a Neo-Archean and
697 a Siderian zircon population peak and a Paleoproterozoic Orosirian (1800 Ma - 2050 Ma) signature
698 of the Bangweulu craton. Five of these Mwashia and Nguba samples are clustered in the far NW
699 of the basin. The other (Z42) is from a location some 500 km to the east (Figure 9a). Given this
700 large separation, we interpret these Neo-Archean and Paleoproterozoic peaks as being sourced
701 from two distinct Archean sources. The five located in the west from the Congo craton of the Kasai
702 area of the DRC and the one in the east from remnants of the adjacent Niassa or Tanzanian cratons
703 (De Waele et al., 2006). The northwestern sourced zircons define a discrete sub basin at the western
704 margin of the Katangan Basin. The Archean footprint reduces markedly at the Kabompo dome.
705 (Z06 & 07) and ends in the area between the Kabompo and Mwombezi domes. This western area
706 we refer to as the Mwinilunga Salt basin and interpret Archaean sedimentary input extended to the
707 Kabompo/Mwombezi Dome area, but not beyond it.
708
709 The second largest MDS cluster (Figure 9b and 10a & 10b, MDS 2) runs from the
710 Kabompo/Mwombezi Dome area eastwards to Mpika along the Zambian Copperbelt and along
711 the eastern edge of the Katangan basin. The provenance area covers the Northern Rift basin (NRB)

712 to the north of the CRZ (Figure 10). Samples of Roan, Mwashia and Nguba are dominated by KDE
713 spikes in the Paleoproterozoic Crosinian (1800 Ma to 2050 Ma). Subordinate spikes come from
714 Stenian (1000 Ma -1200 Ma) Cryogenian (850-635 Ma) and Tonian (~780-720 Ma) aged sources.
715 This distribution indicates an oldest and dominant sediment source from the Bangweulu craton
716 granite and volcanic rocks. The frequent Stenian spikes reflect the late tectonic granitic magmatism
717 of the Irumide orogeny (Daly, 1986 & De Waele et al., 2006). As the majority of MSD2 samples
718 are from the Lower Roan section, and the dominant underlying Katangan basement is of granites
719 from the Bangweulu Crosinian or Irumide Stenian periods, it may be that these rocks have not
720 travelled far. Rather, they are the erosional products of syn rift highs within the Katangan rift basin
721 and have been locally derived. Alternatively, they may have come from the Bangweulu craton core
722 to the NE where large areas of the Bangweulu craton remained exposed until the beginning of
723 Kundulungu times (Figure 11c). Facies supportive of both interpretations are recorded in the
724 Lower Roan.
725
726 This result implies a primary Bangweulu craton margin and Irumide orogen source for the MDS2
727 samples, with either a proximal rift basin, basement drainage area dominating source provenance,
728 or large fluvial drainage and marginal marine systems from the cratonic center to the NE. The
729 latter implies a large fan of Bangweulu detritus passing southwestwards from the present day
730 Muchinga mountain area to the Kabompo/Mwombezhi area and the eastern edge of the
731 Mwinilunga salt basin. Whilst there is a lack of Lower Roan outcrops to be tested in the far west,
732 Nguba sample Z06 indicates the subdued connection to the Archean rocks to the west. On this
733 basis we interpret the Bangweulu basin drainage system to have been largely separated from the
734 Mwinilunga drainage system from the beginning of deposition.
735

736 The third MDS trend (Figure 9 & 10 MDS 3) largely south of the Central Rift basin. Nguba and
737 Kundulungu clastics are the main zircon source rocks. The dominant characteristic between MDS3
738 samples is the strong Stenian (1000 Ma -1200 Ma) link of 1000 to 1050 Ma, Irumide age, granite
739 sourced zircons in samples Z11 to Z35, with two later samples to the NE in sample Z41 from the
740 Kundulungu Group and sample Z44 from the Mwashia Group. Equally striking is how the
741 dominant Bangweulu craton zircons of the Northern Rift have all but disappeared to be replaced
742 by late tectonic Irumide age zircons. Given that by Kundulungu time the centre of the Bangweulu
743 craton and basin generally (Figure 7) was well buried with little evidence of exposed Bangweulu
744 basement within it, we have to look outside of the basin to the northeast and east for the source of
745 these rocks and an exposed area of the Irumide Belt and its late tectonic granites (Daly 1986 & De
746 Waele et al 2006). These granites are most prevalent in the Muchinga Mountains today and we
747 postulate that this was the source area for MDS3 zircons transported on proximal river and more
748 distal marginal marine systems from the exposure of the Irumide basement rocks, possibly due to
749 the onset of early compressional tectonics (Section 3.1).
750
751 In addition to these three distinct regional provenance and drainage system interpretations, two
752 local data discoveries are relevant regionally (Figure 10a). Firstly, zircon sample Z21 comes from
753 a sub-arkosic arenite overlain by a dolomitic section, exposed in a large upright to south verging
754 fold (Figure 10a). This sample of 108 zircons clusters with MDS 2 and reveals a minimum age of
755 859+/-13 Ma. Although the error bar is large, the data indicates that this sub-arkosic arenite outcrop
756 is a time equivalent of the Lower Roan clastics of the Lower Roan of the Copperbelt. As such it is
757 the southernmost Lower Roan exposure and the only area in the Southern Rift Basin where Lower
758 Roan is recorded to date. The overlying dolomite is potentially an Upper Roan equivalent,

759 implying potentially a full Katangan section is possible in the SRB. Such a full section has not
760 been previously described or unequivocally discovered by drilling, which perhaps explains the
761 under explored nature of this complementary basin to the NRB. Our result argues that further
762 stratigraphic research is required in the SRB with a view to testing the deep stratigraphy and the
763 presence or otherwise of a deep "Mine Series" Cu plays.

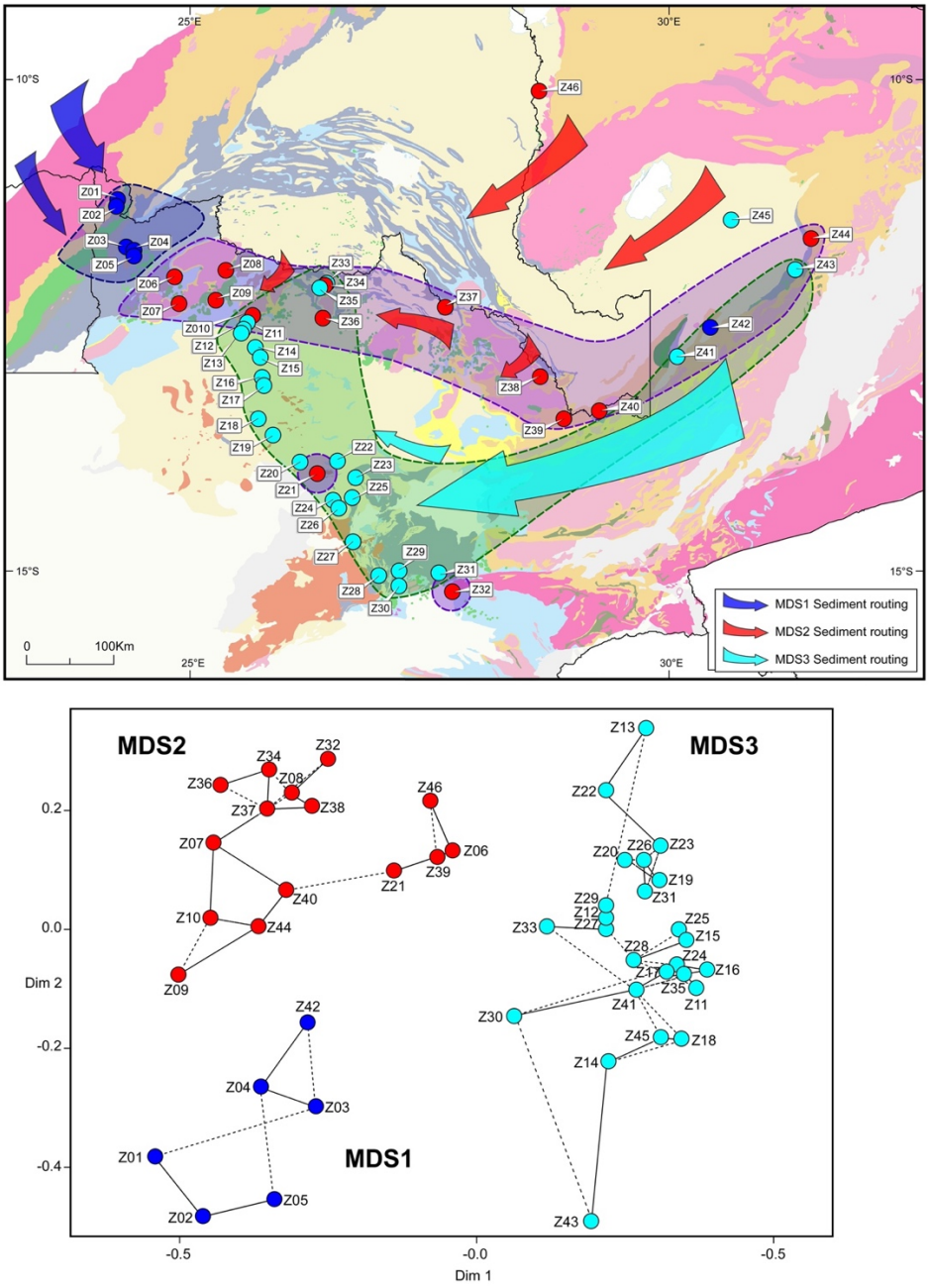

764

765 **Figure 10. Sediment source areas, routing and potential intra basin boundaries**

766 **10a).** The Katangan basin geological map showing the areas of the three MDS clusters marked on the
767 associated MDS chart (Figure 10b).
768 **10b)** The areas show paleogeographically the provenance data-clustering and regional relationships and
769 one pronounced sediment routing boundary. The MDS1 cluster, characterised by frequent Neo-Archean
770 ages ends in Kabompo/Mwombezhi area. This abrupt termination indicates that sediment sourced from the
771 west has not been distributed further east than the Mwombezhi dome area. The MDS2 cluster is dominated
772 by Paleoproterozoic ages of the Bangweulu craton. Finally, MDS3 is characterised by both strong
773 Paleoproterozoic and Mesoproterozoic frequencies during a mature time in the basin's development.
774
775 Secondly, a Mwashia age quartz arenite (sample Z32), located about 10 km south of the MBZ and
776 the southern boundary of the basin, reveals a maximum age of 754+/-33 Ma (Figure 10a). The
777 sample clusters with MDS2 (Figure 10b), suggesting the rock has a provenance compatible with
778 the clastic sediments of the Lower Roan facies, but is younger than the Lower Roan typical of the
779 Katangan basin (Figure 4). The stratigraphic interpretation and its maximum age from zircon
780 provenance analysis, however, suggests the rock represents an extension of the Katangan basin
781 across the MBZ, comprising a similar facies and provenance of younger age. This result will be
782 discussed in Section 3.4 and returned to in the Discussion section.

783

784 **Summary**

785 The above discussion defines three large-scale features of the provenance data: three distinct
786 sediment routing systems and their relationship to the bounding cratons and basement lithologies;
787 a major provenance change across the Kabompo/Mwombezhi area; the possibility of full Katangan
788 stratigraphy in the Southern Rift Basin. For more detailed and precise provenance answers, more
789 locally detailed analyses are required. But for now, this work appears to develop several new
790 stratigraphic and tectonic aspects of the basin.

791

792

3.4 Katangan paleographic development

The integration of field mapping, chronostratigraphic relationships, regional geological maps and the U-Pb zircon provenance data presented above show that the Katangan basin's footprint widened and deepened with time. This growth is indicated by the extensive onlapping stratigraphic relationships described and discussed above (Section 3. Figure 7) and was driven by the multiple basin forming processes and their impact, as discussed in Section 3.1 and figure 5. The subsidence from the Lower Roan rift basins (RF1) (Figure 11a) and associated Upper Roan thermal subsidence results in the drowning of the early rift architecture by an extensive marine carbonate-evaporite system (Figure 11b). This epicontinental environment deepens and widens further with the Mwashia period of extension (RF2) and the association of an extensive igneous event of extrusive and intrusive mafic activity with extension implying intraplate geochemistry (Kampunzu et al. 1990) (Figure 11c). This widespread event is i most obvious in the basin margin sub-basins and along the CRZ (Figure 3, 10c & 12).

The overlying Kundulungu basin in contrast exhibits little to no unequivocal, intra-basinal, rifting activity. It's poorly constrained subsidence profiles are consistent with a convex upward profile that may indicate a load driven flexural basin forming mechanism (Figure 5). The base of the Kundulungu section is the Petit Conglomerat that lies unconformably on the Bangweulu basement on the Mporokoso Arch (Figure 7 locations 23 and 24). The time coincidence of the early ~630 Ma age of the initiation of the Kundulungu stratigraphy (Figure 4), and the regionally extensive Pan African collisions along the eastern margin of Africa is compelling (Goscombe et al 2020). We therefore link the change in subsidence mechanism, from extension and thermal subsidence to crustal loading due to crustal thrust elevation of the marginal areas of the Katangan basin, as a result of distant collisional processes to the east in Tanzania and Mocambique (Goscombe et al.

2020). The consequent subsidence resulted in the fine grained and shallow water clastic and carbonate facies of the Kundulungu Group. This trend culminates ~70 Ma later with the onset of focused north-south closure and deformation of the Katangan basin and the oblique inversion of pre-existing extensional faults (Figure 6) and ultimately the expulsion of the basin fill, localized metamorphism, and emplacement of the allochthonous nappes to the north of the CRZ.

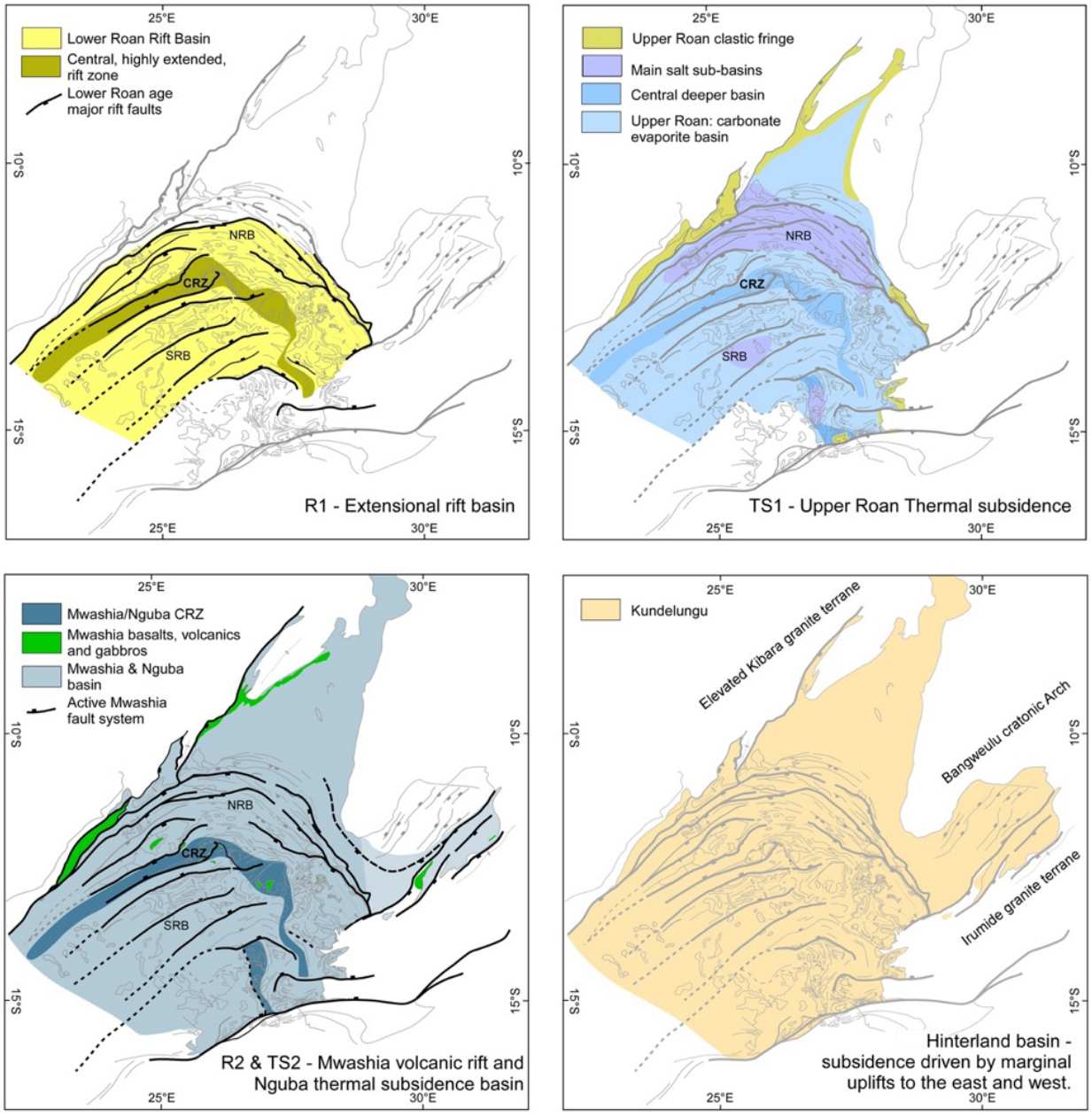

Figure 11 Basin growth through time

Paleo-stratigraphic distribution maps showing the five episodes of Katangan basin formation and the expansion of the basin through time. Note Rift basin 2 and Thermal subsidence 2 are included in a single 11c map. restorations at this time. Abbreviations: NRB Northern rift basin; CRZ Central rift zone, SRB Southern rift basin; R1 and R2 Rift basins; TS Thermal subsidence driven basin.

a). R1 (Rift basin 1) Lower Roan rift basins that developed in the early Tonian, in the period 840-800 Ma. This involved a highly extended Central Rift zone and two broad rifted areas to the north and south.
b) TS1 (Thermal subsidence basin 1) Upper Roan period of passive thermal subsidence that developed large epi-continental carbonate and evaporitic basins to the north and south of a postulated deeper basin resulting from the greater Lower Roan extension 800-745 Ma
c). R2 & TS2 Mwashia-Nguba basin. Oblique, rift basin deepening and widening in the Mwashia period with extensive volcanogenic phases at the basin margins and along the earlier formed Central Rift Zone. This period established in a wide, partly sediment starved basin. It includes the 720-660 Ma Sturtian glaciation event, and the associated complex of debris flows locally known as the Grand Conglomerate. Whole period 745-650 Ma.
d) The Hinterland basin of the Kundulungu Supergroup. Given the extent of the basin, the lack of obvious rifting events and the indication of the subsidence profile being convex, we believe this basin formed due to loading from marginal basement elevations. Such "push down" basins are recognized in Central Asia and the North America today and are generated by distant collisional processes that elevate intra-continental mountains along crustal scale faults.

4. Tectonic Model of the Katangan Basin

4.1 Introduction

Post-dating the active rifting and passive thermal subsidence processes discussed above, two further significant tectonic processes played major roles in the formation of the Katangan basin. Most dominant regionally was the long and incremental process of compressional tectonics, active distally throughout the Ediacaran and more intensely and localized during the Cambrian period (~550 Ma to 500 Ma). This period culminated in widespread rift inversion, fold and thrust related deformation and local metamorphism of the pre-existing extensional rift system. The basin inversion resulted in basement/cover imbrication and recumbent folding and thrusting of basement lithologies with Katangan metasediments along low angle ductile shear zones and thrust faults developed along the relatively narrow, ~50 km wide zone of the CRZ or high strain zone and metamorphic core (Coward & Daly 1984, Cosi et al. 1992) (Figures 6 & 11). The arcuate form of the Katangan basin's structure, described as the Lufilian Arc (Doorninck 1928), is defined by a

series of thick-skinned, basement involved reverse faults, inherited from the Tonian rift basin structure. This reactivation of earlier extensional faults is best recorded in figure 6 and whilst thin skinned, bedding parallel detachments are also evident with large horizontal displacement (Daly et al 1986, Porada and Berhorst 1990 & Kampunzu 1999). In addition, and arguably the more complex, was the long-term movement of Upper Roan age salt in the basin. The understanding of the importance of salt tectonics was first realized by Jackson et al (2002) as a major influence in the detailed structural architecture of the basin. In this paper we focus mostly on the basin scale fault structures as the major fluid pathways within the crust and possibly the lithospheric mantle and include salt activity briefly when directly relevant to an interpretation (eg. Figure 6).

Regarding the arcuate change of structural trends, from NE/SW in Western Zambia, swinging to NW/SE in Central Zambia and the DRC, Garlick (1961) and Unrug (1983) argued that the arcuate shape was the result of major clockwise rotation during the Eo-Cambrian deformation. Unrug (1983) associated the rotation with large scale north vergent thrust sheets in the Kolwezi area of the DRC. Based on detailed mine data from the Nchanga and Chambishi area and regional field data Coward and Daly (1984) and Daly et al. (1984) demonstrated ENE/WSW crustal shortening by basement involved thick skinned thrusts. These basement rooted thrusts verge dominantly ENE along the east of the Kafue Anticline and both ESE and WSW along the western margin of the Anticline. The axial zone between these features has no Lower Roan sediments and basement is locally onlapped directly by Upper Roan carbonates. Porada, (1989) extended the thrust tectonic model to the whole Katangan basin, describing it as a northerly vergent, asymmetric fold and thrust belt and adopting an Alpine asymmetric model for the basin. Cosi et al (1992) increased the thrust tectonic understanding with the recognition of basement cover imbrication in the

Kabompo/Mwombezhi area. Kampunzu & Cailteux (1999) further extrapolated the model in detail to the DRC, interpreting thin skinned detachment folds and thrusts. Porada and Berhorst (2000) further developed their Alpine thrust based deformational model that still prevails today (Selley et al 2006 & Eglinger et al. 2016)

The next major tectonic insight in the basin came with the recognition of widespread salt tectonics in the NW DRC part of the basin. The interpretation of mapped geometry and the extensive breccias as a result of thick, salt related welds associated with extensive salt movement was developed by Jackson et al (2003). Using geometric analogues from modern salt basins, Jackson et al. (2003) interpreted the complex structural geology of the western DRC as product of northerly vergent thrusts and of large volume salt migration. Salt as the tectonic driver of much of the rock deformation in the DRC Katangan basin has been supported by the schematic sections of Selley et al (2018) and detailed structural work of Twigg (2020). The latter showing the link between deep faults and salt perturbation and migration.

Taking a metamorphic perspective on the deformation of the Katangan basin, Johns et al (2004) concluded that a deformation and metamorphic phase of high-pressure amphibolite facies conditions existed in the Domes region of Western Zambia. They attributed it to crustal thickening of the Katangan section resulting in pressure temperature conditions of about 700’C and 10 kbar (Johns et al 2003 & 2004). They interpreted the crustal thickening and pressure as a result of continental collision and subduction at about 530 Ma. Whilst the scale of their estimated PT conditions may have been accentuated by brine conditions (Zimba 2015), nonetheless the petrological evidence for a basin inversion event in the Kabompo, Mwombezi, Solwezi and Luswishi domes area and the western margin of the Kafue anticline around 530 Ma and localized along the previously formed CRZ, is compelling.

To understand these complex and conflicting approaches to the deformation processes of the Katangan basin and ultimately the formation of fluid pathways of the basin, we will take a domain approach to the basin, defining areas of comparable rift, salt and inversion tectonics and their boundaries. The three deformational processes are intricately linked and are discussed as an integrated tectonic model that can be tested as the quantitative geological and geophysical database of the basin grows with time.

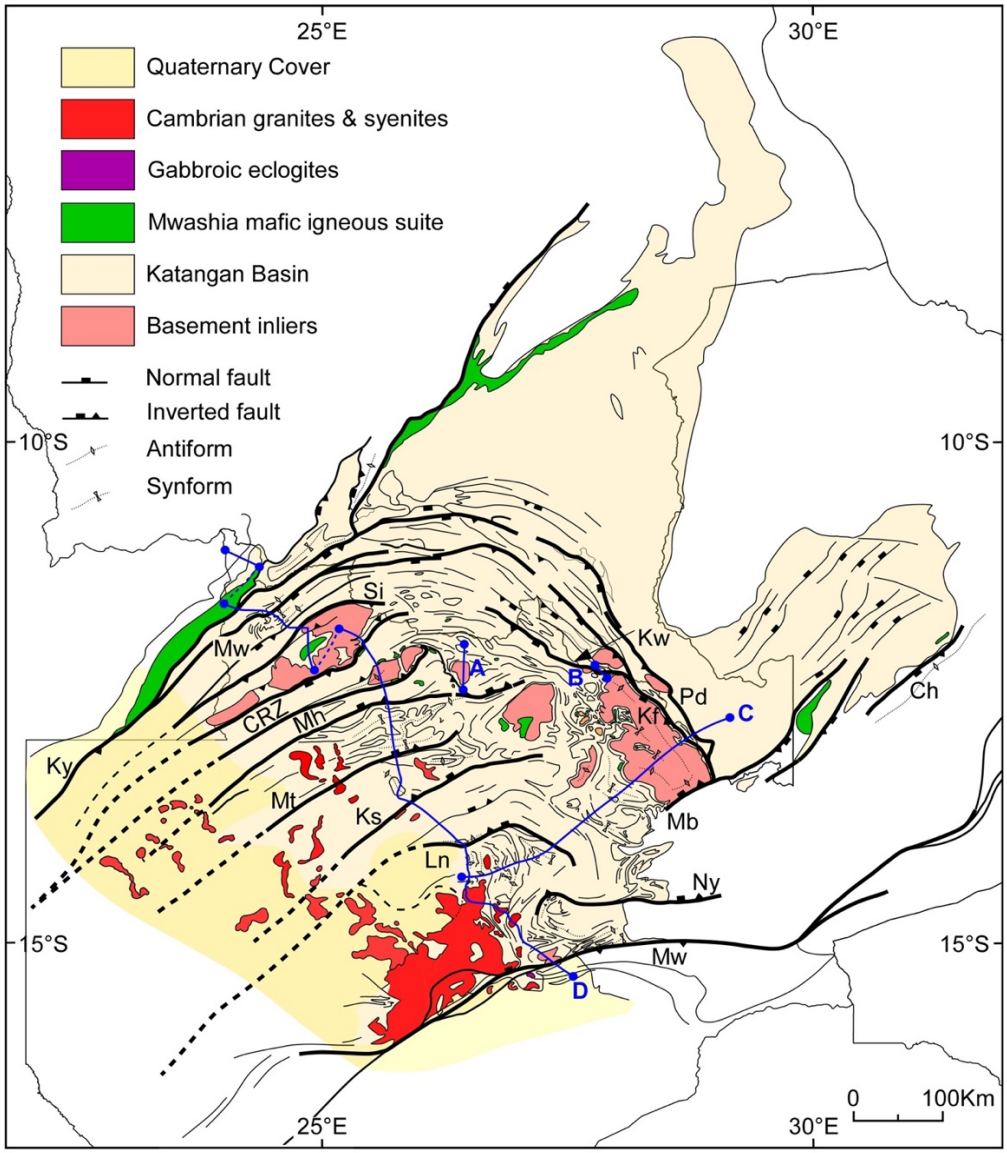

Figure 12. Katangan Basin Structural Map
Structural trend and fault map of the preserved portions of the Katangan basin, built from Geological Survey Department geological (Thieme & Johnson 1981) and field work undertaken during five field regional traverses undertaken between 2016 and 2021. The map highlights the major structures, basement inliers, representative basaltic, gabbroic, and andesitic volcanic units, and syn and post tectonic granite intrusions. Regionally significant fault zones and bedding trends are marked and define the Tectonic Domains discussed in the text. The blue lines A, B, C & D indicate the location of the four cross sections shown in figures 6 and 13.
Initialized are the major fault zones of the basin: Kf Kafue; Ks Kasempa; Kw Kawire; Ky Kanyama; L Lungu; Mb Mubulashi; Mh Maheba; Mt Matebo; Mw Mwinilunga; Mw Mwembeshi; Ny Nyama; Pd Pedicle; Si Sialinga. The Central Rift Zone is labelled CRZ in the west.

4.1 Katangan Basin deformation and the role of the rift basin faults

The regional understanding of the Katangan basin's deformation is highly variable, with great detail available in the mined areas and much less data elsewhere. The regional perspective presented here is portrayed in the structural elements map of figure 12. The map has been built from Geological Survey Department geological and aeromagnetic maps (Thieme & Johnson 1981) and field work undertaken during five field regional traverses undertaken between 2016 and 2021. Figure 12 shows the present-day area of the basin underlain by Katangan stratigraphy together with the major fault zones, structural form-lines, basement inliers and the large volumes of Tonian basic rocks and the Ediacran and Cambrian Hook granites. Structural form lines and associated faults give an impression of the structural style of the basin, it's regional anisotropy and major discontinuities. Many of the major fault zones were formed in the rift phase of the basin and control the later structural form that has resulted in the basins arcuate shape.

The western boundary of the basin is defined by the Katangan sedimentary section onlapping onto Mesoproterozoic Muva stratigraphy (Figure 6) and underlying Paleoproterozoic and Archaean basement (Key et al). Close to this onlapping margin are the Lwawu, Kanyama and Mwinilunga fault zones (Figure 12 & 13), the latter two broadly traceable as fault zones to the NW/SE trending

947 eastern margin of the Kafue Anticline. These features transfer into a series of faults that define the
948 SW boundary zone of the basin (Figure 12). Within the basin a complex series of rift basins are
949 defined, the deepest and most pronounced but also the least understood due to later deformation,
950 occur associated with a series of basement dome inliers.

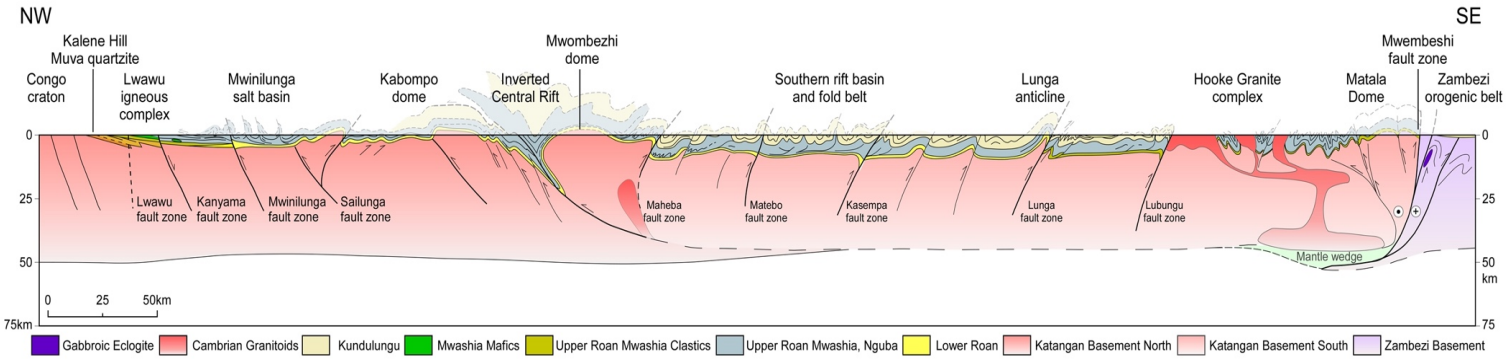

951
952 **Figure 13. Basin cross section.**
953 A geological cross section of the Katanga basin, from Jimbe Bridge in the NW to the Mwembeshi Fault in
954 the SE. The section shows the Katangan sediments onlapping the western basin margin. The Lwawu (Lw),
955 Kanyama (KF) and Mwinilunga (MF) fault zones define the 100 km wide, craton to rift basin transition
956 zone. The Lw fault appears to be the source the extensive Mwashia continental flood basalts (CFB) that
957 occur along the western margin of the basin. The Kanyama fault defines the point of Katangan sediments
958 thickening into the basin and the Mwinilunga fault the edge of the thick salt basin that is the continuation
959 into Zambia of the Kolwezi salt basin to the north (NRB). The ~50 km wide, intense deformation zone of
960 the Kabompo and Mwombezi domes is interpreted as the Central Rift Zone (CRZ), a continental suture
961 zone that marks the boundary between regionally thick >45 km crust to the west and thinner <45 km crust
962 to the east. The folded Southern Rift basin (SRB) are interpreted as a regularly spaced series of inverted,
963 NW dipping extensional faults, with the Lunga fault elevating the only outcrop of Lower Roan arenites in
964 this central area. The Lunga fault also marks the start of the deformed Nguba section of the Kayambe Hills,
965 the western side of which is a slate and phyllite belt north of the Mwembeshi where the Hooke granite
966 cupolas and veins invade the phyllitic Katangan metasediments. The southern basin boundary is marked by
967 the northerly dipping fabrics of the Mwembeshi fault zone and the eclogitic gabbroic intrusions of the
968 Zambezi orogen.
969

970 The primary rift fabric and bounding faults are shown in Figure 13 as a regional, composite
971 geological cross section that offers a vertical dimension to the geological map. There are little data
972 to constrain the section at depths beyond a kilometre. The figure uses CRUST1.0 (Laske et al.
973 2013) to define the moho across the area and on this adds field data across the basin in a NW/SE
974 profile broadly along the profile shown in figure 12. Figures 12 and 13 and their underpinning

975 geology enable the breakdown the Katangan basin into six structural domains (Figure 14) that
976 enable a coherent and comparative discussion of the basin's present structure and tectonic history.
977
978
979 **4.1.1 Domain 1: The Northeastern Katangan basin (NKB)**
980 The Northeastern part of the Katangan basin extends into the areas of the Binda and Kundulungu
981 plateaux of the DRC and the Mporokoso basin and Bangweulu craton of Zambia (Figure 14c).
982 Whilst minor folds and thrusts of the Katangan and Kundulungu stratigraphy are developed within
983 this large region, the sequence is largely characterized by sub-horizontal to gently dipping
984 Kundulungu Supergroup formations and a lack of penetrative deformation, metamorphism or
985 evidence of regional salt movement. Aeromagnetic data imply a strong NE/SW fabric beneath the
986 Kundulungu Group on the Bangweulu craton (Figure 14c), likely reflecting Irumide basement
987 fabrics beneath the Kundulungu cover.
988
989 At the outer edges of this northern extension are a series of Mwashia aged sub-basins that are
990 discussed here as Domain 2. In the middle of the domain a NE trending and SW plunging
991 basement arch, the Mporokoso Arch, occurs within the Bangweulu craton (Figure 14c). To the east
992 the Nguba and basalt bearing Mwashia section reappears towards the Domain 2 basin at the
993 Kasanka and Chilonga Mission areas (Figure 4, 6 & 7 locations 26 & 27) showing a westward
994 onlapping relationship and sedimentary thickening to the east until the section is uplifted, eroded
995 and not seen further east due to elevation of the Muchinga mountains.
996
997 **4.1.2 Domain 2: Mwashia, Basin Margin sub-basins**

The NW and SE margins of the Katangan basin are characterized by a series of fault related sub-basins of dominantly Upper Roan, Mwashia and younger stratigraphy and are the sites of extensive basaltic volcanism and gabbroic intrusions (Kampunzu et al. 1990). Along the SE margin the basins are characterized by a westward onlapping, eastward thickening Katangan section (Figure 6) with extensive basic igneous rocks recorded in the proximity of the Chilonga Mpika (Figure 4 & 7 location 28) and Kasanka (Figure 7 location 26). This section terminates eastwards due to a series of NW facing monoclinal, basement cored folds that define the eastern edge of the basin today (Figure 7 & 13). A series of southeast dipping reverse faults along this margin elevate the Mesoproterozoic Irumide basement. These monoclines are interpreted to be a result of the compressional reactivation of earlier, down to the east, Mwashia age normal faults formed during the Katangan RF2 extension.

On the NW basin margin several comparable Mwashia age basins exist, fault and fold defined and with structural and stratigraphic similarities including extensive volumes of Mwashia basaltic volcanics and gabbroic intrusions. The rifts of this Domain are developed west of the Kanyama fault (Figure 1, 7 & 14). In Zambia, west of the Lwawu fault, Katangan sediments onlap the Proterozoic and Archean basement in the Kalene Mission area. In the DRC the NW margin of the basin Upper Roan and Mwashia stratigraphy onlaps the Mesoproterozic Kibara Mountains. Francois (1987) mapped a similar southeast facing monoclinal relationship with Mwashia correlated rocks overlying basement as discussed for Zambia. The 20-60 degree dips of bedding to the SE indicates significant basement elevation, interpreted as a series of reverse, fault driven monoclinal folds of basement. This complex inverted margin is epitomized by the southern Nzilo

dome area where Mwashia and Nguba aged debris flows are well described against a large basement rooted fault zones (Twite et al 2017).

This basin margin Domain of Mwashia age rift basins (Figure 4 & 14) has extensive basaltic volcanism and intrusions (Figure 12) and no clear evidence of significant volumes of salt. Locally the basins are developed upon coarse clastic sections of potentially Upper Roan and Mwashia age. The associated igneous activity suggests deep rooted basement fault systems were active on both the western and eastern faulted margins. This Domain is also characterized by mild basin inversion and local folds, often driven by elevation of the large, basement cored, monoclinal folds that define the present-day basement – basin cover contact (Figure 12).

4.1.3 Domain 3: Inverted Northern Rift and Salt Basins (NRB)

Domain 3 encompasses a large area of inverted northern rift basins (NRB) and extensive salt tectonics lying to the north of the CRZ. Although representing a contiguous tectonic domain, four subdomains are outlined based on the degree of the basement involved inversion (Figure 14, 3a & 3d) and different degrees of salt activity (Figure 14, 3b &3c). The unifying feature of Domain 3 are the inverted rift basins that has also experienced various styles and degree of salt tectonics locally. We introduce two new observations of salt activity, one interpreted from seismic reflection data in the Konkola area (Figure 6a) and field mapping in Mwinilunga (Figure 15). Otherwise, this brief description leans heavily on the literature of Jackson et al (2002), Selley et al. (2018) and most recently Twigg (2020). Each of the four sub-domains of the northern rift basin is discussed below.

Sub-Domain 3a: The Inverted Northern Rift Basins and Fold Belt

Along the SW margin of the Bangweulu craton lie two long, NW trending, basement rooted fault zones, the Kafue Anticline Fault (KAF) and the Pedicle Fault (PF). These fault zones typify the major structures of the NRB. They are interpreted as basement rooted extensional faults (Figures 6b, 7, 12 & 14) reactivated into reverse and oblique-reverse structures during Ediacaran-Cambrian deformation. The KAF elevates the large and complex Kafue Anticline (Coward and Daly (1986) and links to the Kawira fault (Figure 6) and to the very far west, the Mwinilunga fault (Figure 6b & 14). Outboard of this lies the basement rooted PF that creates the Mokambe dome and can be traced through the DRC to link with the Kanyama Fault Zone (Figure 1 & 14). In the hangingwall of these faults a full Katangan section occurs along the eastern margin of the Kafue anticline with the Lower Roan locally pinching out to the west over the centre of the Kafue anticline and onlapping basement (Garlick 1961). The Roan syn-rift sediments and basin also onlap to the east and terminate east of the of the PF. The Lower and Upper Roan carbonates are not represented at the center of the Bangweulu craton as shown in figure 7.

Coward & Daly (1986) interpreted the Kafue Anticline as the product of the KAF, a SW dipping, NE facing, blind, basement cored thrust fault. To the NW the KAF zone continues for several hundred kilometres and broadly links with the Mwinilunga fault zone (Figure 14). A major play of this fault, the Kawire Fault (Figure 14) defines the NW termination of the Kafue Anticline. This SSW dipping, basement rooted, inverted extensional fault is based on seismic reflection data (Figure 6a) showing it as an integral component of the early Kafue Anticline extensional fault system. The more easterly Pedicle Fault zone (PF) elevates the Mokambe dome, and to the SE links with the KAF that defines the eastern edge of the Kafue anticline, becoming a part of this major system of blind basement rooted faults (Figure 12). Similar inverted extensional fault geometry interpretations can be applied to the Kafue Anticline as a whole, with the frequent reverse

facing folds being a reflection of original antithetic extensional faults formed on the major SW dipping structures.

Sub-Domain 3a continues to the northwest beyond where the Kafue Anticline plunges to the NW and, after the Luina dome, basement inliers no longer appear. These major linear fault systems that define the Zambian Copperbelt continue to the NW for >250 km (Selley et al. 2006 & 2018) and are traceable as continuous, non-cylindrical, surface fold and thrust structures. Two major features stand out in this fold and thrust belt. Firstly, the length of fault zones defined by contiguous individual fault structures, that occur as long, continuous, NW/SE trending fault zones from south of Ndola to Kambove for over 250 km. Linear fault zones of this continuity and scale suggest a deeply penetrating, thick-skinned, basement rooted fault zone penetrating deep into the crust (Cowie & Scholz 1992).

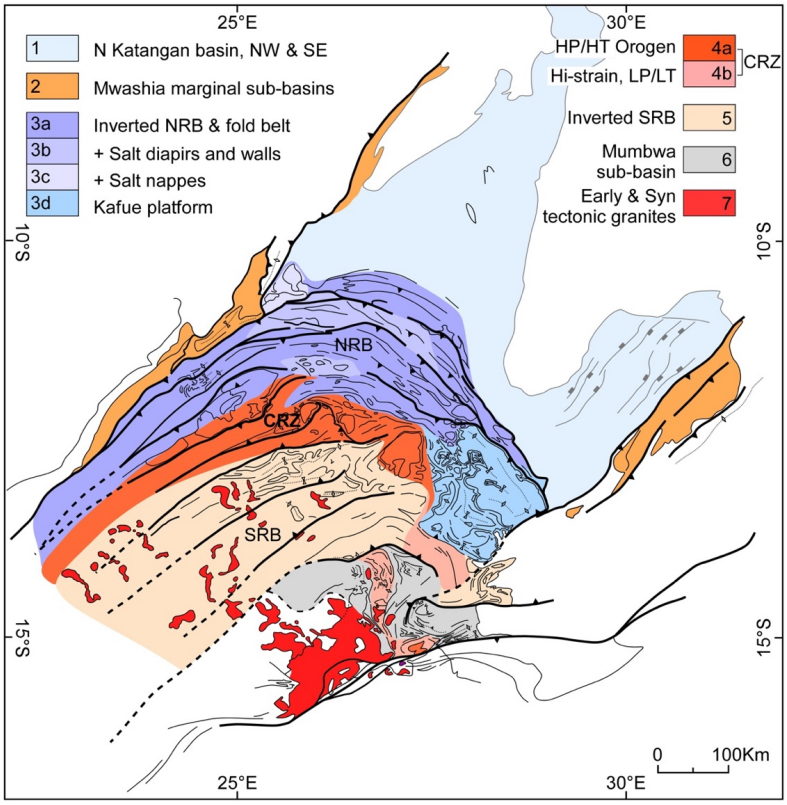

Figure 14 Katangan Basin Tectonic Domains
The tectonic evolution of the Katangan basin is captured as 6 discrete tectonic domains. The domains describe the outcome of a complex and long-lived period of inter-cratonic, Katangan basin formation, rift basin inversion and localized orogenic deformation. The domains of the Northern rift basin (NRB), Southern rift basin (SRB) and Central rift zone (CRZ) are labelled.

The seismic image of the Kawiri fault, north of the Kafue Dome (Figure 6a), shows basement elevated on a pre-existing normal fault. This basic structural model applies to the length of the Kafue fault along the eastern margin of the Kafue Dome. To the NW of Konkola the basement exposures cease and there is little evidence of major basement elevation or involvement. Yet the same long curvilinear fault zones continue to the NW and west and are characterized by extensive and complex structuring. As with the Kawiri interpretation (Figure 6a) we interpret the structures of the DRC as salt related features, localized and triggered by movement on the regionally continuous basement faults of the Kafue/Mwinilunga and Pedicle/Kanyama fault zones (Figure 1, 2, 5c & 10). This interpretation is consistent with the work of Jackson et al (2003), Selley et al (2018) and in more detail, Twigg (2020), who shows clearly the extensional fault triggered and salt driven structural complexity in the vicinity of Kambove.

The continuous anticlinal structures that lie along the surface trace of the Mwinilunga /KAF and KY/PD fault zones for more than two hundred kilometers indicate that the fault zones are crustal in scale. Given the crustal penetration, any significant displacement on these faults would be likely to elevate basement structure, as seen in the domes of Solwezi and Konkola (Figure 5a & 5b). In the DRC the structural complexity of the faults appears to have a different origin. This lack of significant basement elevation can be explained by the pre-existing, rift related basement faults triggering and enhancing salt displacement (Twigg 2020).

Porada & Berhorst (2000) interpreted the DRC fold belt as an extensive thin skinned thrust belt detached above the basement with over 150 km of shortening. Wendorf (2003), arguing that thick breccias are a characteristic of far traveled thrust faults, supported this model on the basis of the extensive breccias being fault related. The lack of evidence of basement involvement in the structures implies the detachment lay above basement for over 300 km. The alternative explanation proposed here, is that the curvilinear, arcuate structural features reflect the pre-existing, basin forming, extensional fault system of the Mw/KAF and KY/PD fault zones (Figure 12). This distinction is clearly a key issue with regard to regional ore genesis, raising the question whether the mines that exist in the sedimentary section are overlying their original, underlying basement fault systems, as in our model, or not, as in the Porada & Berhorst (2020) model of large thin skinned horizontal displacements.

Prior to the thick-skinned thrust tectonics and dome formation, an intense bedding parallel deformation fabric (S1) developed along the western flank of the Kafue Dome (McGowan et al 2003). Coward & Daly (1982) described this S1 deformation fabric as an early bedding parallel fabric resulting from NE directed basement and cover thrusting and detachment of the Katangan section. To the west towards Solwezi and Mwombezhi domes the displacement direction becomes more northerly and northwesterly, with comparable S1 mylonitic fabrics associated with the emplacement of the Solwezi nappe as a thin, high-grade thrust sheet over what is today the Solwezi Dome and Kansanshi mine area (Figure 6a).

Sub-Domain 3b Inverted Northern Rift Basins with Salt Diapirs and Walls

Sub-Domain 3b attempts to cover the parts of the Northern Katangan rift basin where there is widespread evidence that there has been an influence of significant salt mobilisation (Jackson

2002). During the Upper Roan the Katangan basin was a large carbonate/evaporite, epicontinental, marine environment. Today none of the large volumes of mobile salt remains, however, the impacts of it are evident through stratigraphic geometries, structurally displaced rafts of stratigraphy and structural fabrics such as the brecciated welds due to salt diapir, salt wall and salt nappe displacements. On this basis it is likely that salt was deposited everywhere in the Northern Rift Basin Sub-Domian 3b area. Within this large basinal background of the NRB we identify two distinctive styles of salt activity and categorise them as Sub Domain 3b and 3c here: Sub-Domain 3b, characterized by areas of fault related salt diapirs, salt walls and connected salt walls that define sub-basins of Katangan stratigraphy; Sub Domain 3c characterized by areas of large and detached salt fold limbs, canopies and isolated stratigraphic units labelled 'ecaille' in the DRC. Sub-Domain 3d is also considered a likely area of salt deposition but its impact has mostly been removed by erosion resulting in little preservation of post Roan stratigraphy.

Sub-Domain 3b identifies areas within the Domain where multiple diapirs and extensive salt walls have coalesced to from distinct sub-basins. The evolution of the sub-basin formations are difficult to date precisely and are likely diachronous, however, it is also likely that they began to form with or soon after deposition of the evaporite basins of the Upper Roan. These basins were also deformed, potentially enhanced, and also separated completely during the Cambrian deformation. Examples of salt wall and diapir geometries, mapped on the basis of seismic data, current sub-basin structure and surface breccias, are clearly defined in the Konkola (Figure 6b) area of Zambia and along and between the major structures of the DRC Copperbelt, notably in the Kakanda region (Twigg 2020). A similar radial, salt wall convergence is mapped in the Mwinilungu area, and the hanging wall of the Mwinilunga fault zone. The salt wall feature is marked by the three tight radial anticlines, interpreted as three salt walls, converging on a central salt diapir (Figure 15). In the area

to the south of Mwinilunga mapping by Liyunga et al. (2000) describes far more complex fold features that we also interpret as salt related features

Several other sub-basin areas of similar scale to the Kawire and Mwinilinga Sub-Domain basins exist in the Northern Rift basin and are marked in figure 14. Most recently similar features have been described with great detail by Twigg (2002) in the Kakanda area of the DRC. We interpret this wide variation as largely a result of thicker areas of original evaporite deposition, and the presence of an irregular Katangan basement surface, such as a faulted graben that triggers salt instability. Such features were greatly exaggerated during the basin inversion as extensional faults are reactivated as thrusts as shown in the Kawire fault zone (Figure 6a).

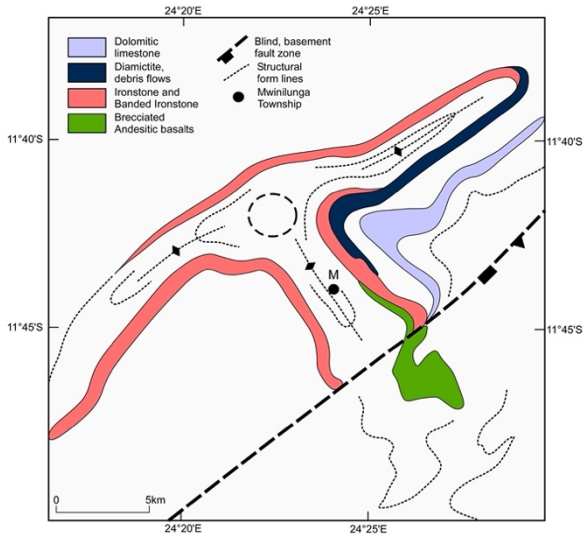

Figure 15. The Mwinilunga salt structure.

Structural sketch map of the Mwinilunga radial fold structure (Modified from Liyunga et al. 2000) The three-way structure is interpreted as radial salt-wall fold features, converging on a central salt diapir. The salt structure interpretation is compatible with further complex folded features to the SE. To the NE it appears that the salt becomes less significant.

Sub-Domain 3c Inverted northern rift basins with salt nappes and welds

The area marked as Sub-Domain 3c in figure 14 is characterized by the development of large, detached blocks of Katangan stratigraphy, up to kilometric dimensions, that are interpreted as having been carried by mobile salt (Jackson 2002 & Selley et al 2018). The interpretation by Jackson et al (2002) indicates a significant amount of stratigraphic shortening in the Katangan

section. They assume that the shortening links to the thrust tectonics of the Domes region of Zambia. Jackson et al (2002) conclude stratigraphic shortening of the order of 80 km. Selley et al (2018), argue for a smaller degree of tectonic shortening in essentially the same area. Suffice to say, movement of salt nappes and tectonics dominate the structures of the Kolwezi area of the basin, is an indicator of thick salt deposition and significant mobility from Upper Roan/Mwashia times onwards. The tectonic detail in terms of geometry and stratigraphic and/or crustal shortening remains to be more precisely defined by subsurface imaging.

Sub-Domain 3d Inverted northern rift basins of minimal preserved salt tectonics

Domain 3d covers the area of the Kafue anticline, it's associated domes, and the extensive Katangan Kabisha platform area to the SW (Figure 3, 6c & 12). Whilst this area has localized indications of salt, most of the surface exposure lies at or below the stratigraphic source of the salt in Upper Roan stratigraphy (Figure 2 & 6). Consequently, little signature remains of salt activity except within synclinal inliers like the Chambishi syncline and the flanks of the Kafue anticline where the Mwashia and Nguba sections arguably record the salt activity preserved. On this SW side of the Kafue Anticline the stratigraphy dips gently off the western flank of the Kafue anticline, defining a flat to west dipping area of Upper Roan carbonates called the Kashiba platform after the large sink hole (Figure 3 & 6c).

The Kashiba platform (Figure 6c) is intensely deformed to the west with horizontal to gently dipping S1 equivalent fabrics and a basal zone of isoclinally folded marbles that become interleaved with steep to vertically dipping phyllites of the Mwashia and Nguba Groups that mark transition to Domain 4b. The bedding parallel fabric and associated, small scale isoclinal folds are the equivalent of the bedding parallel fabric seen extensively in the west of Domain 3 and mark the margin with Domain 4b.

1208
1209 To the north of the Kashiba Platform, a series of NE and SW facing thrusts occur in the Nchanga
1210 region defining the irregular outcrop pattern of the Fitawola and Chililabombwe area. The complex
1211 strain and cleavage patterns (Torremans et al. 2018) described in this area reflect the local
1212 kinematics driven by reactivating a pre-existing and complex rift fault system geometry. Combined
1213 with the cross section of figure 6c this marks the transition from the flat NKB on the Bangweulu
1214 craton, across the basement cored Kafue Anticline and inverted Northern Basin, to an increasingly
1215 intensely deformed flat lying area to the steeply dipping phyllite belt of the Central Rift Inversion
1216 zone and Domain 4.
1217

1218 **4.1.4 Domain 4: High strain and metamorphic zone and basement domes**

1219 Domain 4 is an arcuate zone that defines the southern boundary of Domain 3 and the northern
1220 boundary of Domain 5. The Domain includes the four inliers of the Kabompo, Mwomezhi, Solwezi
1221 and Luswishi Domes and lies to the southwest of the Kafue anticline. The Domain is described as
1222 two sub-domains; a northern Sub-Domain (4a) characterized by a high strain and high-grade
1223 metamorphic section of apparently Katangan metasediments; Sub-Domain 4b, a high strain low
1224 metamorphic grade extension of 4a to the south.
1225
1226 Sub Domain 4a bears a close resemblance to the metamorphic map of Zambia (Ridgeway &
1227 Ramsay 1986) which shows a ~30-50 km wide zone of high grade, garnet amphibolite facies rocks,
1228 developed around the area of the four inliers. The metamorphic facies of Sub-Domain 4a decline
1229 to the SE and become an intensely deformed low greenschist facies rock sequence. More detailed
1230 and localized metamorphic studies corroborate this regional view (John et al. 2003, 2004, Barron
1231 2003), indicating the amphibolite facies rocks have experienced deep tectonic burial during the

Ediacaran/Cambrian time and subsequent emplacement to the north and exhumation. In addition, data from core KRX082 in Solwezi indicates that these high grade tectonites were emplaced over lower grade, Lower Roan clastic rocks (Figure 5b) creating a significant metamorphic inversion (Figure 6a).

The field work undertaken here supports the generality of high grade metamorphosed Katangan metasediments occurring from the eastern flank of the Kabompo dome to the western flank of the Luswishi dome. The lithologies bearing the high-grade mineral assemblages are also intensely deformed with a bedding parallel (S1) fabric developed in pelitic, psammitic and meta-carbonate rocks. As mentioned above, the Solwezi area and core KRX082 specifically (Figure 6), demonstrates this thrust relationship most clearly. The KRX082 core shows the high grade, amphibolite facies highly deformed and folded rocks emplaced over undeformed, but compacted, clastic rocks of the Lower Roan that preserve primary sedimentary structures such as cross bedding and ripple marks. Similar sedimentary features occur at outcrop on the margin of the Solwezi dome at the Kifubwe Falls. The Solwezi thrust sheet is characterized by complex and intense, large, tight to isoclinal, recumbent folds (Arthurs 1974 & Barron) and best seen today in the main pit of the Kansanshi mine. This thin thrust sheet of high-grade rocks ends to the north but outcrops around the Solwezi Dome to the south. The dome itself comprises a core of pre-Katangan crystalline basement of Paleo and Mesoproterozoic ages (Ku et al 2022) and folds the early S1 Katangan tectonic fabric of the thrust sheet. The Dome is interpreted as a late stage, basement cored thrust of relatively minor displacement compared with the earlier and large displacement of the metamorphic thrust sheet. However, the basement cored nature of the late Solwezi thrust structure generates significant vertical topography of the basement/cover boundary zone. The kinematics of the emplacement of the high metamorphic grade rocks of the Solwezi thrust sheet have yet to be

precisely determined. However, the termination of the Solwezi thrust sheets to the north towards the Chagwama Hills, and the extensive outcrops to the west and south with northward verging structures suggests a southern origin and is compatible with the observations described to the west and east of Solwezi.

The zone of high metamorphic grade and intensely deformed thrust sheets can be traced both west and east from Solwezi. To the west it trends WNW and then swings around the northern tip of the Mwombezi dome to lie between and above the Kabompo and Mwombezi basement domes (Figure 14). From there it trends to the SW plunging below the Kalahari sands and towards Angola. The zone is clearly recognized on the eastern margin of the Kabompo zone where highly deformed Katangan meta-pelites, calc-schists and volcanics are imbricated with the basement (Klink 1977). This narrow, 10-15 km wide synform comprises steeply dipping metapelites, intensely deformed volcaniclastic and locally, highly strained pillow basalts, above and to the east of the Kabompo Dome (Klink 1977), together with locally mylonitised carbonates to the north of the Mwombezhi Dome. It's contact with the Kabompo and Mwombezhi basement is marked by quartz, muscovite, kyanite, talc schists recording deep burial (John et al 2004). The high strain zone’s fan-like structure, faces both to NW in the north and to the SE in the south, defining the edge of the Kabompo Dome and apparently surrounding the Mwombezhi Dome (Figure 12 & 13). To the east of Solwezi, the zone swings around north and south of the Luswishi dome where the HSZ swings south alongside the Luswishi dome. The amphibolite facies metamorphic rocks are lost southwards of the Luswishi area where exposures are poor.

Sub-Domain 4b (Figure 14), southwest of the Kafue anticline, starts where metamorphism has declined to middle to low greenschist and the steeply dipping high strain zone continues to the

south (Figure 12 & 14). It then turns southeast towards the poorly exposed Lukanga Wetlands area. Here the zone largely comprises vertical to steeply dipping pelitic phyllites that define the western margin of the Kabisha platform of flat lying intensely deformed Upper Roan carbonates in the Mpongwe mission area (Domain 3b, Figure 10a & 10c). To its west these high strain rocks of indeterminate age overthrust the Nguba and Kundulungu section of the Kayamba Hills along the Lumwala thrust zone described by Vajner (1998b). Along this boundary highly attenuated and asymmetric folds, locally of sheath fold geometry, indicate ENE/WSW displacement consistent with the thrust kinematics of the Kafue Anticline (Coward and Daly 1984). This zone is interpreted as a structural fan, with structures facing both ways away from an upright center but with a clear west facing fold and thrust in the west (Vajner 1998b) and intense ENE facing isoclinal folded in the dolomites to the east (Figure 6c).

The high strain zone then steps to the west and runs north-south from the Lunga fault to the Mwembeshi fault zone (MFZ), broadly along the eastern boundary of the Hook Granite Batholith (HGB). In this southerly section of the HSZ the Mwashia and Nguba phyllites and schists overthrust the Kundulungu Group to the east, and both are widely intruded by Hook related granite cupolas. The southern termination of the HSZ is a broad zone of east-west fold and faulting towards the proximity of the MFZ where deformed dolomites overlie quartzite tectonites that are exposed around the low-lying basement cored Matala dome (Nayendov et al. 2016). Above them the Nguba and Kundulungu sections are folded parallel to the MFZ. The western boundary of the HSZ is defined by the intrusion of Hook granites that appear to occupy the centre and continuation of the HSZ.

In summary, the HSZ and high grade metamorphics of Domain 4 have three prominent structural characteristics that define Domain 4 and are key to its formation. Firstly, it broadly overprints the Central Rift Zone mapped from the stratigraphic, provenance, and quantitative extension analysis presented in section 3.1. This implies that the deformation became focused by an existing, regional, crustal, and possibly lithospheric scale boundary. This focus occurred through reactivation of rifted, highly extended and possibly broken lithosphere with potentially a narrow zone of transitional or oceanic crust developed within it.

Secondly, although dominantly a zone of vertical fabrics at today's outcrop, the marginal zones of the HSZ are characterized by flat lying shear fabrics that indicate significant lateral displacement of deformed and metamorphosed lithologies away from the CRZ. This displacement is generally asymmetric, favouring a NNW to northerly emplacement in the Kabompo and Solwezi area (Figure 6 & 13). The displacement is best seen in the Solwezi area where the garnet amphibolite Solwezi nappe has been emplaced over a little deformed Lower Roan section broadly from the south (Figure 6a). We interpret this far travelled amphibolitic thrust sheet as the content of a series of rifts and passive margin material developed over the highly extended crust interpreted from the quantitative rifting analysis (Section 3.1).

Thirdly, field mapping shows that the sinuous HSZ and associated structural fan becomes narrower and a lower metamorphic grade to the south of the Luswishi Dome and Kafue Anticline (Figure 12). In the region between the Kashiba Platform area and Lumwala Thrust mylonitic simple shear fabrics outcrop on the Kashiba carbonate platform in the east and to a lesser extent in the the Lumwala Fault zone in the west (Figure 6c).

Finally, based on the above interpretation of a CRZ defined by high extension and deep water depositional environments with volcaniclastic and pillow lava facies, we interpret that an Ediacran compressional event exploited this earlier fabric and inverted the CRZ to a narrow orogenic belt inverting the rift contents in the process. The associated strain and metamorphic grade that occurred with the inversion indicates the orogen was most deformed and thickest in the Kabompo to Solwezi area where major thrust sheets have been mapped, and that the deformation continued southwards to Mumbwa but at lower greenschist grades creating a phyllite and, locally, slate belt. Notwithstanding the thermal and pressure variation along the HSZ, the formation of this arcuate zone of deformation and metamorphism represents the most active time in the evolution of the basin, in terms of heat, pressure and the opportunity for dehydration and hydrothermal activity to generate fluid migration. The degree of closure associated with this event is difficult to estimate. There is little stratigraphy to suggest a major oceanic separation, but equally, pillow lavas and extensive mafic intrusions (Kampunzu 2000) may suggest a highly thinned or transitional crust at a minimum was developed during the Tonian extensional events. In addition, the sediment provenance signature across this same area supports a major structure. Given these features together with broad similarity of stratigraphy and geological history to the north and south of the CRZ, we conclude that highly extended lithosphere with a transitional crust or minor oceanic crust component (10-50 km) was the likely outcome of the Tonian rifting. Implying that the most extended crust existed between the Kabompo to Luswishi areas. The degree of extension appears to have declined to the SE. This apparent decline may be the result of greater oblique extension than in the Kabompo area. Similarly, to the southwest of Kabompo the CRZ swings to the south and may again have been of a more oblique character.

4.1.5 Domain 5: Inverted Southern Rift Basin

To the south and west of the HSZ lies the inverted Southern Rift Basin (SRB) that is characterised by a series of ENE trending, NW dipping fault zones that segment the basin (Figure 12 and 14). The SRB lies between the HSZ and the Lunga fault zone (Figure 12 & 13). It comprises a wide, poorly exposed region with no significant economic mineral discoveries but many mineral occurrences. The Domain is segmented by four regionally significant, NW dipping fault zones between 50 and 70 km wide, that separate segments of folded and faulted stratigraphy (Figure 12). Each segment displays a distinct series of form lines defined by regional mapping and aeromagnetic data that define folds and discontinuities (Page 1974 & Loughlin 1980). From NW to SE the fault lines are known as the Maheba Fault, the Mateba Fault, the Kasempa Fault, the Lunga fault and Lubungu fault (Figure 12).

The Maheba fault is a west dipping feature that borders a folded zone of Nguba and Kundulungu rocks dipping gently off the Mwombezhi dome (Figure 12 & 13). The zone between the Mwombezhi Dome and the Maheba fault is of low metamorphic grade, but with post-tectonic biotite growth. To the SE of the Maheba fault lies a folded zone of largely Kundulungu stratigraphy between the Maheba and Mateba faults (Loughlin 1980). The folds are upright to southeasterly vergent and non-cylindrical. East of the Mateba fault lies a large area of easterly and NW trending fold structures that are interpreted as isolated salt related features due to their highly variable orientations and frequent breccias (Figure 12). East of the Kasempa fault zone there are indications of low angle folding up to the west dipping Lunga fault (Figure 12 & 13). In contrast the hanging wall of the Lunga fault contains a large, east west trending and southerly verging anticline exposing steeply dipping, white, quartz and sub-arkosic arenite overlain by a

recrystallized dolomitic carbonate (Figure 13). This fold is arguably one of the most important structures of the SRB from a stratigraphic perspective. The two stratigraphic formations outcropping in the Lungu fold compare closely with the Lower and Upper Roan facies of typical Katangan stratigraphy (Figure 3) widely developed in the NRB. In addition, the arenite's maximum age, from U-Pb zircon provenance dating, is 859+/-13 Ma (Figure 8a Z21). This data supports a Lower Roan age of deposition. Given the structural context and provenance data we conclude that the hangingwall fold of the Lungu fault displays the deepest stratigraphic level exposed in the Southern Basin. The SRB and Domain 5 effectively terminates at the Lungu fault zone where to the south of it in Domain 6, the structural trend is orthogonal to the Lungu fault zone (Figure 14). From this point southwards to the Lubungu fault and beyond, extensive, north-south trending fold structures of low metamorphic grade Nguba and Kundulungu arenites occur. This folded zone is bounded to the east by the similarly trending, but more intensely folded, HSZ Nguba rocks of Domain 4b (Figure 3 & 12), and to the west by Triassic cover (Figure 3). This area is the northern part of Domain 6.

The significance of the SRB and Domain 5 is three-fold. Firstly, in spite of sparse outcrop and relatively shallow drilling to date, we conclude that similar Katangan basin stratigraphy occurs in the SRB as in the NRB. Whilst this implies that there is grossly stratigraphic similarity either side of the CRZ it is therefore unlikely that a major ocean basin existed between them (John et el. 2004). It is far from clear however, how comparable the Katangan sections are in detail. Secondly, the structure of both basins is segmented by ~200 km long, thick skinned basement cored fault systems, separating different structural domains. The east west trending Lunga fault zone that defines the southern boundary of the Domain, elevates the oldest stratigraphic section, proving the

existence of Lower Roan stratigraphy in the SRB and opening the possibility that it is widespread. Thirdly, whilst there is an indication of Upper Roan carbonate/evaporite sequences in both the NRB and SRB, the NRB appears to host far more extensive, and active salt tectonics than the SRB. Throughout much of the NRB salt has been a significant mechanism in driving the basin structuring. In the SRB only the Kasempa area appears to indicate a contribution from salt tectonics, reflected in complex fold geometries.

4.1.6 Domain 6: The Mumbwa sub-basin

To the south of the SRB lies Domain 6 and the Mumbwa sub-basin. Domain 6 is defined the Lunga fault zone in the north and the MBZ to the south, with the Hook Granite Batholith to the west (Figure 12 & 13). The Domain comprises at outcrop, a north-south trending folded belt of fine to medium grained clastics of Nguba age with a large Kundulungu section preserved in the Kayambe Hills (Vajner 1998b) and a synclinal area to the northeast of Mumbwa (Vajner 1998a) (Figure3). A central area of north-south trending upright, penetrative deformation is mapped as the continuation of the HSZ from the NE. To the north of Mumbwa, lies a large, isolated raft of dolomitic carbonate rock that appears to be a salt transported remnant, equivalent to a Congolese “ecaille” (Figure 12 and 14). The large east-west trending syncline to the NE of Mumbwa is defined by the Nyama Fault Zone on its northern flank. It occurs as an oblique thrust zone with mylonitic fabrics (Vajner 1998a) bounding a moderately folded zone of clastic Nguba and Mwashia rocks to the south. These upright folds are underlain by carbonates and a highly deformed quartz arenite and quartz pebble conglomerate that border the contact with the Paleoproterozoic basement of the Matala Dome (Naydenov et al. 2016). To the south of the Mutala dome and across the MFZ lie the gabbroic eclogites described by (John et al 2003) and the high grade amphibolite facies rocks of the Zambezi belt (Hanson 1993).

The MFZ is considered the southern margin of the sedimentary and regionally low grade to unmetamorphosed Katangan Basin. It is arguable that much of the adjacent Zambezi metamorphic belt comprises rocks whose protolith is a continuation of the Katangan basin (Drysdall et al 1974). However, this is unproven as the two regions have different deformational and metamorphic histories, with the Zambezi belt representing a mid-crustal, high-grade metamorphic terrane in comparison with the largely mildly deformed Katangan basin, with the exception of the inverted CRZ. In addition, there is a compelling spatial coincidence of the intersection of the Zambezi Eclogite Belt (John et al 2003), the MFZ and the formation of the Hook Batholith. The implication of this is uncertain but is raised in the Discussion section below.

4.1.7 Domain 7: The Hook Granite Batholith and its offshoots

To the west of Domain 6 lies the large area of Domain 7 and the Hook Granite Batholith (Figure 14). The domain occurs between the northwest dipping Lunga Fault Zone that defines the southern margin of Domain 6, the SRB, and the steep dipping MFZ (Figure 14). To the southwest the batholith appears to intrude Mesoproterozoic gneisses of the Zambezi belt (Griffiths 1998) but is largely covered by the Quaternary sand of the Kalahari Desert.

The Hook Batholith and associated, regionally developed, gabbroic intrusions represent a major period of bimodal magmatism (Milani et al 2014) between 560 and 530 Ma. The batholith is dominated by a largely undeformed core of phenocrystic alkali-feldspar granites, syenite and monzonite granites with occasional rhyolite dykes and associated gabbroic inclusions (Sanz 2005). To the east, several cupolas of similar K-feldspar granites occur in the low-grade metasediments

of the Mumbwa sub-basin (Figure 12 & 13). These smaller granites intrude the north/south trending, upright fold structures of Domain 5 and the arenite and pelitic Nguba sediments of the Katangan Supergroup that define the margin of the batholith. These upright, tight to isoclinal, fold structures are characteristic of the major, low grade, deformational event in the area (Drysdall et al. 1974, Porada 1989). They are also compatible with a highly compressed, inverted, north south trending rift basin margin of the greater Katangan basin.

The coarse phenocrystic to fine grained granitic textures within the batholith, exhibit a undeformed background with highly deformed sheared and mylonitic textures developed in relatively narrow zones. Naydenov et al. (2014) described two such zones, the southern most being a curvilinear splay of the MFZ, with its trend running smoothly from EW to NS over a distance of about 80 km (Figure 12) and linked with the main MFZ to the east and west. In doing so this shear zone and its low strain margins define an elliptical, lower strain lens within the granite, indicating a left lateral slip component and that the granites preceded at least part of the MFZ displacement. Deformation fabrics of the northern shear zone also converge with the batholith's eastern boundary structures of the NNW/SSE trending upright folds of the Nguba sediments. They also curve and smoothly merge with the NNW/SSE folded zone and into the MFZ (Figure 12).

To the SE of the Batholith, along the MFZ, is a large area of gabbroic eclogite outcrop and float (Phillips 1957, John et al. 2003) that appear to represent both mafic rocks linked to the batholith and gabbroic eclogites of a separate genesis. The eclogite rocks represent the termination of a regional trend of gabbroic eclogites, eclogite and meta-gabbro (Prasad & Vrana 1972, Vrana et al. 1975, Johns et al. 2003) that run from the Hook Batholith ~200 km to ESE. On the basis of

kinematic indicators, Coward & Daly (1982) postulated that this zone defined a highly oblique, collisional plate boundary in the Zambezi belt. Johns et al (2003) expanded this model and, on the basis of PT modelling and minor and trace element patterns similar to recent mid-ocean ridge basalts, concluded that the eclogite assemblages were indicative of a large ocean basin, over 1000 km wide, that separated the Congo and Kalahari cratons. Johns et al (2003), reported a Sm-Nd isochron, defining an age of 595+/-10 Ma age for the eclogite facies metamorphism and argued it implies a rapid subduction model to create the Hook Batholith. The lack of any other evidence of a large ocean basin, such as elements of an ophiolitic suite, blueschist facies rocks or major differences in tectono-stratigraphic history across a well-defined plate boundary question the interpretation. The earlier argued stratigraphic commonality across the MFZ and Eclogite Zone between the Katangan basin and Zambezi Belt (De Swardt, et al 1965) perhaps argues for a different solution.

Naydenov et al (2016) describe a range of U-Pb zircon ages for the Hook Batholith granites from 559+/-18 to 533+/-3. Together with fabric trends, they use these dates to argue for an instantaneous, clockwise rotation of compression that generates a complex of different, cross cutting structural fabric orientations. In effect this is for two discrete and sequential orogenic events related to distant and unspecified regional events outside of their study area. In general terms that may or may not be an appropriate geodynamic model and it is certainly difficult to prove. In our view however, the anastomosing, highly heterogeneous, local strain fabrics of the Mumbwa to Lungu fault area represent a single and evolving local strain pattern. This singular and continuous strain is interpreted as a result of an irregular, pre-deformational, rift-based basement and rift fill architecture, being reactivated during a period of intense basin inversion. Such large

trend variation in strain, due to differential rheology between crystalline basement, rift faulted basement margins, associated sedimentary fill, and large intrusive granite bodies is arguably a more likely explanation for the locally complex strain variation and fabric continuum of the Mumbwa area. Such a singular progressive event is also consistent with the relatively large error bars on the U-Pb ages that define the granite protolith as pre to early-tectonic.

Given the early tectonic setting of the Hook Batholith with respect to Katangan deformation, it is likely that the geodynamic process driving them are connected. The bimodal nature of the batholith is consistent with a model of basaltic magmas being emplaced into the lower continental crust causing rapid and voluminous melting and generation of phenocrystic silicic magma (Huppert & Sparks 1988 & Huppert et al. 2011) (Figure 13). The subsequent question is the source of the alteration of gabbroic rock to eclogite and the mechanism of exhumation. Milani et al (2015) proposed a model where the batholith formed due to slab role back along a zone of oceanic subduction with subsequent invasion of basaltic magmas into the crust in turn triggering crustal melting at the base or within the crust. The scenario implies the crustal thickening and roll-back occurred before the Lufilian orogenic cycle in order for the batholith to have formed before significant deformation took place. We propose an alternative tectonic process that relies on mantle lithosphere invasion at the base of the crust and similar crustal melting causing extensive granite formation (Huppert & Sparks 1998), and eclogite formation. We invoke exhumation of the altered mantle derived gabbros by ductile flow (Harris 2007, & Marques 2018) between the upper, Katangan basin plate, and obliquely colliding lower Zambezi plate. Lithospheric scale lateral movement causing oblique, convergent tectonics, crustal fracturing and ingress into the crust of a mantle intrusion would immediately result in extensive crustal melting and granite formation. A

similar process along the active San Andreas fault zone has been argued (Hutton & Reavy 1992). In summary, precisely the cause of partial melting and the emplacement of the basic material is uncertain, however the evidence of a large, subducted ocean is sparse to nonexistent. Consequently, we interpret that the crustal melting and phenocrystic alkali granites, and associated exhumed gabbroic eclogites have resulted from an oblique, convergent process along a broad zone that includes the MFZ.

5. Discussion

The interest in the margins of cratons and their relationship to inter-cratonic areas has developed over the last two decades as surface wave tomography has converged on the definition of the thickness and shape of continental lithospheric thickness (Jackson et al 2020). The notion of mineral systems being associated with the topography of the lithosphere asthenosphere boundary (LAB) has followed (Griffen 2013 & Hoggard et al. 2020). In this paper we have integrated the lithospheric context with a series of geological studies to build a tectonostratigraphic model for this prolific copper basin that is bordered by three cratons. We have used this model to map the compartmental fabric of the basin relevant to the formation of major fluid pathways through time. We argue for a modified Katangan basin tectonostratigraphic model on four, evidence-based aspects of the basin's formation and deformation:

i) lithospheric thickness control on basin location and shape (section 2);

ii) basin formation, rift geometry and crustal stretching trend (3.1 & 3.2);

iii) sedimentary provenance, routing and basin growth with time (3.3 & 3.4);

iv) basin inversion and the role of rift fault reactivation and compartmentalisation (4.1).

The Katangan basin occurs in a lithospheric thickness zone of 170 to 140 km low between the Congo, Bangweulu, and Kalahari craton margins. The major fault systems within the basin parallel the tomographic contours to a large degree (Figure 2), and the highest stretched part of the basin lies approximately in a trough of 140 km thick lithosphere. In spite of large errors on the surface wave tomography these generalities appear to imply lithospheric thickness, and crustal strength, has controlled both where the basin formed, its general shape and the location where thin lithosphere accommodated the Cambrian compressional deformation.

The distribution of crustal stretching data is limited to regions of low grades of metamorphism and deformation of the Katangan stratigraphy, and to the availability of deep cores to estimate basin subsidence shape and scale. What data we have may be uncertain in absolute terms, but as a clear trend we feel it is highly convincing of an increase of lithospheric stretching from the ENE basin margin to the CRZ. These data both supports a rifting process for the basin formation and also identify the thinnest, and therefore potentially weakest part of the underlying lithosphere. It does, however, not imply a major ocean, but nor does it rule out one. Given the minimum of 70% stretching experienced in the CRZ it seems likely that a highly extended rift system existed in Mwashia time and lithospheric breakup was possible. Together with the field evidence of pillow lavas in the CRZ and the widespread igneous activity (Kampunzu et al. 2000) a highly extended rift system, with a small ocean basin, in the Kabompo/Mwombeshi/Solwezi area is our preferred interpretation. To the southeast it is less likely and to the southwest the Kalahari sand hides any direct evidence. We interpret the CRZ to have been a highly extended rift zone that likely produced a narrow (10’s km) and relatively short (200-500 km long) zone of oceanic crust in the Kabompo

to Luswishi area due to NNW/SSE rifting. As the CRZ becomes increasing oblique to the southeast and southwest the extension has increasingly a strike-slip form with less opening.

The U-Pb zircon provenance studies further support the idea of a major rift basin associated with the CRZ by defining a potential, rift-controlled sediment boundary zone that prevented the widespread distribution of Archean age zircon detritus east of the CRZ in the Kabompo area. This provenance boundary is further evidence of the area being a major discontinuity in the basin and supports the CRZ being a major depocenteracross which material from the west could not pass. The size and duration of the boundary is unclear, but it was an active boundary from at least Mwashia through Nguba times (760-620 Ma). Elsewhere the data implies both locally sourced Lower Roan sediments and regionally sourced sediment routing systems in the Nguba and Kundulungu.

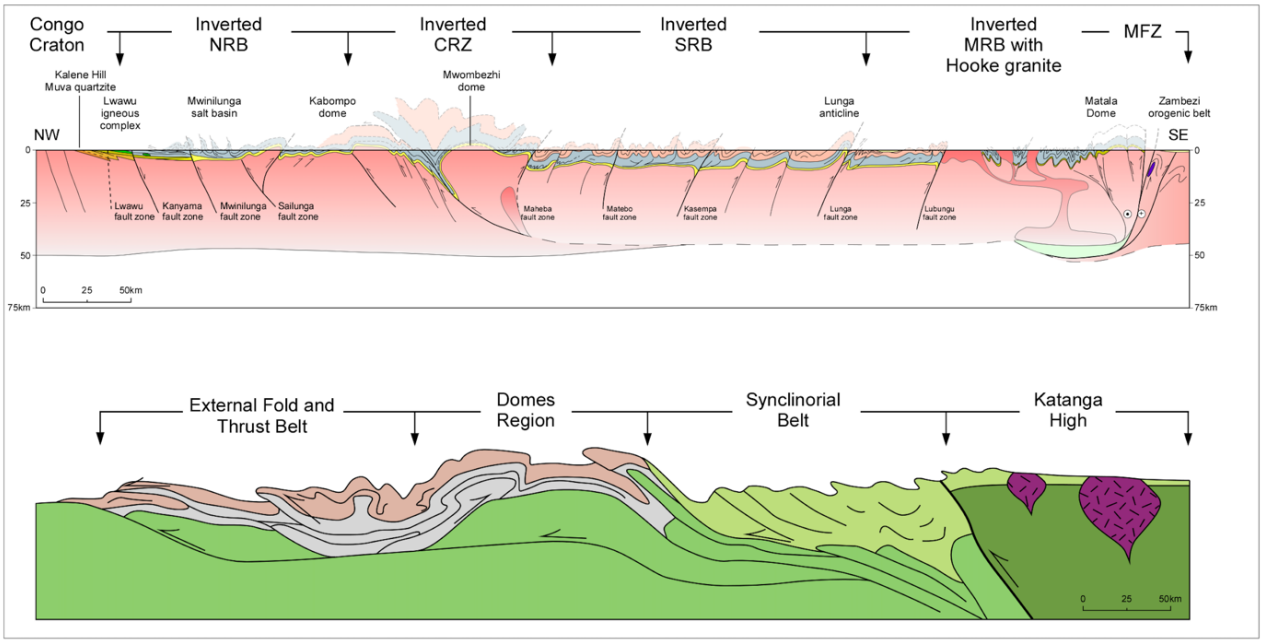

Figure 16. Comparative sections across the Katangan basin.
A comparison of composite basin profiles discussed in this paper, (Figure 12) and the long-accepted basin model first published by Porada (1989). Section (a) is broadly to scale whilst section (b) has an approximately 2x vertical exaggeration.

(a) The structural profile from figure 12 outlining the Katangan basin tectono-stratigraphic interpretation developed in this paper. Wide rift basins (NRB and SRB) developed either side of a highly extended Central Rift Zone (CRZ). Virtually the whole rifted area is deformed to varying degrees by the EoCambrian orogenic inversion. Further explanation of the section detail is on figure 12.
(b) The Zientek et al (2014) schematic section of the Katangan basin developed from Porada (1989) and Porada & Berhorst (2000). The section is markedly asymmetric with a hard boundary to the south defined by a north verging boundary fault of the Katangan High. The fault borders a synclinorium between the Katanga High and the domes region. The Mwembeshi fault zone and associated eclogites are not indicated.

We interpret many of the long, steep, reverse faults active in the EoCambrian inversion to be reactivated rift forming extensional faults. The best example of this behaviour is seen in the reflection seismic interpretation or figure 6b and the core constrained Solwezi Rift interpretation in figure 6a. There are however, other reasons that support the existence of large rift forming extensional faults that later reactivated. The chronostratigraphic section shows the presence of the major rift forming faults and their associated stratigraphy (Figure 7). Each of these rift boundary faults has experienced significant degrees of contractional, oblique inversion as the deformation front developed from being initially upper crustal and dominantly flat lying and parallel to bedding (S1) to thick skinned and basement rooted across the basin. The early fabric is most intensely developed in proximity to the closure of the CRZ, the thicker-skinned, basement rooted faults activate later and elevated the Kafue Anticline and triggered salt diapirs through pre-salt perturbations. Finally, the mapping of the major reverse faults shows extensive stratigraphic evidence indicative of syn-sedimentary movement.

The implications of the existing model and our tectonic model, outlined in profiles in figure 16, are widespread and significant for the formation of the basin and the search for its minerals. Figure 16 compares our model with the existing model originated by Porada (1989) and developed subsequently (Porada & Berhorst 2000, Selley et al. 2006, & Eglinger et al 2015). In this discussion we focus on the aspects of the evolution of the Katangan basin relevant to major fluid pathways through time, notably: the controls implied by formation of the Katangan rift basin; the fill of the rift basin; and the deformation of the rift basin architecture at the time of deformation and maximum heat and pressure in basin. The work has produced a very different profile, similar in the immediate area of the domes regiona but elsewhere very different. The four main differences are discussed below.

Firstly, we have established a close connection between lithospheric thickness and the onlapping margin of the basin. Similarly, large and contiguous crustal scale fault zones that define the center of the basin appear to lie within lithosphere of the order of 170-140 km. Central to that 170-140 km zone, lithospheric extension analysis of the basin indicates the presence of a highly extended CRZ indicating a degree of localized lithospheric break up at the core of the thinnest lithosphere. However, the regional geology does not support the formation of a major ocean basin.

Secondly, on basin formation, the deep core and reflection seismic data has brought clear evidence of the rifting geometry of the basin (Figure 6 & 13) and together with the quantified crustal stretching analysis, shown a clear trend of extension across the basin. The stretching trend has led us to interpret a CRZ associated with of highest crustal extension. In addition, chronostratigraphic analysis has brought basin scale evidence of two rift phases, the second associated with a large

1626 volcanic association and the growth of the basin on to the Congo and Bangweulu cratons with
1627 time.
1628
1629 Thirdly, regarding basin fill, our regional, sedimentary provenance approach to sediment routing
1630 using U-Pb ages of detrital zircons (Figures 8, 9 & 10) has demonstrated that the drainage was
1631 highly compartmentalized west and north of the CRZ. The significant input of Neo-Archaean
1632 zircons into the Mwashia and Nguba sediments of the Mwinilungu sub-basin and their termination
1633 eastwards of the CRZ is dramatic. We interpret this relatively abrupt change in provenance
1634 material as the CRZ of the Kabompo Mwombezhi area representing a major sediment routing
1635 change. This conclusion of a deep basin acting as a provenance boundary is further supported by
1636 associated pillow basalt lavas in the Kabompo area implying a highly thinned crust and deep rift
1637 separating the Mwinilungu sub-basin of the NRB from the SRB.
1638
1639 Finally, regional structural analysis indicates that the Ediacran/Cambrian (560-500 Ma)
1640 deformation reactivated a large part of existing extensional fault structures causing the widespread
1641 inversion of the Tonian rift basins. Deformation ranged from complete closure of the highly
1642 extended CRZ and the development of a ~50 km wide zone of intense, basement involved, thrust
1643 tectonics and high grade metamorphism (Coward & Daly 1984, Ridgeway & Ramsay 1986, Johns
1644 et al 2004), to isolated fold structures due to local, mildly compressional reactivation of individual
1645 faults. The southward continuation of the inverted CRZ appears to be localized along the western
1646 margin of the Kashiba Platform (Figure 13). It is defined by a low temperature, high strain upright
1647 fold belt of Mwashia and Nguba phyllites, interpreted as an intensely folded example of the CRZ
1648 and shown schematically in figure 6c.

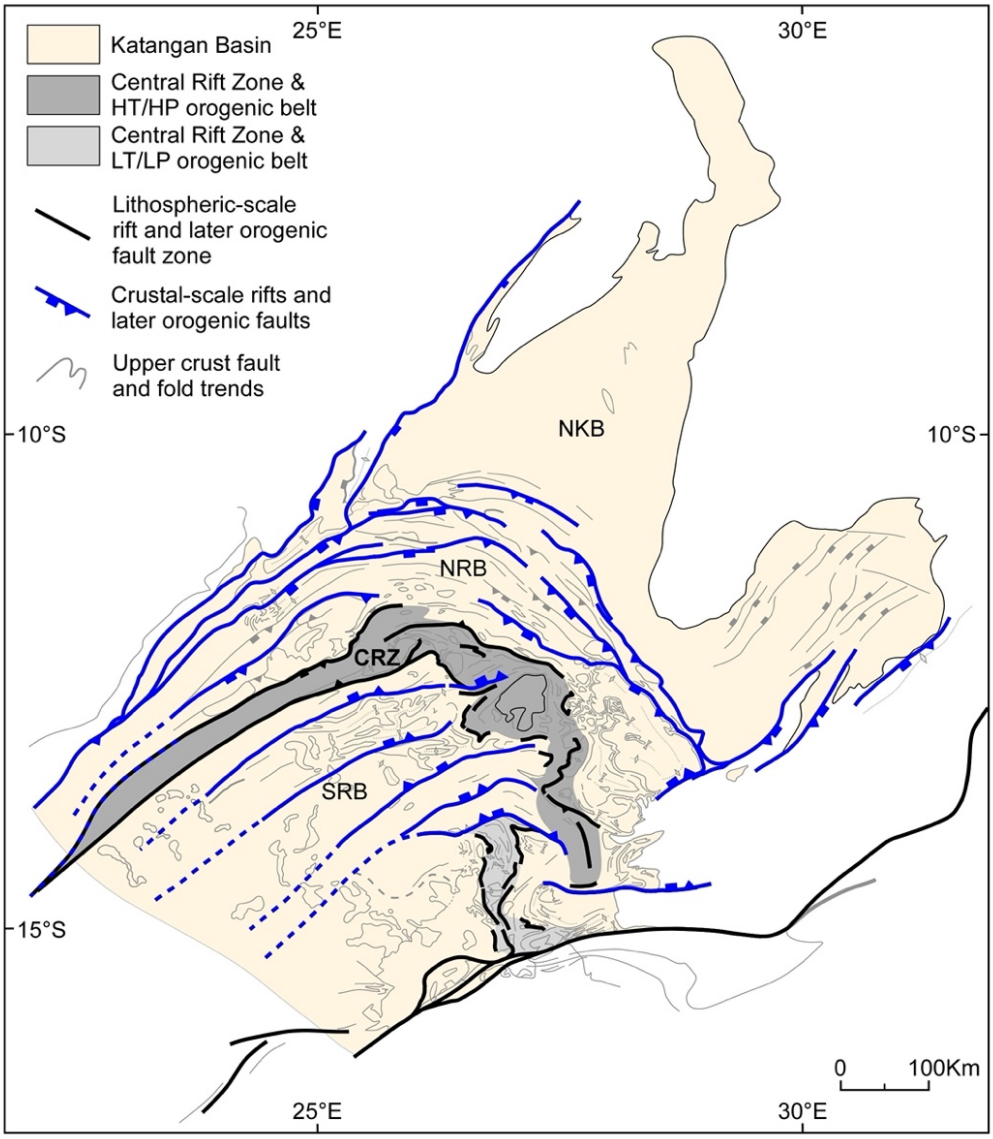

Figure 17 Crustal scale fault systems within the Katangan basin.

The schematic map shows three different scales of regional structures that may have acted as pathways for major hydrothermal fluid movement during the EoCambrian orogenesis, and earlier in the Tonian as magmatic conduits. The grey area represents the most profound, High Strain zone that likely penetrates the whole crust and closed a highly extended CRZ and possibly lithospheric scale break-up. Associated with it are the highest PT conditions experienced by the basin and therefore the source of most fluid movement away from it. The blue faults represent deep crustal structures with major reach laterally. The remaining grey features represent background structural trends showing the extent of upper crustal and surface structure in the terms of fold and faulted Katangan sediments.

1661 This geological heterogenity across long lived fault zones that defines the compartmentalization
1662 of the basin is further complicated by the highly active salt tectonics in the NRB and Mumbwa
1663 area. The early salt tectonics would have been driven initially by local, load driven pressure
1664 gradients and tilting triggered by rift fault heterogeneities. However, the 200 Myr later regional
1665 inversion tectonics, are believed to have exacerbated this complexity and remobilized whatever
1666 salt that remained.
1667
1668 Our tectono-stratigraphic model for the Katangan basin attributes the fundamental deformation
1669 pattern of the basin to the reactivation of the fabric defined by original extensional faults (Figure
1670 17). Original structures of lithospheric scale such as the CRZ and MFZ dominate the basin; crustal
1671 scale structures such as the major Kanyama-Pedicle and Mwinilunga-Kafue fault zones (Figure
1672 12). In addition there is a widespread and more ephemeral upper crustal fault population that exists.
1673 The extensional thermal pulse of the rifting events, and much greater thermal impact of the
1674 compressional orogenic and inversion tectonics and associated amphibolite grade metamorphism,
1675 represent the two main, high heat flow events and, with the inversion, high pressure event of the
1676 basin's history. This focus on the evolution of the early rift basins and their resultant role in the
1677 basins deformation is what makes our interpretation profoundly different to the earlier Porada
1678 (1989) model. The anisotropy and heterogeneity indicated in the basin by both the stratigraphic
1679 and structural analysis and the associated PT highs, has strongly influenced the hydrothermal
1680 pathways available for large volumes of hydrothermal fluids to be focused and penetrate for their
1681 contents to become concentrated. This perspective arguably offers fresh insight into mineral
1682 exploration, both around existing mines and also in the under explored areas such as the SRB and
1683 the marginal Mwashia sub-basins.

6. Conclusions

The paper presents several analyses and conclusions about the Katangan Basin that are new, and others that support or modify previous work. Our interpretations come from the fusion of a large scale lithospheric view together with detailed shallow crust (<5 km) and surface analyses and observations. We list our specific conclusions from this spectrum and offer a small number of questions and a direction for further regional scale research.

1. A profound aspect of the Katangan basin is its location around the margins of three Archean and Early Proterozoic cratons. The basin, as preserved, overlies an area of lithospheric thickness of 170-140 km. This is relatively warm and weak, compared to adjacent cratonic lithosphere of, between 240-200 km that is cold and stronger. The influence of this relationship is evident as inverted rift faults broadly overlie and parallel the craton contours.
2. The basin to lithospheric crustal relationship is defined by the Katangan stratigraphy and is etched in the crust by major fault zones defining the basin margin and the CRZ. These 200 km plus complex fault zones define a curvilinear NW basin margin, an arcuate NE margin and a curvilinear southern margin. The faults have been reactivated throughout the life of the basin and some are active today.
3. ENE to WSW stratigraphic profiling of the Katangan sediments has enabled the quantitative estimation of lithospheric extension across the basin. These data show a concave subsidence form developed in two phases (RF1 and RF2). The degree of subsidence increases progressively from the basin margin to a Central Rift Zone (CRZ). Cumulative extension increases from beta factors of <1.1 at the NE margins of the basin to >1.7 at the Central Rift Zone (CRZ) around Solwezi. This coincidence of highest extension and most intense deformation suggests the most extended and weakest part of the basin to some degree

controlled the highest deformed and metamorphosed part of the basin. Associated with RF2 is a widespread basic and intermediate, intraplate igneous event focussed along the NW and SE basin margins and around the CRZ

4. Regional zircon U-Pb provenance data highlight the structurally driven, stratigraphic compartmentalisation of the basin and major sediment routing over time. In particular, the presence of a CRZ that separates the NRB and the SRB, across which sediment provenance changes dramatically. The high frequency of zircons from the Congo Archean craton in the NW, cease to exist eastwards of the CRZ and the Mwombezhi dome. In the northern rift basin (NRB), the provenance of Lower Roan clastics is dominated by Paleoproterozoic granites of the age of the immediate Katangan basement. Proximal facies interpretation indicates these are likely to be local, rift shoulder sources, from Bangweulu craton basement. In the southern rift basin (SRB) both Paleoproterozoic (Bangweulu craton) and Mesoproterozoic (Irumide orogen) sources are strongly represented. As the rocks sampled are mostly Kundulungu in age, it is unlikely that a mid-basin source was active. Hence the sediment routing here is more likely distal and from the NE where Ediacaran uplift must be generating a sediment source area. The SRB also raises an interesting provenance result at the Lungu fault anticline. In the anticlinal core a sub-arkosic to quartz arenite is overlain by dolomite. The former recorded an 859 Ma maximum age indicating that a Lower Roan section is present deep in the SRB.
5. Chronostratigraphic interpretation shows that the basin progressively onlapped it's margins over time, supporting the implication of rifts followed by periods of thermal subsidence expanding the basin. The final of these periods is the Kundulungu Group that is interpreted as a load driven basin driven by the onset of distal collisional events and the elevation of basement

massifs and loading of adjacent basins. This latter idea may be tested by modelling the thermal evolution of the basin margins and their uplift.

6. Structural analysis describes the Katangan basin as a wide rift basin with a series of fault bounded segments to the north (NRB) and south (SRB) of a deep CRZ. The whole basin experienced degrees of structural inversion during the Eo-Cambrian, along early rift faults most dramatically in the CRZ. Associated with the CRZ is a series of major thrusts that carry amphibolite facies, Katangan age rocks and basement, to the northwest to northeast. These sequences are interpreted as the metamorphosed products expelled due to the closure of the CRZ during the EoCambrian (560-500 Ma) orogenic period. This relationship is well appreciated at the Solwezi area and in the KRX082 core where a mylonitic basal shear zone unit carries garnet-kyanite metasediments over undeformed Lower Roan, subarkosic/quartz arenites. This orogenic zone is traceable from SW of the Kabompo Dome, in a crude arcuate sweep to the SW of the Kafue Anticline where the metamorphic grade declines and the deformation is displayed by largely vertical upright folds. To the north of and outside of the narrow (50 km wide) CRZ, the NRB is largely a series of thick-skinned basement involved structures and extensive salt generated folds, diapirs, salt walls and in the Kolwezi area, large and often detached, salt emplaced nappes. To the south of the CRZ, the SRB is constructed by a series of ENE trending and NNW dipping fault segments on average about 60 km wide and comprising separate, folded zones of outcropping Nguba and Kundulungu stratigraphy. Although dominantly segmented by blind fault structures, the Lungu fault, and associated Lungu anticline, reveal an ESE verging fold of quartz arenites and dolomite interpreted from field and U-Pb provenance ages as Lower and Upper Roan respectively.

7. The arcuate nature of the Katangan basin structure is interpreted to be the result of structural inheritance of pre-existing basement rheology and rift geometry. The contrasts between the NRB, CRZ and SRB are in part a result of crustal thickness variation as seen in CRUST-1, with NRB being thicker than SRB (Figure 13). The regional orthogonal structural trends, carved out by extensional faults and later compression and inversion, may have exploited a weak, earlier tectonic boundary or fault zone along the margin of the Bangweulu craton and Irumide orogen. The complex, locally driven fold and strain fabric relationships, particularly during compressional closure of the CRZ as seen in the Mumbwa and Kafue Dome areas, we also interpret as largely a result of primary basement structure. Complex crenulated fabrics are a response to this basement structure and are unlikely to be a result of multiple different fold phases driven by distal external events.
8. The southern boundary of the Katangan basin is defined by the Mwembeshi fault zone (MBZ). South of the MBZ, deeper exposure with few metasedimentary inliers, regional metamorphism, gabbroic eclogite facies rocks and potentially different stratigraphy raises the possibility of a discrete plate in spite of the similarities north of the MFZ. Whatever the protolith to the present gneisses and granitic rocks of the Zambezi Belt, the deformation and burial as a whole has been significantly greater than in the Katangan basin to the north. Associated with this major boundary is the Hook granite complex, believed to be the result of melting of mafic source rocks associated with gabbroic intrusion/emplacement into the Katangan lower crust. The granite batholith and it's cupolas formed as a result of the lower crust melt and the oblique collisional history of the MFZ and the associated E-W trending Nyama-Mubalashi faults. We conclude the tectonic situation implies a highly oblique

displacement along the MFZ and a crustal thickening context for the gabbroic eclogite assemblages.

9. To consider new basin hosted transition metal (eg. Cu, Ni & Co) exploration options we need to be able to reliably forecast where future, deep mineral deposits will be found. To do this we need to better understand deep crustal structure, its anisotropy and heterogeneity, its connections and permeability through time, and the impact of the resultant compartmentalisation of the basin. Most and probably all of the major copper deposits of the Katangan basin are linked with major fault structures and many with stratigraphic aquifers. Yet the deep crustal relationship of pathway to mineralisation remains difficult to define in both pathway and focus. Large scale diffusive events may be sufficient to create the large low grade ore bodies currently mined, but the role of specific fluid pathways is also a likely and potentially the major focussing conduit. To understand this we need crust penetrating, integrated geophysical data sets to explore this deep space. In this paper we have tried to expand the understanding of the surface geology of the Katangan basin. The next steps need to use integrated geophysical tools to verify the existence of the heterogeneity described here and its deeper subsurface linkages and origins. Only with both these will we be able to successfully explore for the deeper resources required to support the electrification of the energy transition.

Acknowledgements

The authors acknowledge Mike Christie and First Quantum Minerals Exploration Team of Zambia, for supporting the field and analytical work that underpins this paper. We also acknowledge Josh Goldman and KoBold Metals for allowing the inclusion of their seismic reflection data. Country-wide access and field support was provided by the Geological Survey of Zambia, Ministry of Mines, Lusaka. M. C. Daly and M. Purkiss were supported by the UKRI/NERC Copper Basin Exploration Science (CuBES) Project (NERC Grant Reference: NE/T003170/1). The authors acknowledge the late James Mwale as a colleague and early contributor to the work presented here.

The Authors have no conflicts to declare with respect to this work or its publication.

Open Research

The paper includes two Supplementary data sets, S1, referring to the core logs and computations done for the quantitative extensional analysis, and S2, for the analytical detail of the U-Pb zircon analyses. The place of storage for these differing datasets has not yet been decided. Both datasets are included here in the spirit of transparency and open access. Both data bases are included below and remain confidential during the review:

S1. Quantitative analysis of core data for section 3.1.
S2. Sediment provenance age data from zircon U-Pb Data, section 3.3.

References

Alessio, B.L., Collins, A.S., Siegfried, P., Glorie, S., De Waele, B., Payne, J. and Archibald, D.B., 2019. Neoproterozoic tectonic geography of the south-east Congo Craton in Zambia as deduced from the age and composition of detrital zircons. *Geoscience Frontiers*, *10*(6), pp.2045-2061.

Allen, P.A. and Allen, J.R., 2013. *Basin analysis: Principles and application to petroleum play assessment*. John Wiley & Sons.

Andersen, L. S. & Unrug, R. 1984. Geodynamic evolution of the Bangweulu Block, northern Zambia. Precambrian Research, 25, 187–212.

Armstrong, R.A., Master, S. and Robb, L.J., 2005. Geochronology of the Nchanga Granite, and constraints on the maximum age of the Katanga Supergroup, Zambian Copperbelt. *Journal of African Earth Sciences*, *42*(1-5), pp.32-40.

Arthurs, J. W. 1974. Geology of the Solwezi area, degree sheets 1226, NW quarter and 1126 SW quarter. Report 36. Geol. Surv. Dept., Ministry of Mines, Zambia. Published by Gov. Printer, Lusaka.

Baker, J., Peate, D., Waight, T. and Meyzen, C., 2004. Pb isotopic analysis of standards and samples using a Pb-207-Pb-204 double spike and thallium to correct for mass bias with a double-focusing MC-ICP-MS. Chemical Geology, 211, 275-303.

Barron, J. W., 2003, The stratigraphy, metamorphism, and tectonic history of the Solwezi area, Northwest Province, Zambia: Integrating geological field observations and airborne geophysics in the interpretation of regional geology: Ph.D. thesis, Golden, Colorado, Colorado School of Mines, 233 p.

Barton, P. and Wood, R., 1984. Tectonic evolution of the North Sea basin: crustal stretching and subsidence. Geophysical Journal International, 79 (3), pp.987-1022.

Binda, P.L. (1994) Stratigraphy of Zambian orebodies. In: Kampunzu, A.B. and Lubala, R.T. (Eds.), Neoproterozoic Belts of Zambia, Zaire and Namibia. J. Afr. Earth Sci., v. 19.

Black, L. P., Kamos, L., Allen, C.M., Aleinikoff, J.N., Davis, D.W., Korsch, R.J., Foudoulis, C., 2003, TEMORA 1: a new zircon standard for Phanerozoic U–Pb geochronology. Chemical Geology 200, 155– 170.

Bull, S., Selley, D., Broughton, D., Hitzman, M., Cailteux, J., Large, R. & Goldrick, P. 2011. Sequence and carbon stratigraphy of the Neoproterozoic Roan Group strata of the Zambian Copperbelt. Precambrian Research 190 (2011) 70– 89.

Cahen, L., Delhal, J., Ledent, D., 1970a. On the age and petrogenesis of the microcline-bearing pegmatite veins at Roan Antelope and at Musoshi (Copperbelt of Zambia and S-E Katanga). Annales Musée royale de l'Afrique Centrale, Sci. géol. 65, 43–68.

Cailteux, J., 1994. Lithostratigraphy of the Neoproterozoic Shaba-type (Zaire) Roan Supergroup and metallogenesis of associated stratiform mineralization. J. Afr. Earth Sci. 19, 279–301.

Cailteux, J. L. H. & De Putter, T., 2018, The Neoproterozoic Katanga Supergroup (D. R. Congo): State-of-the-art and revisions of the lithostratigraphy, sedimentary basin and geodynamic evolution. https://doi.org/10.1016/j.jafrearsci.2018.07.020.

Cohen, K. M., Finney, S.C., Gibbard, P.L. & Fan, J.-X. 2018 The ICS International Chronostratigraphic Chart. Episodes 36: 199-204 http://www.stratigraphy.org/

Cosi, M.; De Bonis, A.; Gosso, G.; Hunziker, J.; Martinotti, G.; Moratto, S.; Robert, J. P.; et al. 1992. Late Proterozoic thrust tectonics, high-pressure metamorphism and uranium mineralization in the Domes area, Lufilian Arc, northwest Zambia. Precamb. Res. 58: 215–240.

Coward, M.P and Daly, M.C., 1984. Crustal lineaments and shear zones in Africa: their relationship to plate movements. Precamb. Res., v. 24, pp. 27-45.

Cowie, P.A. & Scholz, C. H. 1992. Displacement-length scaling relationship for faults: Data synthesis and discussion. *J. struct. Geol.*, 14, 1149-1156.

Daly, M.C. & Tosca, N. 2020 A Geodynamic Model of the Kansanshi Cu-Au System, Zambia. SEG Conference: https://www.segweb.org/pdf/events/2020/20rmwale/session-1/Session-1-Talk-9.pdf

Daly, M.C. and Unrug, R. 1983. The Muva Supergroup: a craton to mobile belt sedimentary sequence. Trans. Geol. Soc. South Africa, 85, p155-165.

Daly, M.C., Chakraborty, S.K., Kasolo, P., Musiwa, M., Mumba, P., Naidu, B., Nameteba, C., Ngambi, O., and Coward, M.P., 1984, The Lufilian arc and Irumide belt of Zambia: Results of a geotraverse across their intersection: Journal of African Earth Sciences, v. 2, p. 311–318.

Daly, M. C**.** 1986. The Intra-cratonic Irumide Belt of Zambia and its bearing on collision orogeny during the Proterozoic of Africa. In (Eds.) Coward, M. P. C. & Ries, A. C. Collision Tectonics, Spec. Publ. of the Geol. Soc. London, No. 19, pp 321-328.

Daly, M. C., Green, P., Watts, A. B., Davies, O., Chibesakunda, F. & Walker, R. (2020) Tectonic and Landscape evolution of Central Africa and implications for a propagating Southwestern Rift in Africa. Geochemistry, Geophysics & Geosystems, 21, https://doi.org/10.1029/2019GC008746

De Swardt, A.M., Garrard, P., Simpson, J. G. 1965. Major zones of transcurrent dislocation and superposition of orogenic belts in parts of Central Africa. Bull. Geol. Soc. Am. 76, 89-102.

De Waele, B., Liégeois, J.-P., Nemchin, A.A., Tembo, F., 2006. Isotopic and geochemical evidence of Proterozoic episodic crustal reworking within the Irumide Belt of southcentralAfrica, the southern metacratonic boundary of an Archaean Bangweulu Craton. Precambrian Research 148, 225–256.

De Waele, B. and Fitzsimons, I.C.W., 2007. The nature and timing of Palaeoproterozoic sedimentation at the southeastern margin of the Congo Craton; zircon U–Pb geochronology of plutonic, volcanic and clastic units in northern Zambia. Precambrian Research, 159(1-2), pp.95-116.

Drysdall, A.R., Johnson, R.L., Moore, T.A., Thieme, J.G., 1974. Outline of the geology of Zambia. Geologie en Mijnbouw 51, 265–276.

Eglinger, A., Vanderhaeghe, O., André-Mayer, A-S., Goncalves, P., Zeh, A., Durand, C. & Deloule, E. 2016. Tectono-metamorphic evolution of the internal zone of the Pan-African Lufilian orogenic belt (Zambia): Implications for crustal reworking and syn-orogenic uranium mineralizations. Lithos, 240–243, pp 167–188. http://dx.doi.org/10.1016/j.lithos.2015.10.021.

Fleischer, V.D., Garlick, W.G., and Haldane, R., 1976, Geology of the Zambian Copperbelt Wolf, K.H., ed., Handbook of strata-bound and stratiform ore deposits: v. 6, p. 223–352.
Francois, A. P. 1987. Synthese geologique sur l'Arc cuprifere du Shaba (Rep. du Zaire). Bull. Soc. Belge Geol., Centenaire1987, Hors serie, 15-65.

François, A.P., & Cailteux, J., 1981, La Couverture Katangienne entre les Socles de Zilo et de la Kambompo, République du Zaire—Région de Kolwezi. Musée Royal de l'Afrique Centrale, Tervuren, Belgique, Annales Serie In 8o, Sciences Géologiques, no. 87, 50 p.

Garlick, W. G. 1961. Structural Evolution of the Copperbelt. In: Ed. Mendelsohn, F. 1961, The Geology of the Northern Rhodeisan Copperbelt. Published by MacDonald, London.

Goscombe, B., Foster, D. A., Gray, D. & Wade, B. 2020. Assembly of central Gondwana along the Zambezi Belt: Metamorphic response and basement reactivation during the Kuunga Orogeny. Gondwana Research 80, 410–465. https://doi.org/10.1016/j.gr.2019.11.004

Griffiths, C. M. 1998. Geology of the Ngoma area, degree sheet 1525, SE quarter. Report 77. Geol. Surv. Dept., Ministry of Mines, Zambia. Published by Gov. Printer, Lusaka.

Halpin, J. A., Jensen, T., McGoldrick, P., Meffre, S., Berry, R. F., Everard, J. L., Calver, C. Thompson, R., Goemann, K., and Whittaker, J. M., 2014. Authigenic monazite and detrital zircon dating from the Proterozoic Rocky Cape Group, Tasmania: Links to the Belt-Purcell Supergroup, North America: Precambrian Research 250, 50-67.

Halpin, J., Broughton, D., 2018. Structural Configuration of the Central African Copperbelt: Roles of Evaporites in Structural Evolution, Basin Hydrology, and Ore Location. Society of Economic Geologists Special Publication 21, 115–156.

Halverson, G., Porter, S. and Shields, G., 2020. The Tonian and Cryogenian Periods. In Geologic Time Scale 2020 (pp. 495-519). Elsevier.

Hanson, R. E., Wardlaw, M. S., Wilson, T. & Mwale, G. 1993. U-Pb ages from the Hook granite massif and Mwembeshi dislocation: constraints on Pan African deformation, plutonism and transcurrent shearing in central Zambia. Precambrian Research, Vol. 63, 189-209.

Hanson, R. E. 2003. Proterozoic geochronology and tectonic evolution of southern Africa. 2003. In Eds. Yoshida, M., Windly, B. F. & Dasgupta, S. (eds) 2003. Proterozoic East Gondwana: Supercontinent Assembly and Breakup. Geological Society, London, Special Publications, 206, 427–463. 0305–8719/03/$15 © The Geological Society of London.

Hinsbergen, D.J.J., Buiter, S.J.H., Torsvik, T.H., Gaina, C., Webb, S.J. (Eds.), The Formation and Evolution of Africa: A Synopsis of 3.8 Ga of Earth History, Geological Society of London Special Publications, vol. 357. pp. 69–83.

Hitzman, M.W., 2000, Source basins for sediment-hosted stratiform Cu deposits: Implications for the structure of the Zambian Copperbelt: Journal of African Earth Sciences, v. 30, p. 855–863.

Hitzman, M.W., Kirkham, R., Broughton, D., Thorson, J., and Selley, D., 2005, The sediment-hosted stratiform copper ore system: Economic Geology 100th Anniversary Volume, p. 609–642.

Hitzman, M.W., Broughton, D., Selley, D., Woodhead, J., Wood, D., and Bull, S., 2012, The Central African Copperbelt: Diverse stratigraphic, structural, and temporal settings in the world's largest sedimentary copper district: Society of Economic Geologists Special Publication 16, p. 487–514.

Hitzman, M.W., and Broughton, D.W., 2017, Discussion: "Age of the Zambian Copperbelt": Mineralium Deposita, v. 52, p. 1273–1275.

Hoggard, M. J., Czarnota, K., Richards, F. D., Huston, D. L., Jaques, A. L. & Ghelichkhan, S. 2020. Global distribution of sediment-hosted metals by craton edge stability. Nature Geoscience, Vol. 13, 504-510, https://doi.org/10.1038/s41561-020-0593-2

Huismans, R.S., Podladchikov, Y.Y. and Cloetingh, S., 2001. Transition from passive to active rifting: Relative importance of asthenospheric doming and passive extension of the lithosphere. *Journal of Geophysical Research: Solid Earth*, *106*(B6), pp.11271-11291.

Huppert, H. E. & Sparks, R. S. J. 1988. The Generation of Granitic Magmas by Intrusion of Basalt into Continental Crust. Journal of Petrology, Vol. 29, Part 3, pp 599-624.

Hutton, D. H. W. and Reavy, R. J. 1992. Strike-slip tectonics and granite petrogenesis. Tectonics, 11(5), pp. 960-967. https://doi.org:/10.1029/92TC00336

Intiomale, M.M., and Oosterbosch, R., 1974, Géologie et géochimie du gisement de Kipushi–Zaire, in Bartholome, P., ed., Gisements stratiformes et provinces cupifères: Centenaire de la Société Géologique Belgique de

Liège, p. 123–164.

Jackson, J., McKenzie, D., & Priestley, K. 2021. Relations between earthquake distributions, geological history, tectonics and rheology on the continents. Phil. Trans. R. Soc. A 379: 20190412. https://doi.org/10.1098/rsta.2019.0412

Jackson, M.P.A., Warin, O.N., Woad, G.M., and Hudec, M.R., 2003, Neoproterozoic allochthonous salt tectonics during the Lufilian orogeny in the Katangan Copperbelt, central Africa: Geological Society of America Bulletin, V. 115, p. 314–330.

Jochum,K. P., U. Weis, B. Stoll, D. Kuzmin, Q. Yang, I. Raczek, D. E. Jacob, A. Stracke, K. Birbaum, D. A. Frick, D. Gunther and J. Enzweiler, 2011, Determination of Reference

John, T., Schenk, V., Haase, K., Scherer, E. & Tembo F. 2003. Evidence for a Neoproterozoic ocean in south-central Africa from mid-oceanic-ridge–type geochemical signatures and pressure temperature estimates of Zambian eclogites. Geology; V. 31; no. 3; p. 243–246.

John, T., Schenk, V., Mezger, K. and Tembo, F. 2004, Timing and PT Evolution of Whiteschist Metamorphism in the Lufilian Arc Zambezi Belt Orogen (Zambia): Implications for the Assembly of Gondwana. The Journal of Geology, 2004, volume 112, p. 71–90

Jove, C. F. & Coleman, R. G. 1998. Extension and mantle upwelling within the San Andreas fault zone, San Francisco Bay area, California. Tectonics Vol. 17, No.. 6, pp 883-890.

Laske, G., Masters, G., Ma, Z. & Pasyanos, M. 2013. Update on CRUST1.0 – A1 – degree Global modelof Earth's Crust, Geophys. Res. Abstracts, 15, Abstract EGU2013-2658.

Kampunzu, A.B., Kapenda, D. and Manteka, B., 1991. Basic magmatism and geotectonic evolution of the Pan African belt in central Africa: evidence from the Katangan and West Congolian segments. *Tectonophysics*, *190*(2-4), pp.363-371.

Kampunzu, A.B. & Cailteux, J., 1999. Tectonic evolution of the Lufilian arc (Central Africa Copperbelt) during the Neoproterozoic Pan-african orogenesis. Gondwana Res. 2, 401–421.

Kampunzu, A. B., Tembo, F., Matheis, G., Kapenda, D. and Huntsman-Mapila, P., 2000. Geochemistry and Tectonic Setting of Mafic Igneous Units in the Neoproterozoic Katangan Basin, Central Africa: Implications for Rodina Break-up. Gondwana Res., V. 3, No. 2, pp125-153.

Kampunzu, A.B., Cailteux, J.L.H., Moine, B. and Loris, H.N.B.T., 2005. Geochemical characterisation, provenance, source and depositional environment of 'Roches Argilo-Talqueuses'(RAT) and Mines Subgroups sedimentary rocks in the Neoproterozoic Katangan Belt (Congo): Lithostratigraphic implications. Journal of African Earth Sciences, 42(1-5), pp.119-133.

Kang-kang X., Wei Xie, Kai Sun, Jun-ping, R., Peng-hui, G., Sheng-fei, H. Yi-guan, Lu. &

Hang, Zhang. 2022. Geochronology, geochemistry, and petrogenesis of I- and A-type granites in the Solwezi Dome of the Lufilian Arc: implicationsfor the late-Mesoproterozoic magmatic and geodynamic evolution in northern Zambia. Arabian Journal of Geosciences 15:1729. https://doi.org/10.1007/s12517-022-10971-0

Kennedy, K. Nicholas, E. & Broughton, D. 2019. Basinal setting and origin of thick (1· 8 km) mass-flow dominated Grand Conglomérat diamictites, Kamoa, Democratic Republic of Congo: Resolving climate and tectonic controls during Neoproterozoic glaciations. Sedimentology 66, no. 2 (2019): 556-589.

Keppie, J. D. 1977. The Geology of the Mukubwe area, degree sheet 1327, SE quarter. Report of the Geol. Surv. Dept., Ministry of Mines, Zambia, No. 48, pp. Published by Gov. Printer, Lusaka.

Klink, B. A. 1977. The Geology of the Kabompo Dome area, degree sheet1224, NE quarter. Report of the Geol. Surv. Dept., Ministry of Mines, Zambia, No. 44, pp. 44. Published by Gov. Printer, Lusaka.

Key, R. and Banda, J. 2000. The geology of the Kalene Hills area; explanation of degree sheets 1023 SE, 1024 SW and 1124 NW quarters. Report of the Geological Survey of Zambia, No. 107, pp. 34. Published by Gov. Printer, Lusaka.

Key, R. M., Liyungu, A. K., Njamu, F. M., Somwe, V., Banda, J., Mosley, P. N. & Armstrong, R. A. 2001. The western arm of the Lufilian Arc in NW Zambia and its potential for copper mineralisation. Journal of African Earth Sciences, V. 33, 503–528.

Kober, L., 1921. Der Bau der Erde, Gebr uder Borntraeger

Liyunga, A. K., Mosley, P. N, Njamu, F. M. and Banda, J. 2000, Geology of the Mwinilunga Area; explanation of Degree Sheet 1124, southwest quarter and that part of 1123, southeast quarter that lies in Zambia. Report of the Geological Survey of Zambia, No. 110, pp. 36.

Loughlin, W. P. 1980. The Geology of the Matebo and Luma River Areas, degree sheets 1225, SE quarter and 1226, SW quarter. Report of the Geological Survey of Zambia, No. 90, pp. 20. Published by Gov. Printer, Lusaka.

Loughlin, W. P. 1998. Geology of the Idiamala Pool area, degree sheet 1626, NW quarter. Report of the Geological Survey of Zambia, No. 87, pp. 36. Published by Gov. Printer, Lusaka.

Mambwe, P., Swennen, R., Cailteux, J., Mumba, C., Dewaele, S. and Muchez, P., 2023. Review of the origin of breccias and their resource potential in the Central Africa Copperbelt. Ore Geology Reviews, https://doi.org/10.1016/j.oregeorev.2023.105389

Mendelsohn, F., ed., 1961, The geology of the Northern Rhodesian Copperbelt: Published by MacDonald & Co. Ltd., London W.1, 523 pp.

Master, S., Rainaud, C., Armstrong, R.A., Phillips, D. and Robb, L.J., 2005. Provenance ages of the Neoproterozoic Katanga Supergroup (Central African Copperbelt), with implications for basin evolution. Journal of African Earth Sciences, 42(1-5), pp.41-60.

McGowan, R.R., Roberts, S., Foster, R.P., Boyce, A.J., and Coller, D., 2003, Origin of the copper-cobalt deposits of the Zambian Copperbelt: An epigenetic view from Nchanga: Geology, v. 31, p. 497–500.

Milani, L, Lehmanna, J., Naydenova, K. V., Saalmanna, K., Kinnaird, J. A., Daly, J. S., Freie, D. & Sanz, A. L. G. 2015. A-type magmatism in a syn-collisional setting: The case of the Pan-African Hook Batholith in Central Zambia. Lithos, http://dx.doi.org/10.1016/j.lithos.2014.11.029

Miller, R. 2013. Comparative Stratigraphic and Geochronological Evolution of the NorthernDamara Supergroup in Namibia and the Katanga Supergroup in the Lufilian Arc of Central Africa Geoscience Canada, v. 40, http://dx.doi.org/10.12789/geocanj.2013.40.007

Muchez, P., André-Mayer, A.S., El Desouky, H.A. and Reisberg, L., 2015. Diagenetic origin of the stratiform Cu–Co deposit at Kamoto in the Central African Copperbelt. *Mineralium Deposita*, *50*(4), pp.437-447.

Naydenov, K. V., Lehmann, J., Saalmann, K. Milani, L., Kinnaird, J. A., Charlesworth, G. Frei, D. & Rankin, W. 2014. New constraints on the Pan-African Orogeny in Central Zambia: A structural and geochronological study of the Hook Batholith and the Mwembeshi Zone. Tectonophysics, http://dx.doi.org/10.1016/j.tecto.2014.09.010

Naydenov, K. V., Lehmann, J., Saalmann, K. Milani, L., Poterai, J., Kinnaird, J. A., Charlesworth, G. & Kramers, J. D. 2016 The geology of the Matala Dome: an important piece of the Pan-African puzzle in Central Zambia. Int J Earth Sci. pp. 695–712, http://dx.doi.org/10.1007/s00531-015-1222-y

Page, J. 1974. Geology of the Lubungu and Lunga areas, degree sheets 1426, NW and SW quarters. Report of the Geological Survey of Zambia, No. 56, pp. 23. Published by Gov. Printer, Lusaka.

Page, J. 1974. The geology of the Chilonga Mission area, degree sheet 1231, NW quarter. Report of the Geol. Surv. of Zambia, No. 56, pp. 28. Published by Gov. Printer, Lusaka.

Phillips, K. A. 1957.. The Geology and metalliferous deposits of the Luiri Hill area (Mumbwa District). Report of the Geological Survey of Zambia, No. 10, pp. 82. Published by Gov. Printer, Lusaka.

Porada, H., 1989. Pan-African rifting and orogenesis in Southern to Equatorial Africa and Eastern Brazil. Precambrian Research 44, 103-136.

Porada, H. and Berhorst, V., 2000, Towards a new understanding of the Neoproterozoic-Early Paleozoic Lufilian and Northern Zambezi belts in Zambia and Congo/Zaire: Journal of

African Earth Sciences, v. 30, p. 727–771.

Prasad, R., Vrana, S. 1972. The intrusives of the Chombwa area with special reference to the eclogites. Geol. Surv. Zambia Rap. 12, 131-137 {1972)

Priestley, K., and McKenzie, D., 2013, The relationship between shear wave velocity, temperature, attenuation and viscosity in the shallow part ofthe mantle: Earth and Planetary Science Letters, v. 381, p. 78–91, https://doi.org/10.1016/j.epsl.2013.08.022

Ridgway, J. & Ramsay, C. R. 1986. A provisional Metamorphic Map of Zambia & Explanatory Notes. J. Afr. Earth Sciences Vol. 5, pp. 441-446.

Rooney, A.D., Strauss, J.V., Brandon, A.D. and Macdonald, F.A., 2015. A Cryogenian chronology: Two long-lasting synchronous Neoproterozoic glaciations. *Geology*, *43*(5), pp.459-462.

Sanz, A. L-G. 2005. Pre- and Post-Katangan granitoids of the greater Lufilian Arc – geology, geochemistry, geochronology and metallogenic significance. Unpublished Doctor of Philosophy Thesis Science Thesis, Faculty of Science, University of Witswatersrand, Johannesburg. pp. 734.

Sarafian, E., Evans, R. L., Abdelsalam, M. J. D., Atekwana, E., Elsenbeck, J., Jones, A., & Chikambwe, E. 2018. Imaging Precambrian lithospheric structure in Zambia using electromagnetic methods. Gondwana Research, 54, 38–49. https://doi.org/10.1016/j.gr.2017.09.007

Schaeffer, A. J., & Lebedev, S. 2013. Global shear speed structure of the uppermantle and transition zone. Geophys. J. Int. 194, 417–449. https://doi:10.1093/gji/ggt095

Scholz, C. H. 2007. The Scaling of Geological Faults. doi: 10.1201/9780203936115.ch1.

Sclater, J.G. and Christie, P.A., 1980. Continental stretching: An explanation of the post-mid-Cretaceous subsidence of the central North Sea basin. Journal of Geophysical Research: Solid Earth, 85(B7), pp.3711-3739.

Selley, D., Broughton, D., Scott, R., Hitzmann, M.,Bull, S., Large, R., McGoldrick, P., Croaker, M. & Pollington 2018. N. 2006. A New Look at the Geology of the Zambian Copperbelt. Selley, D., Scott, R., Emsbo, P., Koziy, L., Hitzman, M., Bull, S. W., Duffett, M., Sabagenzi, S., Halpin, J & Broughton, D. W. 2018. Structural configuration of the Central African Copperbelt: roles of evaporites in structural evolution, basin hydrology, and ore location, Metals, Minerals, and Society: Society of Economic Geologists Special Publication, Number 21 pp. 115-156. ISSN 1547-3112 (2018)

Slama, J., Kosler, J., Condon, D.J., Crowley, J.L., Gerdes, A., Hanchar, J.M., Horstwood, M.S.A., Morris, G.A., Nasdala, L., Norberg, N., Schaltegger, U., Schoene, B., Tubrett, M.N., Whitehouse, M.J., 2008. Plesovice zircon - A new natural reference material for U-Pb and Hf isotopic microanalysis. Chem Geol 249, 1-35.

Stacey J. S., Kramers J. D. 1975. Approximation of terrestrial lead isotope evolution by a two-stage model. Earth and Planetary Science Letters 26, 207-221.

Torrealday, H.I., Hitzman, M.W., Stein, H.J., Markley, R.J., Armstrong, R. and Broughton, D., 2000. Re-Os and U-Pb dating of the vein-hosted mineralization at the Kansanshi copper deposit, northern Zambia. Economic Geology, 95(5), pp.1165-1170.

Torremans, K., Muchez, P. & Sintubin, M. 2018. Non-cylindrical parasitic folding and strain partitioning during the Pan-African Lufilian orogeny in the Chambishi–Nkana Basin, Central African Copperbelt. *Solid Earth*, 9 (4). 1011-1033 doi:10.5194/se-9-1011-2018

Turer, D. and Maynard, J.B., 2003. Combining subsidence analysis and detrital modes of sandstones to constrain basin history: an example from the eastern pontides of Turkey. *International Geology Review*, *45*(4), pp.329-345.

Twigg, H. 2020. The geology of Kakanda, DRC – implications for lithological and structural controls of Cu-Co mineralisation of the Roan Group. Unpublished Master of Science Thesis, Golden, Colorado School of Science, pp. 154.

Taverner-Smith, R. 1961. The geology of the Mpanza Mission area, degree sheet 1626, NE quarter. Report 10. Geol. Surv. Dept., Ministry of Mines, Zambia. Published by Gov. Printer, Lusaka.

Thieme, J. G., 1969. The geology of the Mansa area, degree sheet 1128, NE & SW quarters. Report 26. Geol. Surv. Dept., Ministry of Mines, Zambia. Published by Gov. Printer, Lusaka.

Thieme, J. G., 1971. The geology of the Musonda Falls area, degree sheet 1028, SE quarter. Report 32. Geol. Surv. Dept., Ministry of Mines, Zambia. Published by Gov. Printer, Lusaka.

Thieme, J. G. & Johnson, R. L. 1981. The Geological Map of the Republic of Zambia, 1:1,000,000. Geol. Surv. Dept., Ministry of Mines, Zambia. Published by Gov. Printer, Lusaka.

Thompson, J. M., Meffre S, Danyushevsky L. 2018. Impact of air, laser pulse width and fluence on U–Pb dating of zircons by LA-ICPMS. Journal of Analytical Atomic Spectrometry 33: 221–230. DOI: 10.1039/C7JA00357A

Twite, F., Broughton, D., Nex, P., Kinnaird, J., Gilchrist, J. & Edward, D. 2017 Lithostratigraphic and structural controls on sulphide mineralisation at the Kamoa copper deposit, Democratic Republic of Congo. Journal of African Earth Sciences, https://doi.org/10.1016/j.jafrearsci.2018.12.016

Unrug, R., 1983, The Lufilian Arc: A microplate in the Pan African collision zone of the Congo and the Kalahari cratons. Precambrian Research, V21, p181-196.

Vajner, P. G. 1998a. Geology of the country north-east of Mumbwa, degree sheet 1427, SW quarter. Report 29. Geol. Surv. Dept., Ministry of Mines, Zambia. Published by Gov. Printer, Lusaka.

Vajner, P. G. 1998b. Geology of the Luamala and Lukunga areas, degree sheet 1427, NE and NW quarters. Report 52. Geol. Surv. Dept., Ministry of Mines, Zambia. Published by Gov. Printer, Lusaka.

Van Doorninck, H. H. 1928. De Lufilisch plooiing in den Boven Katanga. G. Naeff. Den Hague, Netherlands.

Veevers, J.J., 1981. Morphotectonics of rifted continental margins in embryo (East Africa), youth (Africa-Arabia), and maturity (Australia). *The Journal of Geology*, *89*(1), pp.57-82.
Vrana, S., Prasad, R. & Fediukova, 1975. Metamorphic Kyanite Eclogites in the Lufilian Arc of Zambia. Contrib. Mineral. Petrol. 51,139—160.

Watts, A.B. and Ryan, W.B.F., 1976. Flexure of the lithosphere and continental margin basins. In *Developments in geotectonics* (Vol. 12, pp. 25-44). Elsevier.

Wendorff, M., 2003. Stratigraphy of the Fungurume group – evolving foreland basin succession in the Lufilian fold-thrust belt, Neoproterozoic-Lower Palaeozoic, Democratic Republic of Congo. S. Afr. J. Geol. 106, 17–34.

Wendorff, M., 2005. Evolution of Neoproterozoic-Lower Paleozoic Lufilian arc, Central Africa: a new model based on syn-tectonic conglomerates. J. Soc. Lond. 162, 5–8.

Wendorff, M., 2011. Tectonosedimentary expressions of the evolution of the Fungurume foreland basin in the Lufillian arc, neoproterozoic-lower Palaeozoic, central Africa. In: Van Hinsbergen, D. J. J., Buiter, S. J. H., Torsvik, T. H., Gaina, C. &Webb, S. J. (eds) The Formation and Evolution of Africa: A Synopsis of 3.8 Ga of Earth History. Geological Society, London, Special Publications, 357, 69–83. DOI: 10.1144/SP357.5 0305-8719/11

Wiedenbeck, M., Alle, P., Corfu, F., Griffin W.L., Meier, M., Oberli, F., Vonquadt A., Roddick, J.C., Speigel W., 1995, 3 Natural Zircon Standards for U-Th-Pb, Lu-Hf, Trace-Element and REE Analyses. Geostandards Newsletter 19, 1-23.

Xie, X. and Heller, P.L., 2009. Plate tectonics and basin subsidence history. *Geological Society of America Bulletin*, *121*(1-2), pp.55-64.

Zientek, M.L., Bliss, J.D., Broughton, D.W., Christie, Michael, Denning, P.D., Hayes, T.S., Hitzman, M.W., Horton, J.D., Frost-Killian, Susan, Jack, D.J., Master, Sharad, Parks, H.L., Taylor, C.D., Wilson, A.B., Wintzer, N.E., and Woodhead, Jon, 2014, Sediment-Hosted stratabound copper assessment of the Neoproterozoic Roan Group, Central African Copperbelt, Katanga Basin, Democratic Republic of the Congo and Zambia: U.S. Geological Survey Scientific Investigations Report 2010–5090–T, 162 p., and spatial data, http://dx.doi.org/10.3133/sir20105090T.